

*Abrams*

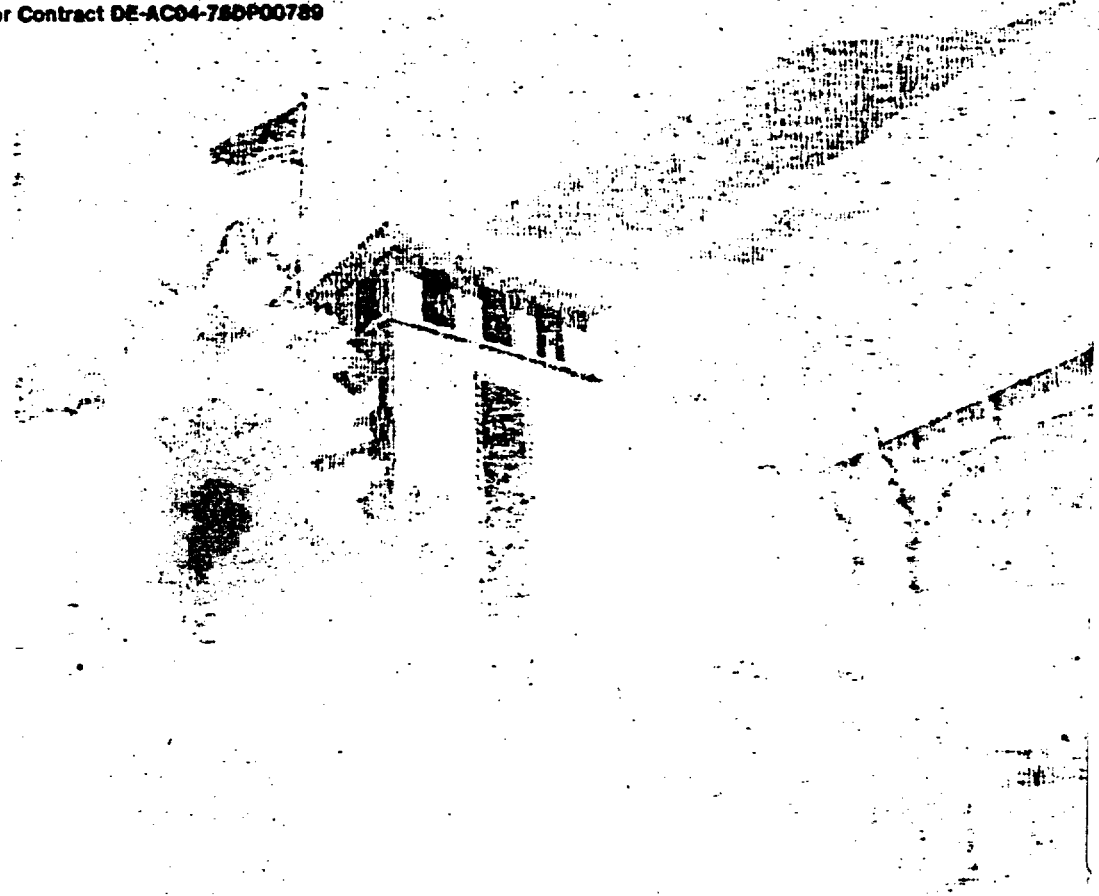
# SANDIA REPORT

SAN 87-1685 • UC-70  
Unlimited Release  
Printed December 1988

## Preliminary Evaluation of the Exploratory Shaft Representativeness for the Yucca Mountain Project

F. B. Nimick, L. E. Shephard, T. E. Blawas

Prepared by  
Sandia National Laboratories  
Albuquerque, New Mexico 87185 and Livermore, California 94550  
for the United States Department of Energy  
under Contract DE-AC04-78DP00789



HYDROLOGY DOCUMENT NUMBER 591

"Prepared by Yucca Mountain Project (YMP) participants as part of the Civilian Radioactive Waste Management Program (CRWM). The YMP is managed by the Yucca Mountain Project Office of the U. S. Department of Energy, Nevada Operations Office (DOE/NV). YMP work is sponsored by the Office of Geologic Repositories (OGR) of the DOE Office of Civilian Radioactive Waste Management (OCRWM)."

Issued by Sandia National Laboratories, operated for the United States Department of Energy by Sandia Corporation.

**NOTICE:** This report was prepared as an account of work sponsored by an agency of the United States Government. Neither the United States Government nor any agency thereof, nor any of their employees, nor any of their contractors, subcontractors, or their employees, makes any warranty, express or implied, or assumes any legal liability or responsibility for the accuracy, completeness, or usefulness of any information, apparatus, product, or process disclosed, or represents that its use would not infringe privately owned rights. Reference herein to any specific commercial product, process, or service by trade name, trademark, manufacturer, or otherwise, does not necessarily constitute or imply its endorsement, recommendation, or favoring by the United States Government, any agency thereof or any of their contractors or subcontractors. The views and opinions expressed herein do not necessarily state or reflect those of the United States Government, any agency thereof or any of their contractors or subcontractors.

Printed in the United States of America  
Available from  
National Technical Information Service  
U.S. Department of Commerce  
5285 Port Royal Road  
Springfield, VA 22161

NTIS price codes  
Printed copy: A07  
Microfiche copy: A01

PRELIMINARY EVALUATION OF THE EXPLORATORY SHAFT REPRESENTATIVENESS  
FOR THE YUCCA MOUNTAIN PROJECT

F. B. Nimick, L. E. Shephard, and T. E. Blejwas  
Geotechnical Projects Division  
Sandia National Laboratories  
Albuquerque, NM 87185

ABSTRACT

Experiments planned in the Exploratory Shaft (ES) play an integral role in the site characterization effort to provide the necessary information for evaluating the Yucca Mountain site as a potential high-level waste repository. An important part of the planning process for the ES is to evaluate the representativeness of the data and information to be obtained in the ES relative to the remainder of the area and environs. This evaluation is based on evolving interpretations of a limited suite of data, many of which were obtained adjacent to or outside the designated boundaries of the primary area.

The representativeness of information scheduled to be obtained in the ES has been evaluated for a number of technical disciplines including geology, mineralogy, rock mechanics, hydrology, waste package and repository design, and performance assessment. The representativeness in some areas is considered in greater detail than in other areas because of the disparity in the amount of data available and the level of confidence in the data analysis and interpretation. Results of this evaluation indicate that most data obtained in the ES are expected to be representative of the primary area at Yucca Mountain. The conclusion also is drawn that the selected location of the ES is at least as good as any other single location within the primary area.

This report was prepared  
for a QA Level III Task.  
The data used was all  
either NQ or QA III.

## CONTENTS

<u>Section</u>	<u>Page</u>
1.0 Introduction .....	1
2.0 Approach to Evaluation of the Representativeness of the ESF ...	5
3.0 Physical Considerations .....	9
3.1 Surface Location of ES-1 .....	9
3.2 Design of the ESF .....	9
4.0 Geological Characteristics .....	15
4.1 Strata of the Proposed Waste-Emplacement Unit and Above ..	15
4.2 Strata Between the Proposed Waste-Emplacement Horizon and the Water Table .....	22
4.2.1 Unit TSw3 .....	22
4.2.2 Unit CHn1 .....	27
4.2.3 Unit CHn2 .....	30
4.2.4 Unit CHn3 .....	30
4.3 Abundances of Lithophysal Cavities and Vapor-Phase- Altered Material Within the Welded, Devitrified Topopah Spring Member .....	35
4.3.1 Lithophysal Cavities .....	35
4.3.2 Vapor-Phase Altered Material .....	40
5.0 Mineralogical Characteristics .....	43
5.1 Distribution of SiO <sub>2</sub> Phases Within the Welded, Devitrified Portion of the Topopah Spring Member .....	43
5.1.1 Tridymite .....	43
5.1.2 Cristobalite .....	46
5.2 Fracture Mineralogy .....	50
5.3 Clay Content of the Welded, Devitrified Portion of the Topopah Spring Member .....	52
5.4 Sorptive Mineralogy Between the Proposed Waste- Emplacement Unit and the Water Table .....	56
5.4.1 Clinoptilolite .....	56
5.4.2 Mordenite .....	58
5.4.3 Smectite Clay .....	62
5.4.4 Glass .....	62
6.0 Rock Mechanics Characteristics .....	67
6.1 In Situ Stress State at the ES-1 Location .....	67

CONTENTS  
(Continued)

<u>Section</u>	<u>Page</u>
6.1.1 Vertical Stress .....	67
6.1.2 Horizontal Stresses.....	72
6.2 Physical Properties of the Welded, Devitrified Portion of the Topopah Spring Member .....	72
6.2.1 Grain Density .....	72
6.2.2 Matrix Porosity .....	73
6.3 Mechanical Properties of the Welded, Devitrified Portion of the Topopah Spring Member .....	76
6.3.1 Poisson's Ratio .....	76
6.3.2 Unconfined Compressive Strength .....	80
6.3.3 Young's Modulus .....	83
6.3.4 Mohr-Coulomb Parameters .....	83
6.3.5 Tensile Strength .....	86
6.4 Thermal Properties of the Welded, Devitrified Portion of the Topopah Spring Member .....	86
6.4.1 Thermal Conductivity .....	86
6.4.2 Heat Capacity .....	87
6.5 Thermal Expansion Behavior of the Welded, Devitrified Portion of the Topopah Spring Member .....	89
6.6 Fracture Characteristics of the Welded, Devitrified Portion of the Topopah Spring Member .....	90
7.0 Hydrologic Characteristics .....	93
7.1 Unit TSw1 .....	94
7.2 Unit TSw2 .....	94
7.3 Unit TSw3 .....	94
7.4 Unit CHnv .....	94
7.5 Unit CHnz .....	98
8.0 Waste Package Environment .....	101
8.1 Natural and Perturbed Physical Environment .....	101
8.2 Natural and Perturbed Chemical Environment .....	101
9.0 Repository-Design Parameters .....	105
9.1 Variations in the Depth of the ESF .....	105
9.2 Excavation Techniques, Orientations, and Sizes of the Underground Openings in the ESF .....	107
9.3 Ground Support Systems in the ESF .....	108
9.4 Construction-Related Conditions in the ESF .....	110
9.5 Effects of Potential Vibratory Ground Motion .....	110
9.6 Ventilation Requirements in the ESF .....	111

**CONTENTS**  
**(Concluded)**

<u>Section</u>	<u>Page</u>
10.0 Performance-Assessment Parameters .....	113
11.0 Conclusions .....	115
12.0 References .....	119
Appendix A: Revision of Input Data for the TSw1 - TSw2 Contact ....	123
Appendix B: Thermal Conductivity Data .....	125
Appendix C: Information From, and Candidate Information For, the Reference Information Base .....	127
Appendix D: Information From, and Candidate Information For, the Site and Engineering Property Data Base .....	129

TABLES

<u>Table</u>		<u>Page</u>
3.2-1	Summary of Elevations and Depths for the Breakouts Planned in ES-1 .....	12
3.2-2	Characteristics, Properties, and Features for Which Representativeness is Assessed .....	13
4.3-1	Comparison of Range in Abundance of Vapor-Phase Altered Material in the Depth Intervals Corresponding With the Upper Breakout and Main Test Level and in Wider Depth Intervals Bounding These Levels .....	40
9.3-1	Recommended Ground Support Requirements for the Expected Rock Conditions Within the ESF .....	109
11.0-1	Summary of Representativeness Evaluation for Each of the Technical Areas Considered .....	116

## FIGURES

<u>Figure</u>	<u>Page</u>
1.0-1 Location of the Exploratory Shaft (ES-1) Within the Present Boundary of the Underground Facilities .....	3
3.2-1 Schematic Cross Section of the Current Design for the Exploratory Shaft .....	10
3.2-2 Schematic Plan View of the Main Test Level in the Exploratory Shaft .....	11
4.1-1 Isopach Map of Unit TCw .....	17
4.1-2 Histogram of Thicknesses for Unit TCw .....	18
4.1-3 Isopach Map of Unit PTn .....	19
4.1-4 Histogram of Thicknesses for Unit PTn .....	20
4.1-5 Isopach Map of Unit TSw1 .....	21
4.1-6 Histogram of Thicknesses for Unit TSw1 .....	23
4.1-7 Isopach Map of Unit TSw2 .....	24
4.1-8 Histogram of Thicknesses for Unit TSw2 .....	25
4.2-1 Isopach Map of Unit TSw3 .....	26
4.2-2 Isopach Map of Unit CHn1 Above the Water Table .....	28
4.2-3 Histogram of Thicknesses of Unit CHn1 Above the Water Table .	29
4.2-4 Isopach Map of Unit CHn2 Above the Water Table .....	31
4.2-5 Histogram of Thicknesses of Unit CHn2 Above the Water Table .	32
4.2-6 Isopach Map of Unit CHn3 Above the Water Table .....	33
4.2-7 Histogram of Thicknesses of Unit CHn3 Above the Water Table .	34
4.3-1 Abundance of Lithophysal Cavities in the Welded, Devitrified Topopah Spring Member as a Function of Depth in USW G-4 .....	36
4.3-2 Comparison of Abundances of Lithophysal Cavities in the Upper Lithophysal Zone of the Topopah Spring Member .....	38
4.3-3 Comparison of Abundances of Lithophysal Cavities in the Zone Equivalent to the Main Test Level in the ES .....	39
4.3-4 Abundance of Vapor-Phase-Altered Material in the Welded, Devitrified Topopah Spring Member as a Function of Depth in USW G-4 .....	41

FIGURES  
(Continued)

<u>Figure</u>		<u>Page</u>
5.1-1	Abundance of Tridymite in the Welded, Devitrified Topopah Spring Member as a Function of Depth in USW G-4 ...	44
5.1-2	Comparison of Abundances of Tridymite in the Upper Lithophysal Zone of the Topopah Spring Member .....	45
5.1-3	Comparison of Abundances of Tridymite in the Zone Equivalent to the Main Test Level in the ES .....	47
5.1-4	Abundance of Cristobalite in the Welded, Devitrified Topopah Spring Member as a Function of Depth in USW G-4 ...	48
5.1-5	Comparison of Abundances of Cristobalite in the Upper Lithophysal Zone of the Topopah Spring Member .....	49
5.1-6	Comparison of Abundances of Cristobalite in the Zone Equivalent to the Main Test Level in the ES .....	51
5.3-1	Abundance of Clay in the Welded, Devitrified Topopah Spring Member as a Function of Depth in USW G-4 .....	53
5.3-2	Comparison of Abundances of Clay in the Welded, Devitrified Topopah Spring Member .....	54
5.4-1	Comparison of Cumulative Contents of Clinoptilolite Between the Base of Unit TSw2 and the Water Table .....	57
5.4-2	Comparison of Expected Ranges in Cumulative Content of Clinoptilolite .....	59
5.4-3	Comparison of Cumulative Contents of Mordenite Between the Base of Unit TSw2 and the Water Table .....	60
5.4-4	Comparison of Expected Ranges in Cumulative Content of Mordenite .....	61
5.4-5	Comparison of Cumulative Contents of Clay Between the Base of Unit TSw2 and the Water Table .....	63
5.4-6	Comparison of Expected Ranges in Cumulative Content of Clay .....	64
5.4-7	Comparison of Cumulative Contents of Glass Between the Base of Unit TSw2 and the Water Table .....	65
5.4-8	Comparison of Expected Ranges in Cumulative Content of Glass .....	66
6.1-1	Estimated Vertical Stresses at the Base of Unit TSw1 .....	69

**FIGURES  
(Concluded)**

<u>Figure</u>		<u>Page</u>
6.1-2	Estimated Vertical Stresses at the Floor of the Design Subsurface Facilities .....	70
6.1-3	Estimated Vertical Stresses at the Base of Unit TSw2 .....	71
6.2-1	Comparison of Ranges of Grain Density for Unit TSw2 .....	74
6.2-2	Comparison of Ranges of Grain Density for Unit TSw1 .....	75
6.2-3	Comparison of Ranges of Matrix Porosity for Unit TSw2 ....	77
6.2-4	Comparison of Ranges of Matrix Porosity for Unit TSw1 ....	78
6.3-1	Comparison of Ranges of Poisson's Ratio for Unit TSw2 ....	79
6.3-2	Comparison of Ranges of Unconfined Compressive Strength for Unit TSw1 .....	81
6.3-3	Comparison of Ranges of Unconfined Compressive Strength for Unit TSw2 .....	82
6.3-4	Comparison of Ranges of Young's Modulus for Unit TSw1 ....	84
6.3-5	Comparison of Ranges of Young's Modulus for Unit TSw2 ....	85
6.4-1	Comparison of Ranges of Thermal Conductivity for Units TSw1 and TSw2 .....	88
7.1-1	Comparison of Matrix Sample Travel Times for Unit TSw1 ...	95
7.2-1	Comparison of Matrix Sample Travel Times for Unit TSw2 ...	96
7.3-1	Comparison of Matrix Sample Travel Times for Unit CHnv ...	97
7.5-1	Comparison of Matrix Sample Travel Times for Unit CHnz ...	99
9.1-1	Thickness of the Overburden Overlying the Proposed Waste-Emplacement Horizon and the ESF .....	106

## ACKNOWLEDGMENTS

The authors would like to acknowledge the assistance of Bruce Whittet, Bob Williams, and Sam Dengler, without whom the information and figures related to unit thicknesses could not have been developed. Ralph Peters, Brenda Langkopf, and Bob Stinebaugh all provided useful technical comments during review of the document.

This document has greatly benefited from the input provided by several principal investigators working on the Yucca Mountain Project, including Dave Vaniman, Dave Broxton, and Paul Aamodt (LANL), Jim Neal and Hugh MacDougall (SNL), and Dean Eppler, Ernie Hardin, Bill Sublette, Dick Morissette, and Dwayne Chesnut (SAIC). The conclusions relative to representativeness that have been drawn in this document, however, are the full responsibility of the authors.

## 1.0 INTRODUCTION

The Nuclear Waste Policy Act of 1982 assigned the responsibility for siting, designing, constructing, and operating geological repositories for spent nuclear fuel and high-level waste to the Department of Energy (DOE). The Act describes the procedural methods, requirements, and schedules to be followed by the DOE when selecting, characterizing, and licensing sites; developing repositories; and complying with environmental and quality assurance regulations. Guidelines summarizing the technical requirements and criteria for siting geological repositories have been summarized and implemented by the DOE. These guidelines were used in the area-to-location screening process that resulted in the selection of Yucca Mountain as a candidate site.

One element of the site characterization process is the excavation of an exploratory shaft for use in making in situ measurements and observations within the repository block at Yucca Mountain. These measurements and observations are required to fulfill many of the information needs identified under the key technical issues (U.S. Department of Energy, 1986) requiring resolution. The location of the exploratory shaft at Yucca Mountain was selected based on scientific, engineering, environmental, and nontechnical criteria that were used for evaluating surface and subsurface characteristics (Bertram, 1984). The location of the shaft was intended to (1) permit the exploration of specific stratigraphic horizons within the primary area; (2) allow access to both saturated and unsaturated stratigraphic horizons, if necessary, for confirmation of expected favorable conditions and to assess potentially adverse conditions; (3) to avoid potentially adverse conditions during shaft siting but to permit access to these areas from the shaft; and (4) to minimize the environmental impact of the shaft construction on the surrounding area (Bertram, 1984). Utilizing these criteria and guidelines, the location of the Yucca Mountain Project (YMP)

Exploratory Shaft (ES-1\*) was selected on the eastern side of Yucca Mountain in Coyote Wash near the mouth of Drill Hole Wash (Nevada Coordinates 766000N, 563300E). Subsequent evaluation has resulted in a small change of the location to 766255N, 563630E. Figure 1.0-1 shows the locations of ES-1 relative to existing deep core holes at Yucca Mountain and relative to the repository block as a whole.

A desirable attribute of site-characterization data collected from the ES is that a large portion of the data be representative of the entire primary area. This report presents a preliminary assessment of the representativeness of the data to be obtained from the ES, and is intended to contribute to the YMP position on the representativeness of the ES location.

We recognize that the ES alone cannot provide all of the necessary site characterization data, and thus in a sense can never be completely representative. The discussion that comprises the remainder of this document is presented with the understanding that we are analyzing representativeness only to the degree to which a single exploratory shaft (and associated underground openings) can be representative.

The design of the ESF has been, and is, evolving toward the final version to be followed during construction and operation. As a result, some of the description of the design as used in this document may have been changed in more recent versions of the design. Because of the evolving nature of the design, no attempt has been made to keep the analyses in this document completely current. The reader is cautioned to keep this fact in mind when text addressing "the correct design" is encountered.

---

\*In this report, the Exploratory Shaft Facility (ESF) includes all shafts, the lateral exploration drifts, and any facilities located on the surface and underground that support the experimental program. Two shafts are planned as part of the ESF; discussion in this document is focused specifically on shaft ES-1.

● USW G-2

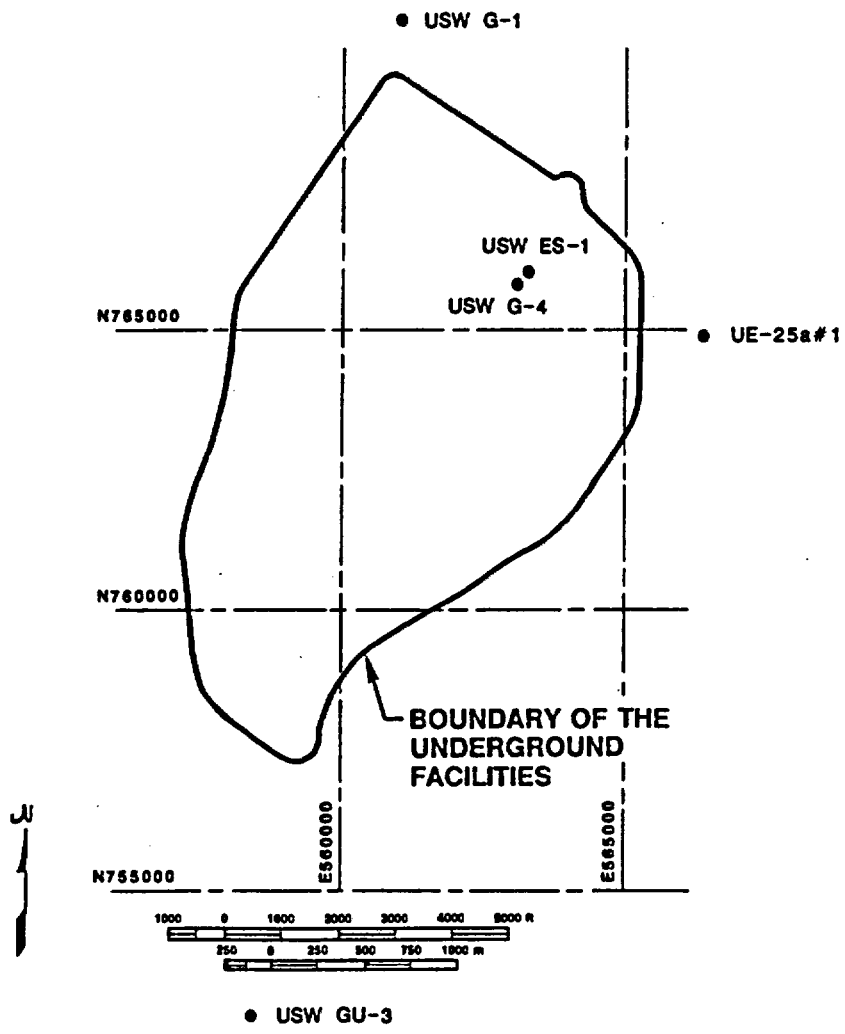


Figure 1.0-1. Location of the Exploratory Shaft (ES-1) Within the Present Boundary of the Underground Facilities

## 2.0 APPROACH TO EVALUATION OF THE REPRESENTATIVENESS OF THE ESF

One of the questions raised during the discussions about the ESF between the DOE, the Nuclear Regulatory Commission (NRC) and the State of Nevada is the following:

Will it be possible to show that the measurements in the ESF are representative of conditions and processes throughout the underground portion of the repository?

This question of representativeness has been raised frequently about the ESF, but a working definition of representativeness has not been established. In fact, the usual connotation of representative (being a typical or characteristic example) does not apply to measurements in a situation where material properties are expected to show spatial variability, variability resulting from material heterogeneity, or both.

Within the context of property variability, several alternative working definitions of a representative value or values can be considered:

- a value close to a presently observed mean value;
- a set of values spanning a large portion of the existing range of values;
- a value anywhere within the existing range of values;
- any value that is not anomalous.

The last two of these alternatives are similar, although the last one can be construed to exclude values that have been observed previously but are uncommon.

For properties or characteristics for which sufficient data are available, the second definition of "representative" given above is preferable, and is used in this document whenever appropriate. For a number of characteristics for which representativeness needs to be assessed, existing data are extremely limited. Consequently, decisions about representativeness cannot be made using working definitions that rely on knowledge of mean values or ranges. In addition, determination of representativeness for some categories (e.g., waste package environment, ground support systems) does not allow use of quantitative measures.

In view of the potential limitations mentioned in the preceding paragraph, assessment of representativeness in this document often uses the last alternative working definition presented previously. Thus, a property, characteristic, or design feature is considered to be representative if it is not anomalous relative to available information.

"Anomalous" is used in several ways in this document. For data that are approximately normally distributed, an anomalous value is arbitrarily defined to be a value that is more than two standard deviations from the mean value. For data that have non-normal distributions, an anomalous value is defined to be a value that is located outside the portion of the distribution occupied by 95 percent of the existing values. Finally, if a parameter is characterized by discrete values (e.g., (1) vitric or zeolitized; (2) drifts are or are not a certain size, etc.), then a value would be anomalous only if it were not one of the (expected) possible choices.

It is recognized that one of the criteria used in the original selection of the ES location was the allowance for exploration of abnormal structural features if necessary. For example, existing plans call for lateral drifting from the main underground test facility to several faults near ES-1. Inclusion of these faults in a discussion of representativeness changes the flavor of "representative" from being non-anomalous to the idea of point-sampling of a range of conditions. Such changes in connotation are discussed for specific properties or features in later sections of this document.

Before continuing with analysis of representativeness for specific topics, it should be emphasized that the original selection process for the ES location ensured that potential waste-emplacment horizons as well as nearby structural features could be explored. At this time, there is no reason to expect that the properties and characteristics at the selected location will be any less representative than those that would be found at any other specific location within the primary area.

### 3.0 PHYSICAL CONSIDERATIONS

In order to assess representativeness, the physical setting must be defined. Such a definition includes the location and design of the ESF together with the stratigraphic units (and characteristics thereof) expected to be encountered underground.

#### 3.1 Surface Location of ES-1

As stated earlier, the surface location originally selected for the exploratory shaft was 766000N, 563300E. Several concerns, including possible erosion of alluvium and possible flooding, have led to a relocation of the collar of ES-1 to 766255N, 563630E, a move of approximately 420 ft (128 m). In the new location, the collar will be situated in bedrock.

#### 3.2 Design of the ESF

The current design of the ESF is shown in Figures 3.2-1 and 3.2-2. Also shown in Figure 3.2-1 are the stratigraphic units that will be penetrated by the underground openings. Figure 3.2-2 includes the drifts to be driven to intersect the structural features that will be investigated according to current plans.

Previous versions of the ESF design called for breakouts from the shaft at three depths: 520 ft (158 m), 1020 ft (311 m), and 1400 ft (427 m). With the change in surface location, these depths have changed. In the remainder of this document, the "upper demonstration breakout room" refers to the breakout in the lithophysae rich portion (upper lithophysal zone) of the Topopah Spring Member, the "main test level" refers to the breakout in which most in situ testing will occur, and the "Calico Hills drill room" refers to the breakout for exploration of the upper part of the rhyolite of Calico Hills. Estimated elevations and depths for the breakouts for the current ES-1 location are summarized in Table 3.2-1.

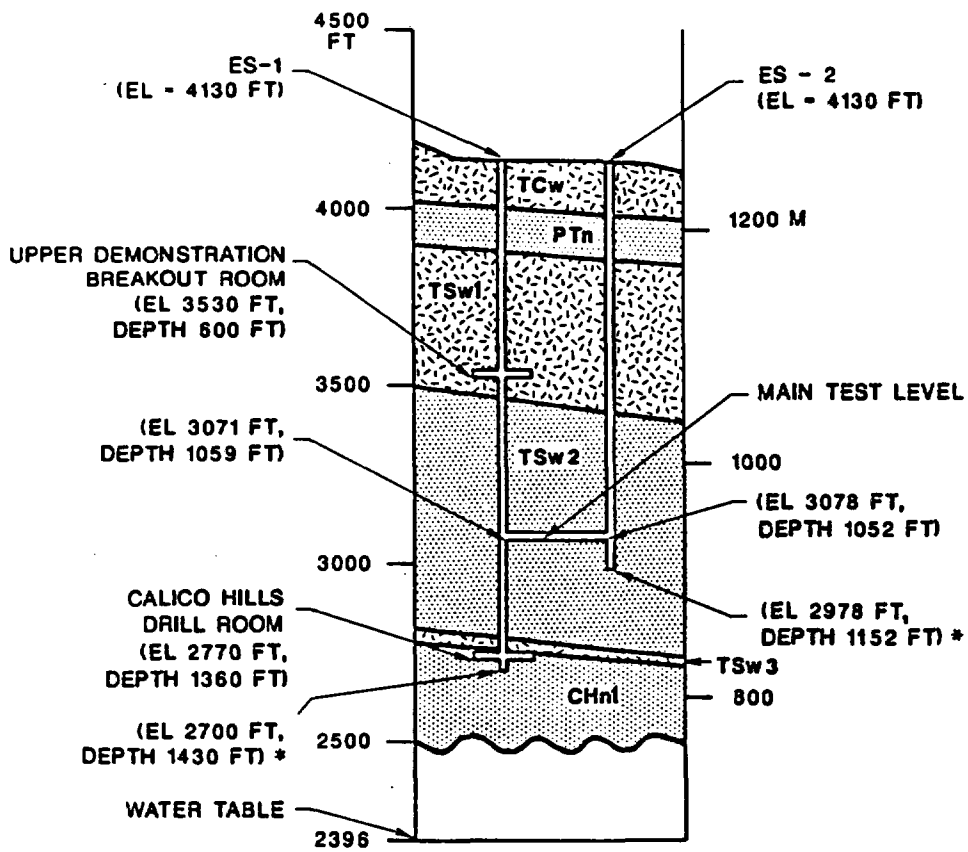


Figure 3.2-1. Schematic Cross Section of the Current Design for the Exploratory Shaft. Elevations given for openings are for the floors of the openings.

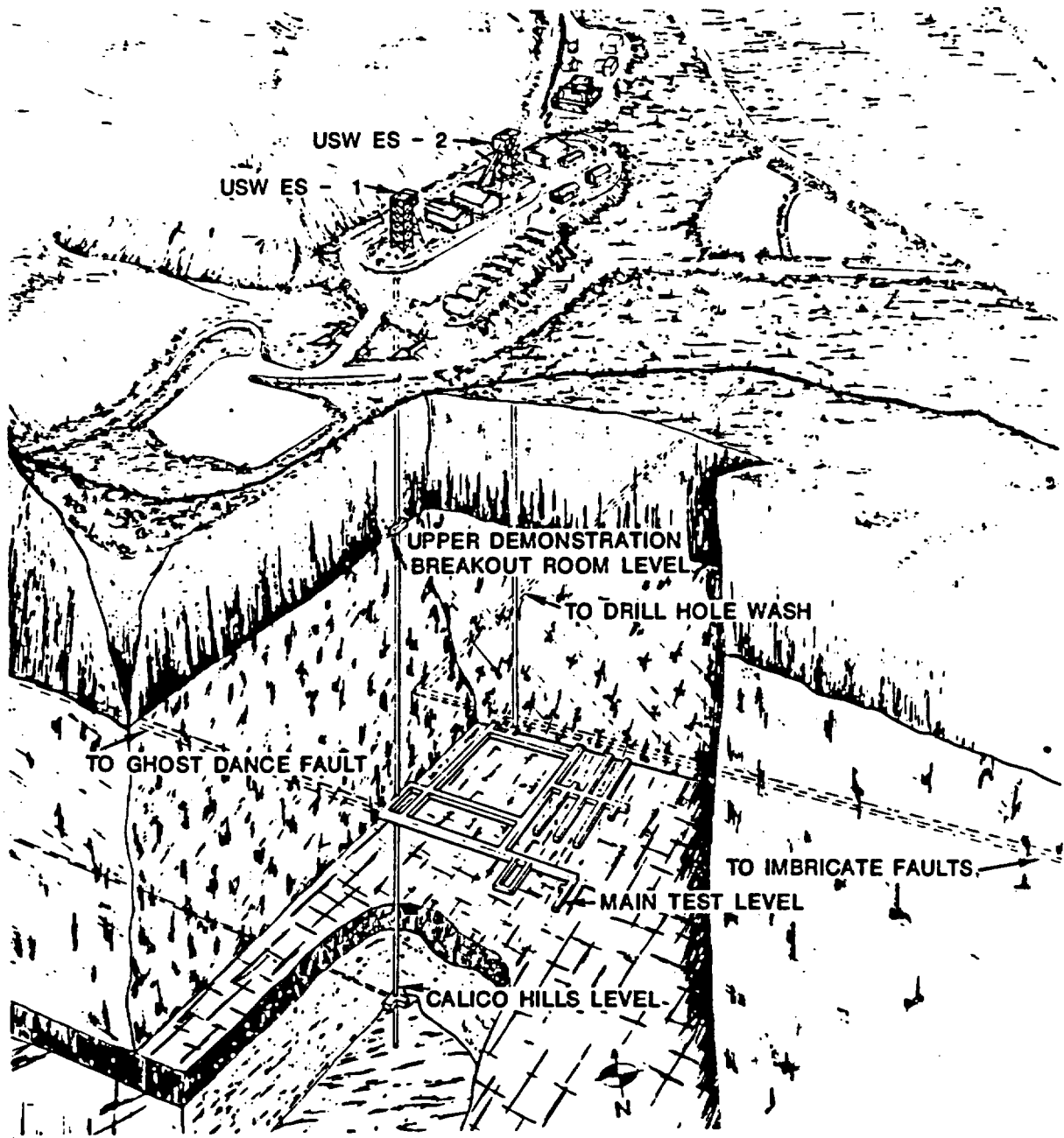


Figure 3.2-2. Schematic View of the Main Test Level in the Exploratory Shaft

Table 3.2-1. Summary of Elevations and Depths for the Breakouts Planned in ES-1

<u>Breakout Level</u>	<u>Elevation [ft(m)]</u>	<u>Depth [ft(m)]</u>
Upper Demonstration Breakout Room	3530 (1076)	600 (183)
Main Test Level	~3076 (~938)	~1054 (~321)
Calico Hills Drill Room	2770 (844)	1360 (415)
Shaft Bottom	2700 (823)*	1430 (436)*

\*Estimate only; may be revised as design develops.

Table 3.2-2 lists the characteristics, properties, and design features that are discussed in the remainder of the document. A few of the items listed, especially design features, may change before actual construction of the ES. Any conclusions about representativeness of such items also may change.

The list provided in Table 3.2-2 is not intended to be exhaustive. Rather, the intent has been to evaluate a sufficient number of parameters to provide a determination of representativeness. Because representativeness is a subjective, nonscientific quality, others might emphasize different parameters. We expect that most readers will find sufficient parameters in Table 3.2-2 to be able to draw conclusions similar to those of the authors.

In general, data to be used in evaluations of representativeness are available only from one or more of the five deep core holes at Yucca Mountain (UE-25a#1, USW G-1, USW G-2, USW GU-3, and USW G-4) (Figure 1.0-1). Of these, USW G-4 is the core hole closest to the ES-1 location; the data available from USW G-4 serve as the basis for properties and characteristics expected in the ESF for much of this report. This is not intended to imply that properties of material from the ESF will be the same as those from USW G-4. Rather, the comparison allows an evaluation of whether the properties from the ESF also are expected to be similar.

Table 3.2-2. Characteristics, Properties, and Features for Which Representativeness is Assessed

---

**Geology**

Strata - Proposed Waste Emplacement Unit and Above  
Strata - Below Proposed Waste-Emplacement Unit to Water Table  
Lithophysal Cavities and Vapor-Phase-Altered Material

**Mineralogy**

Distribution of SiO<sub>2</sub> Phases  
Fracture Mineralogy  
Clay Content  
Volume of Sorptive Minerals

**Rock Mechanics**

In Situ Stress (Vertical)  
Grain Density  
Matrix Porosity  
Young's Modulus  
Poisson's Ratio  
Unconfined Compressive Strength  
Mohr-Coulomb Parameters  
Tensile Strength  
Thermal Conductivity  
Heat Capacity  
Thermal Expansion Behavior  
Fracture Characteristics

**Waste Package**

Ambient and Perturbed Physical Environment  
Ambient and Perturbed Chemical Environment

**Repository Design**

Depth of ESF  
Opening Sizes and Orientations  
Excavation Techniques  
Ground Support Systems  
Construction-Related Impacts  
Weapons-Induced Seismicity  
Ventilation

**Performance Assessment**

Age of Groundwater  
Hydrologic Properties of Units Between Proposed Waste-Emplacement Unit and Accessible Environment  
Solubility of Radionuclides in Groundwater

---

Of the five deep core holes, only USW G-4 lies within the primary area (Figure 1.0-1). However, evaluations have been performed using data from the other four core holes in order to evaluate in a preliminary fashion the potential spatial variability of properties and characteristics.

We recognize that some data that are of potential use in an evaluation of representativeness (e.g., geophysical logs) have not been included in the discussion in this document. Our intent has not been to perform an exhaustive analysis of data. Rather, we have concentrated on readily available and interpretable data. Our analyses well may have been enhanced by use of additional information, but the additional interpretation required to convert the information to an easily manageable form was never intended to be part of this effort. However, we do not expect that use of the additional data would change the conclusion stated at the end of Section 2.0 that the selected location for the ES should be as representative as any other specific location within the primary area.

## 4.0 GEOLOGICAL CHARACTERISTICS

Sections 4.1 and 4.2 address the thickness of a number of thermal/mechanical units. The thicknesses have been calculated using three dimensional representations of the unit contacts. These representations were generated using the modeling technique described by Nimick and Williams (1984) and implemented by Ortiz et al. (1985). Contouring of the isopachs utilized a 250-ft-by-250-ft (76-m-by-76-m) grid and interpolation thereon. Histograms of thicknesses were generated using data for all grid points lying within the boundary of the underground facilities.

### 4.1 Strata of the Proposed Waste-Emplacement Unit and Above

The ESF will be excavated through strata that will vary in lithology, fracture density, and other properties. As a result, the requirements for shaft lining, the potential for inflow of perched water, and the rate at which mining can proceed will vary.

The strata to be excavated at the location of ES-1 are expected to be similar to those found in USW G-4: (1) a portion of the welded Tiva Canyon Member (TCw\*); (2) a nonwelded portion of the Paintbrush Tuff (PTn); (3) the welded, devitrified portion of the Topopah Spring Member [TSw1 (the upper, relatively lithophysae-rich portion) and TSw2 (the lower, relatively lithophysae-poor portion that is the proposed waste-emplacement horizon)]; and (4) the basal vitrophyre of the Topopah Spring Member (TSw3). The ES also will penetrate into the lower portion of the

---

\*Note: Designators in parentheses represent thermal/mechanical units as described by Ortiz et al. (1985). Subdivision of the strata into thermal/mechanical units rather than formal stratigraphic units provides a more reasonable framework for discussion of representativeness of properties in later sections of this report. The remainder of this section is based on the results of three-dimensional modeling summarized in Ortiz et al. (1985) except for units TSw1 and TSw2. For these two units, the input data have been revised as discussed in Appendix A. In this report, the revision applies only to the thickness data; property data for TSw1 and TSw2 have been compiled (Nimick and Schwartz, 1987) based on the previous definition of the units.

Topopah Spring Member and the upper part of the rhyolite of Calico Hills (thermal/mechanical unit CHn1). These strata are discussed in Section 4.2.

Unit TCw is expected to be represented by approximately 156 ft (47 m) of rock at the ES-1 location. By comparison, this unit has a thickness range of 0 to 522 ft (0 to 159 m) within the boundary of the underground facilities (Figure 4.1-1), with thicknesses greater than 100 ft (30 m) over most of the area. ES-1, located on the northeastern side of the primary area, will sample a relatively thin portion of unit TCw, but will not be anomalous with respect to the range of thicknesses (Figure 4.1-2).

Unit PTn ranges in thickness from 0 to 202 ft (0 to 62 m) within the boundary of the underground facilities (Figure 4.1-3). At the ES-1 location, the expected thickness of approximately 124 ft (38 m) is similar to the mean thickness for unit PTn (Figure 4.1-4). Thicknesses less than 100 ft (30 m) are confined to the southeastern side and western edge of the area. Thicknesses greater than 150 ft (46 m) are found only toward the northern boundary.

Unit PTn is a collection of nonwelded ash-flow tuffs and bedded tuffs. The ash-flow tuffs are distal portions of Members of the Paintbrush Tuff, and as such might be expected to be less welded and to have higher porosity at greater distances from the source area to the north and west. However, the area for the underground facilities is located sufficiently far from the source area that all ash flows of PTn in the area for the underground facilities are nonwelded and should be relatively homogeneous. In addition, the thinning to zero thickness near the western boundary of the area is the result of present topography rather than depositional thinning.

The thickness of unit TSw1 has been estimated to range from 82 to 483 ft (25 to 147 m) within the boundary of the underground facilities (Figure 4.1-5). It is thinnest along the western boundary, with a continuous gradual increase in thickness to the north and east. The thickness at the ES-1 location is estimated to be 413 ft (126 m). This

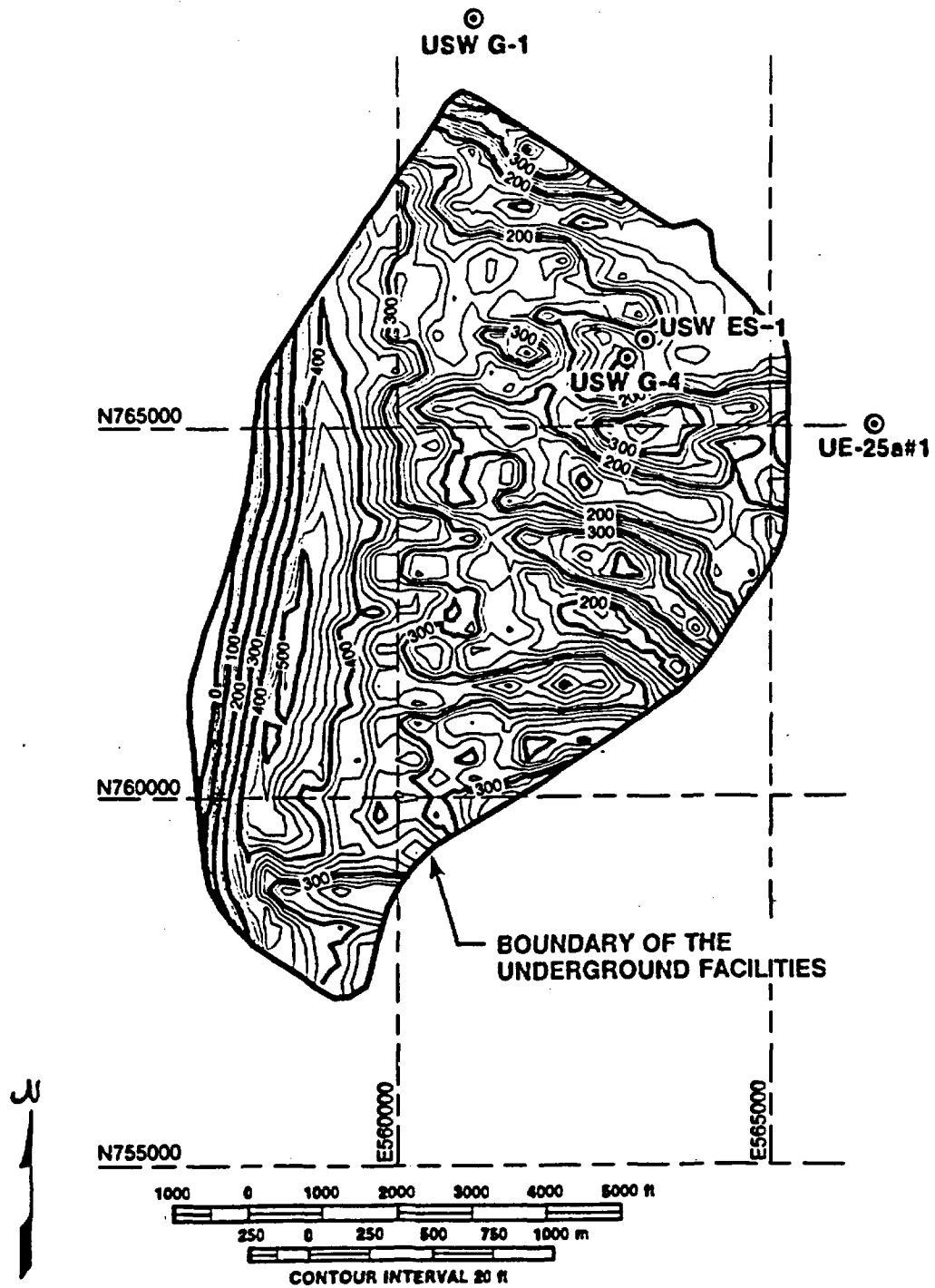


Figure 4.1-1. Isopach Map of Unit TCw. Thickness calculated using the three-dimensional modeling technique discussed in Ortiz et al. (1985).

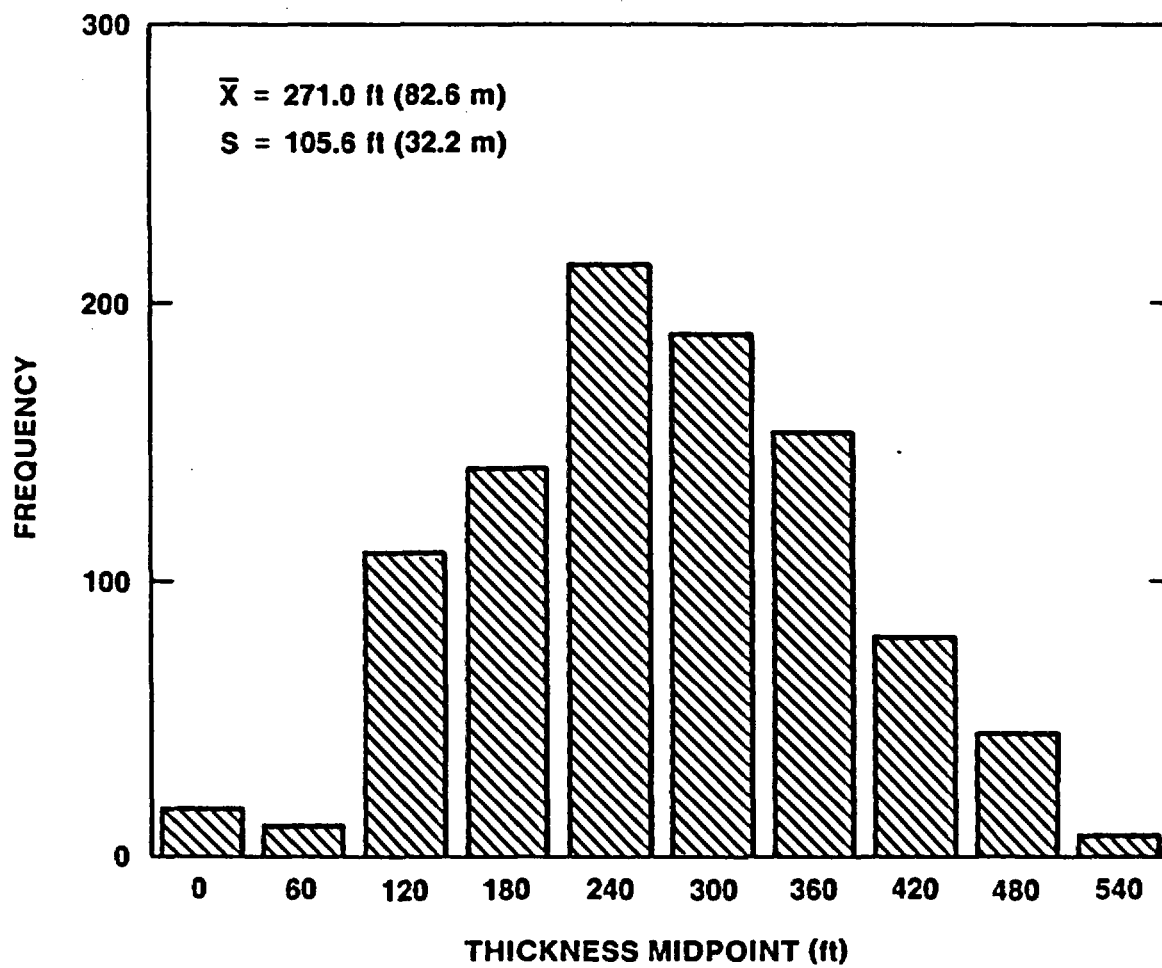


Figure 4.1-2. Histogram of Thicknesses for Unit TCw

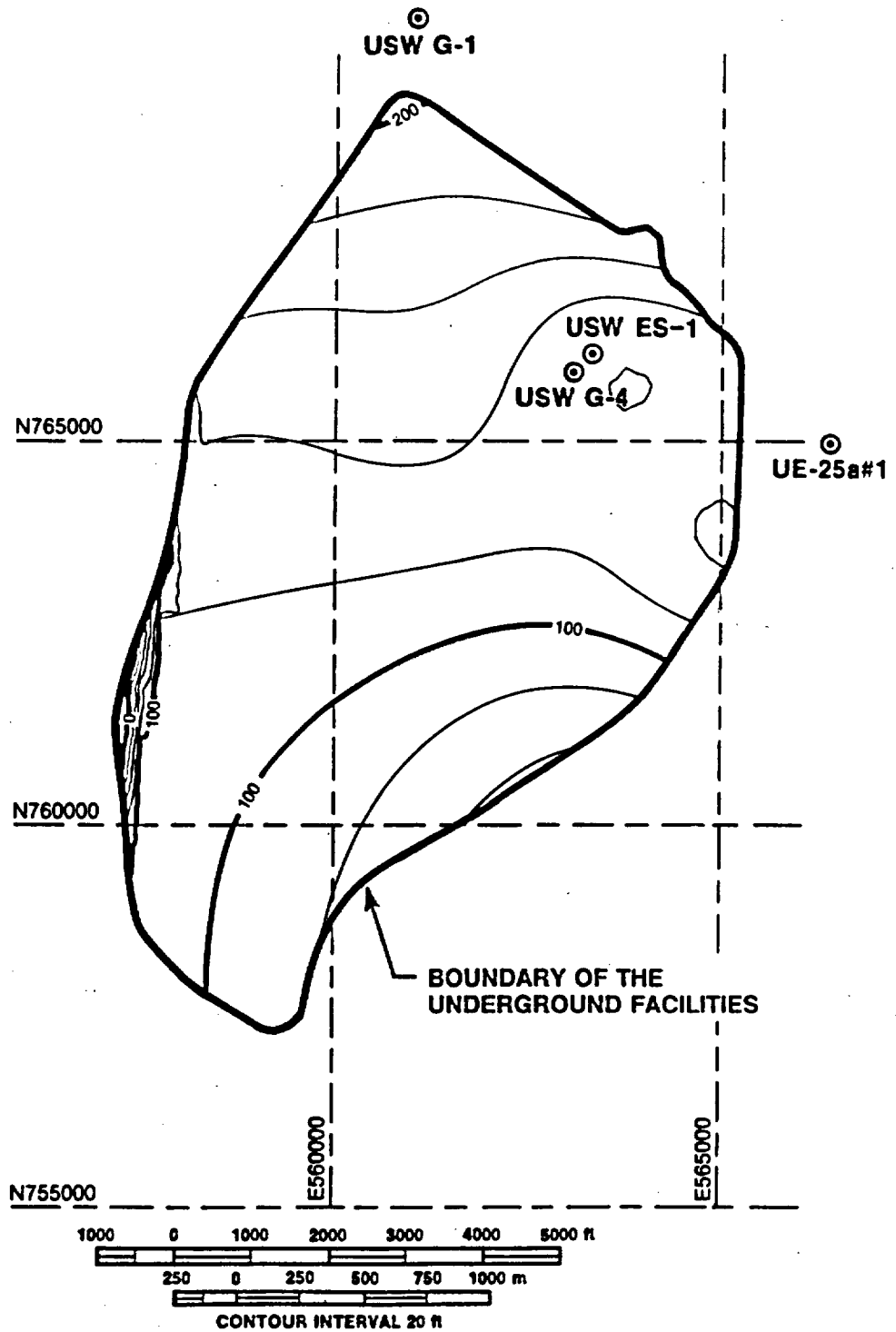


Figure 4.1-3. Isopach Map of Unit PTn. Thickness calculated using the three-dimensional modeling technique discussed in Ortiz et al. (1985).

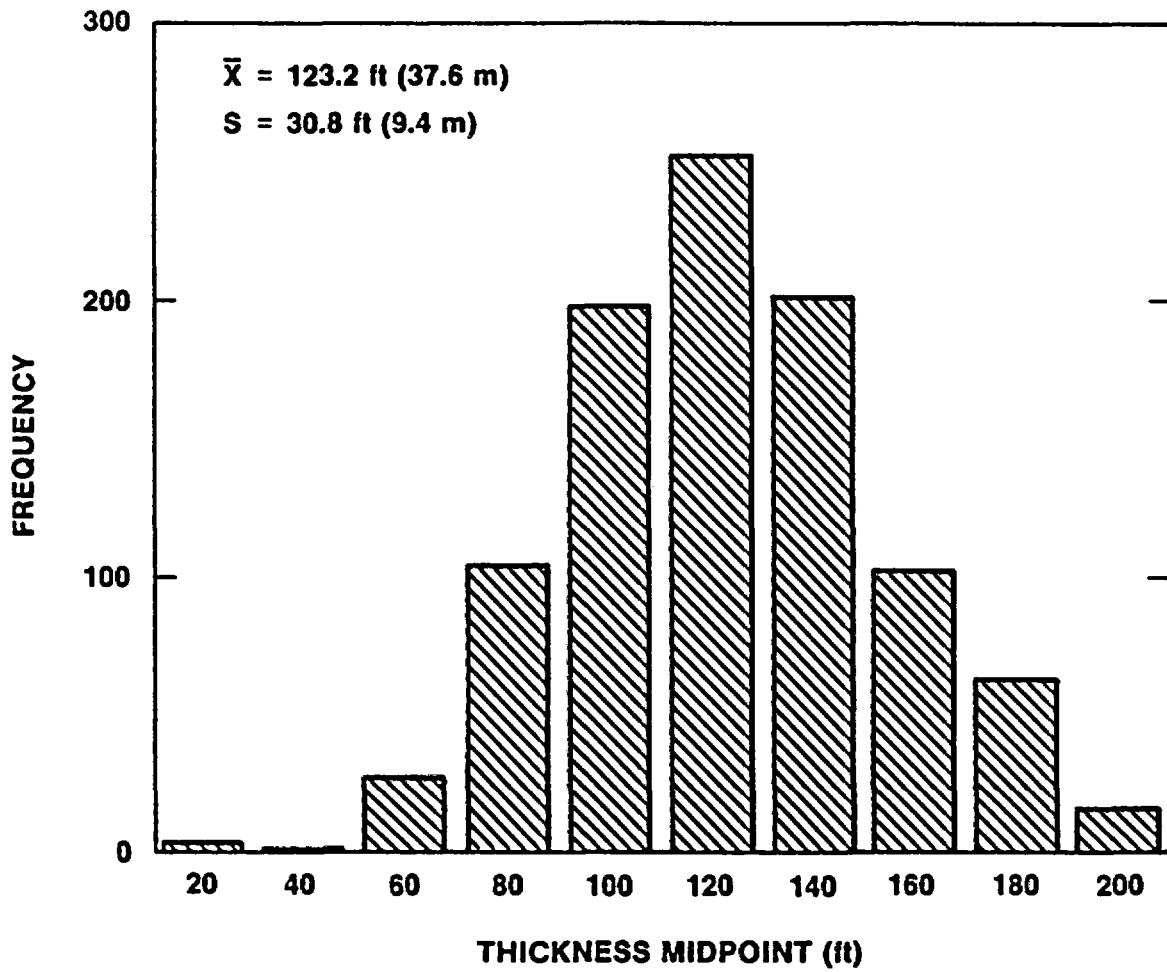


Figure 4.1-4. Histogram of Thicknesses for Unit PTn

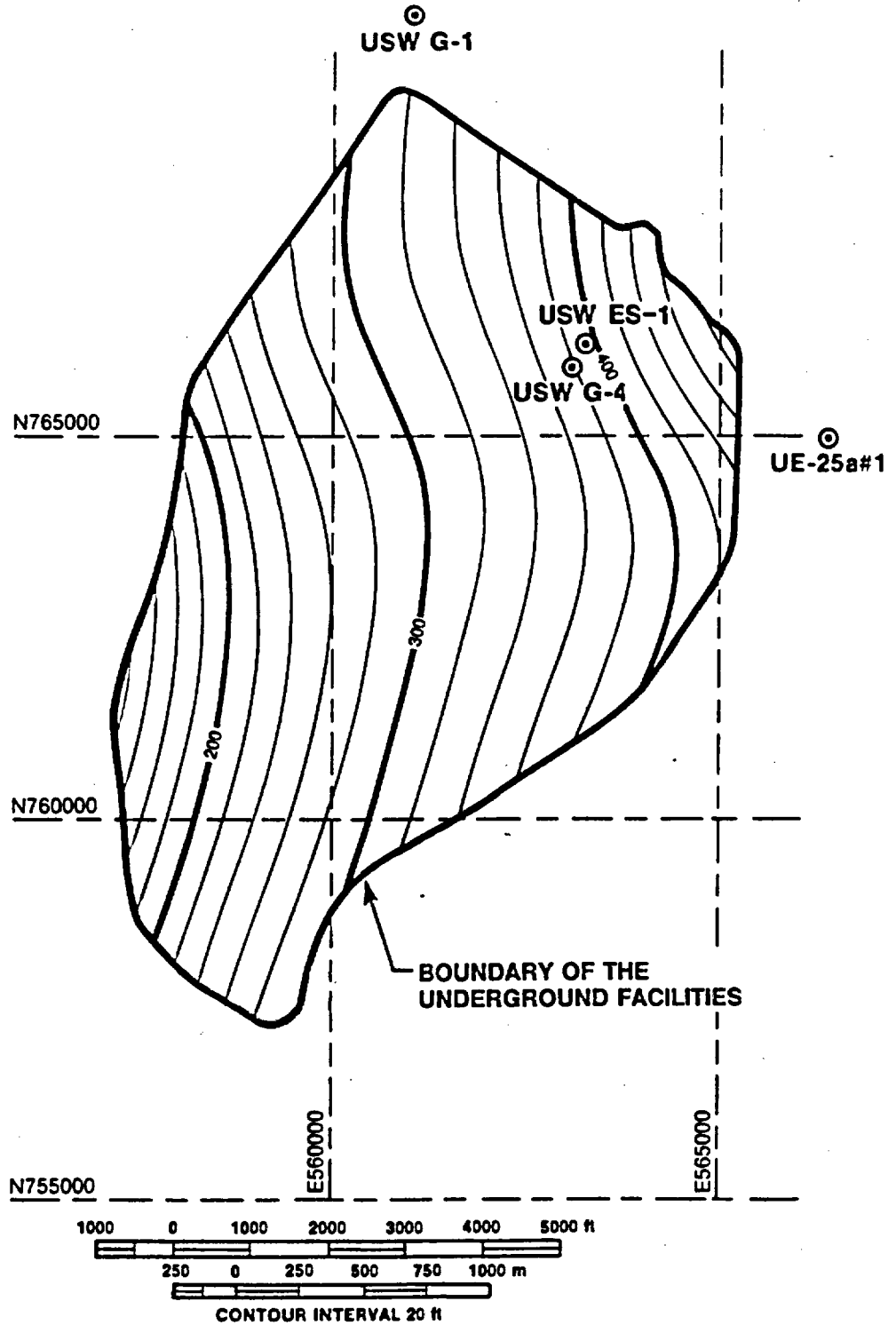


Figure 4.1-5. Isopach Map of Unit TSw1. Thickness calculated using the three-dimensional modeling technique discussed in Ortiz et al. (1985).

thickness is at the high end of the range for unit TSw1 (Figure 4.1-6), but is representative in the sense of being nonanomalous.

Unit TSw2, which includes the target waste emplacement horizon, is estimated to be 672 ft (205 m) thick at the ES-1 location. This compares with the range of 482 to 802 ft (147 to 244 m) within the boundary of the underground facilities (Figure 4.1-7). In contrast to unit TSw1, the thinnest portion of unit TSw2 is at the southern tip of the area for the underground facilities, with increasing thickness to the north and west. The thickness at the ES-1 location is close to the mean thickness for the unit (Figure 4.1-8) and is considered to be representative.

#### 4.2 Strata Between the Proposed Waste Emplacement Horizon and the Water Table

The strata below the proposed waste emplacement horizon are important in that water-borne radionuclides will generally travel downward through the underlying units to reach the accessible environment. The thicknesses of these underlying strata are one of the characteristics that play a role in the calculation of groundwater and radionuclide travel times (for a discussion of the sorptive mineralogy in this material, see Section 5.4). The depth to the water table at the ES-1 location is expected to be approximately 1734 ft (529 m). The strata that occur at USW G-4 between the proposed waste emplacement horizon and the water table include (1) the welded, vitric (vitrophyre) portion of the Topopah Spring Member (unit TSw3); and (2) a sequence of ash-flow tuffs and bedded tuffs that form the rhyolite of Calico Hills (unit CHn1). In addition, the basal portion of the rhyolite of Calico Hills (unit CHn2) and the uppermost portion of the ash-flow tuffs of the Prow Pass Member of the Crater Flat Tuff (unit CHn3) occur above the water table in parts of the area for the underground facilities and are discussed in this section.

##### 4.2.1 Unit TSw3

Figure 4.2-1 shows an isopach map of the estimated thickness for unit TSw3. The zero-thickness contours are believed to be an artifact of the estimation technique. Actual thicknesses are expected to be nonzero in

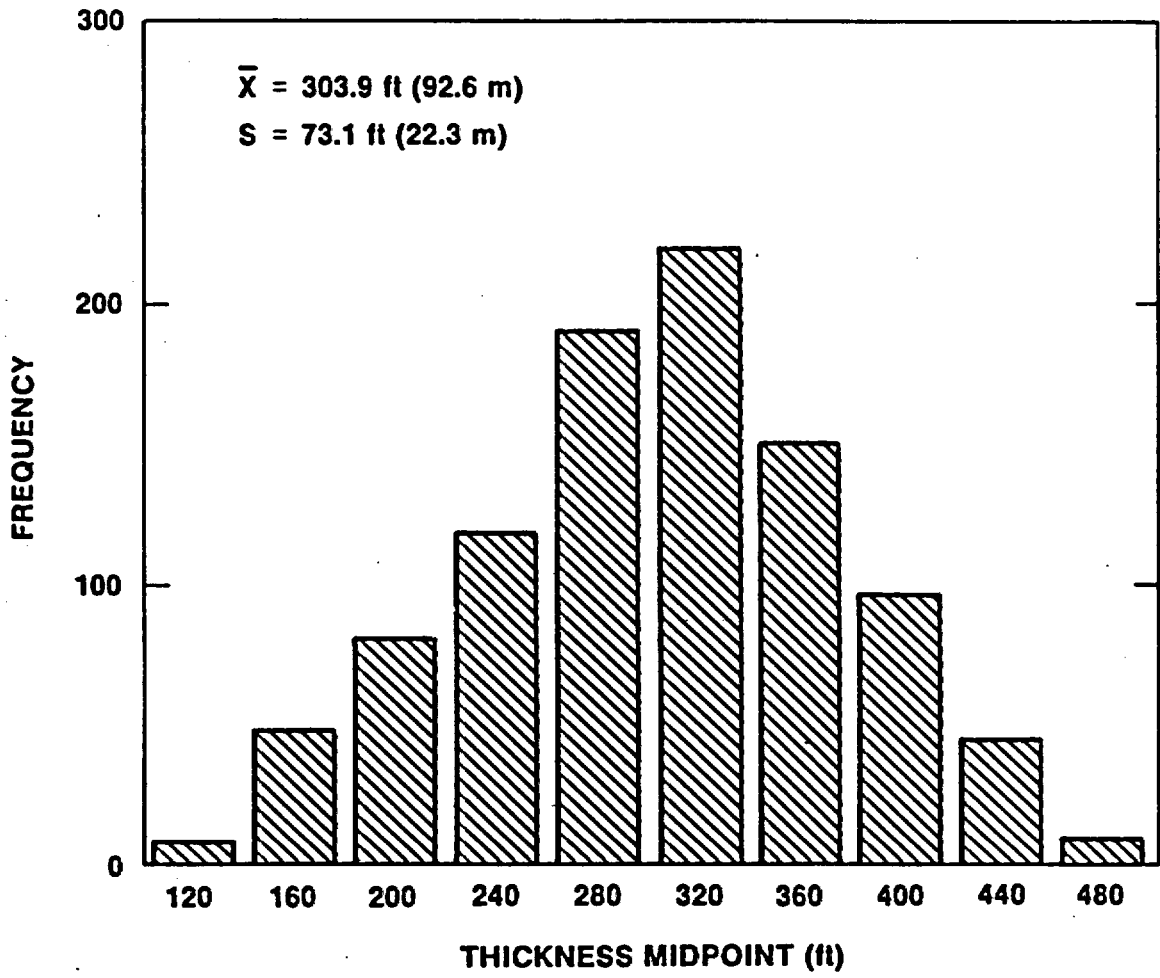


Figure 4.1-6. Histogram of Thicknesses for Unit TSwl

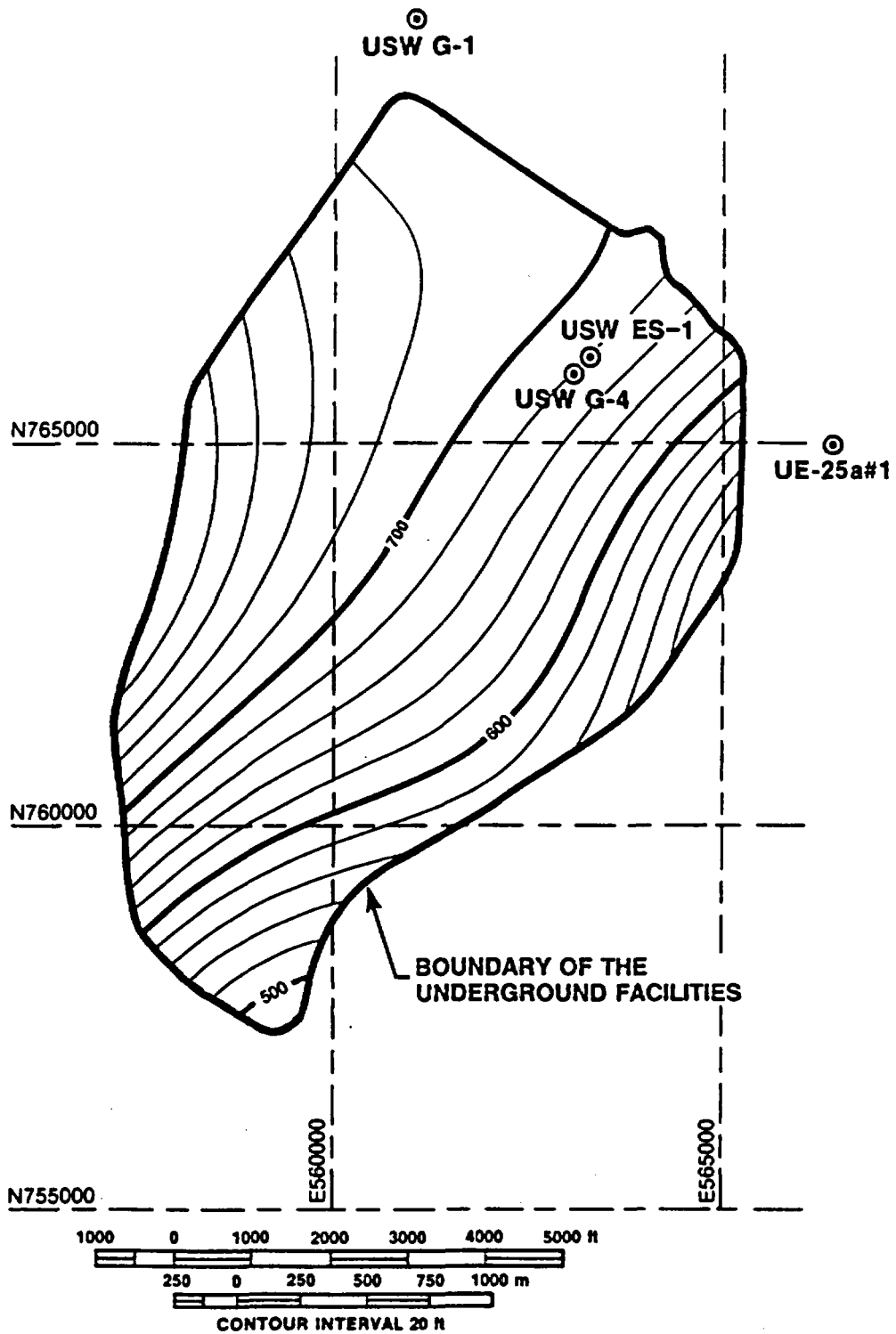


Figure 4.1-7. Isopach Map of Unit TSw2. Thickness calculated using the three-dimensional modeling technique discussed in Ortiz et al. (1985).

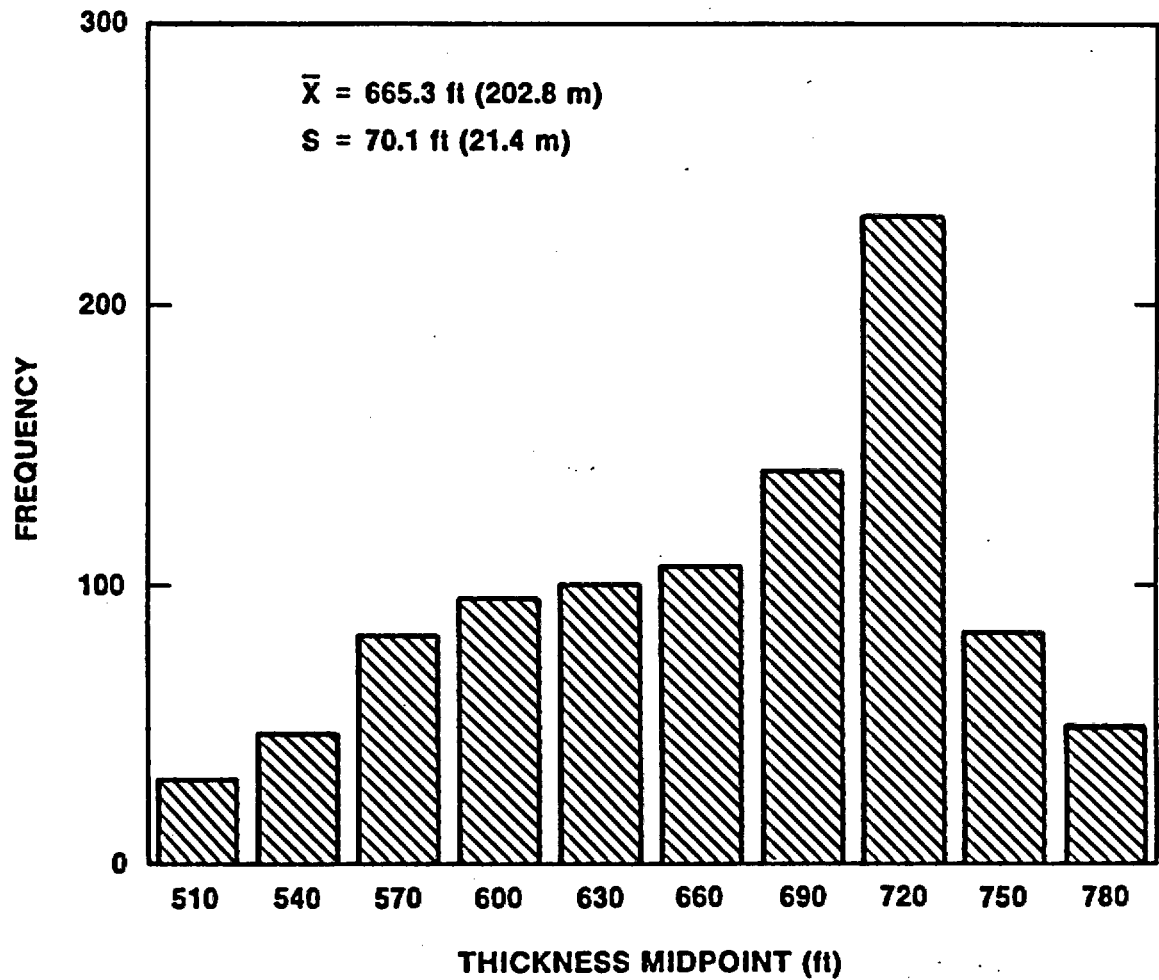


Figure 4.1-8. Histogram of Thicknesses of Unit TSw2. Note that distribution is non-normal, so that statistical parameters must be used with caution.

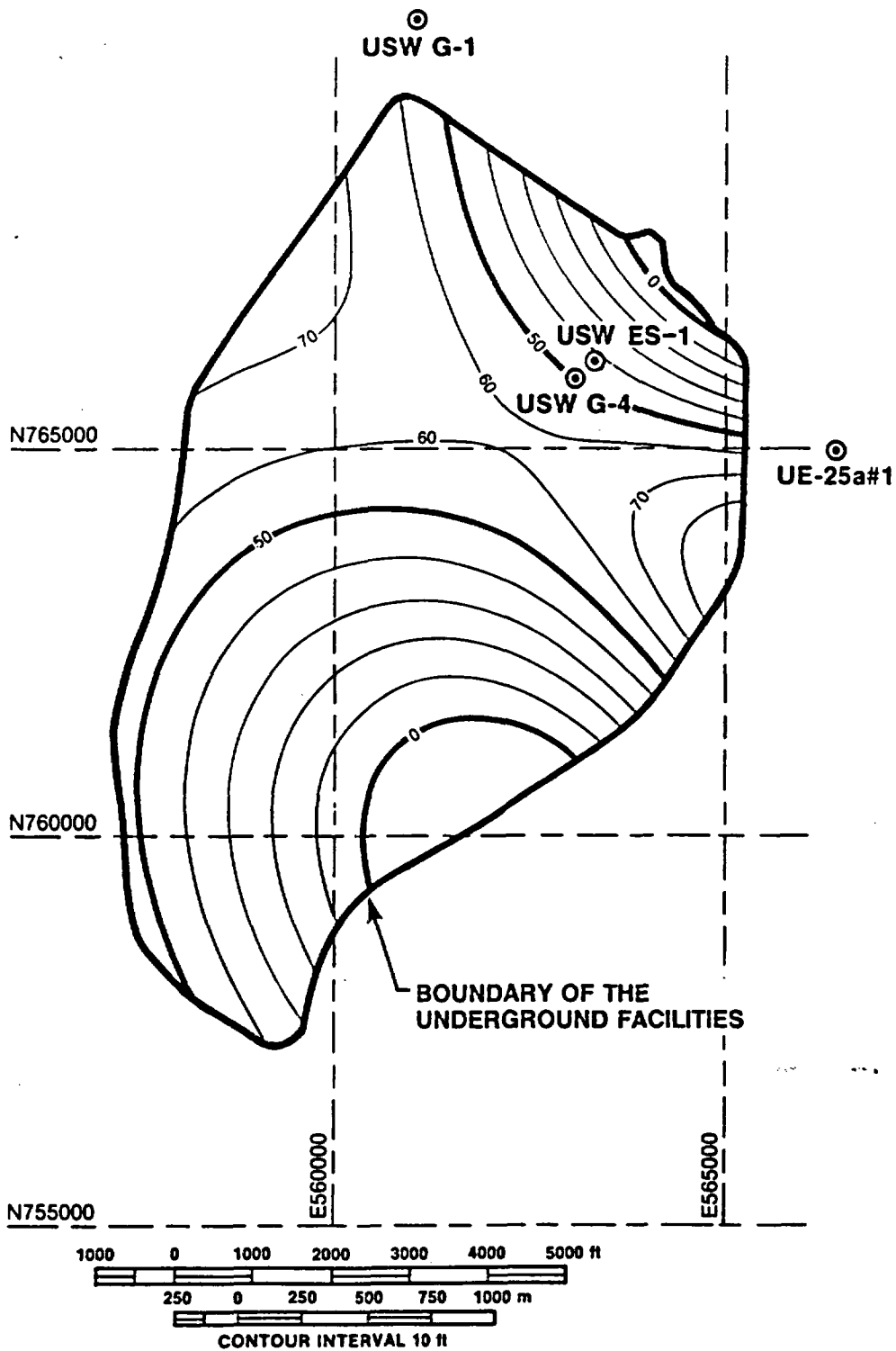


Figure 4.2-1. Isopach Map of Unit TSw3. Thickness calculated using the three-dimensional modeling technique discussed by Ortiz et al. (1985).

the affected regions. In addition, much of the thickness variation shown in Figure 4.2-1 is believed to be incorrect, based on the range of actual thicknesses observed in core holes within or close to the area for the underground facilities [52 ft (16 m) to 82 ft (25 m)]. The thickness of unit TSw3 in USW G-4 is the lowest value in these core holes, with 55 ft (17-m) thicknesses in USW G-1 and UE-25a#1. The thickness of unit TSw3 at the ES-1 location, although unquantified, is expected to be representative of the northern portion of the area for the underground facilities because of the uniformity of thicknesses in the three core holes in the region. The thickness will not be representative of the southern part of the area for the underground facilities.

#### 4.2.2 Unit CHn1

All material between the base of unit TSw3 and the top of the lowermost bedded unit of the rhyolite of Calico Hills is included in unit CHn1. Figure 4.2-2 is an isopach map of the thickness of the unit that occurs above the water table. The thickness above the water table at the ES-1 location is estimated to be 358 ft (109 m), which is at the high end of the expected range of thicknesses (Figure 4.2-3).

Also included as a part of Figure 4.2-2 are estimates of the regions of different dominant mineralogies. The region in which CHn1 is dominated by zeolites throughout is confined to the northeastern portion of the area for the underground facilities. Totally nonzeolitized CHn1 occurs in the southern and southwestern portions of the area. In the region shown as "transitional" on Figure 4.2-2, CHn1 is vitric in the upper portion and zeolitized in the lower portion, with the proportions varying through the region.

Unit CHn1 at the ES location will be representative in both thickness and mineralogy in the sense of being nonanomalous. However, the vitric portion of unit CHn1 is estimated to be less than 25 ft (8 m) thick, a thickness that is nearly anomalous in terms of being able to represent the parts of unit CHn1 that are totally vitric.

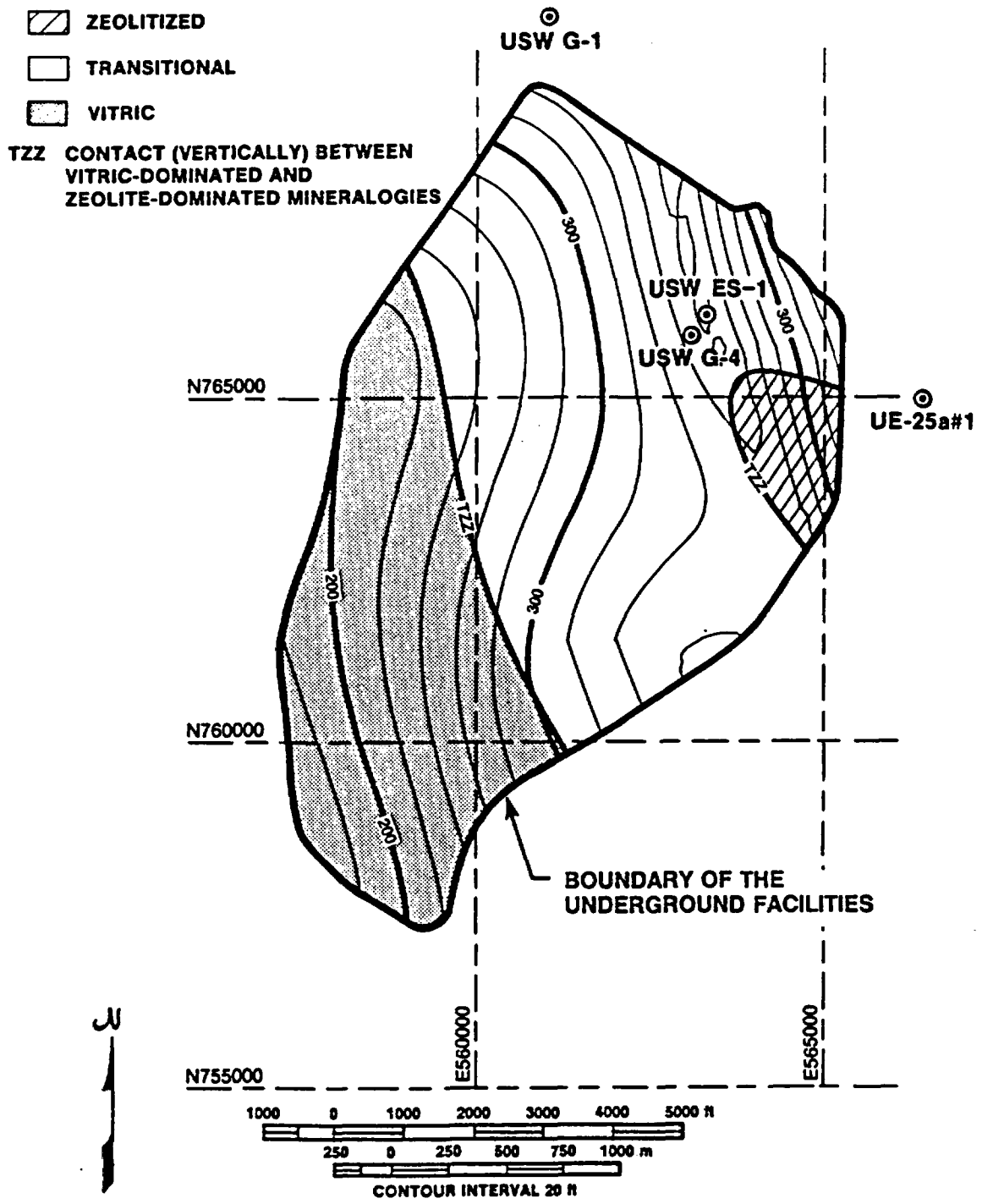


Figure 4.2-2. Isopach Map of Unit CHn1 Above the Water Table. Thickness (and location of TZZ) calculated using the three-dimensional modeling technique discussed by Ortiz et al. (1985).

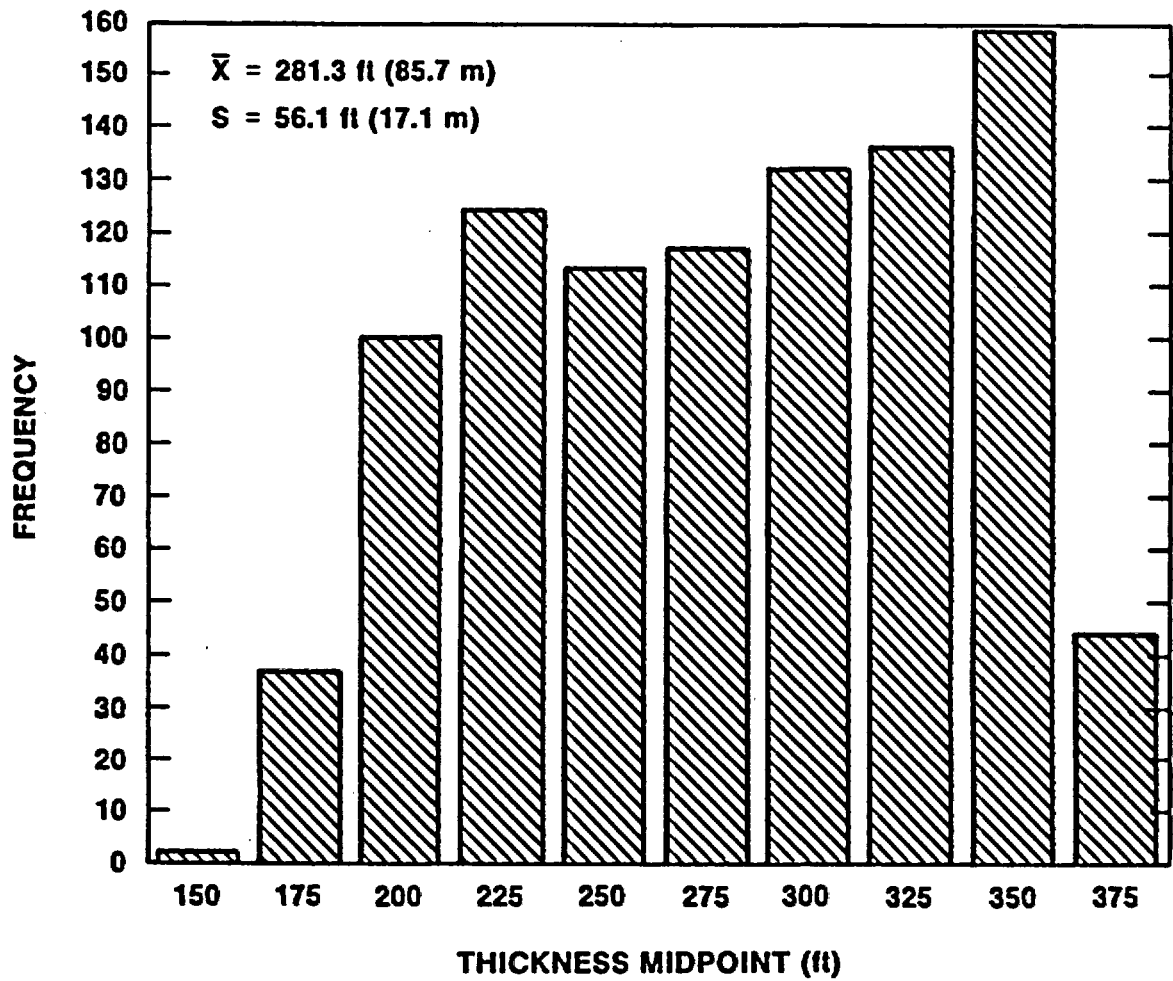


Figure 4.2-3. Histogram of Thicknesses of Unit CHn1 Above the Water Table. Note that distribution is non-normal, so that statistical parameters must be used with caution.

#### 4.2.3 Unit CHn2

The lowermost bedded tuff of the rhyolite of Calico Hills is thermal/mechanical unit CHn2. An isopach map for the thickness of this unit above the water table is shown in Figure 4.2-4. In the northeastern corner of the area for the underground facilities, the water table occurs in or above unit CHn2. The expected thickness of unit CHn2 at the ES-1 location is 40 ft (12 m), which is close to the mean thickness for the unit (Figure 4.2-5).

The ES-1 location is in the portion of the area for the underground facilities in which unit CHn2 is zeolitized (Figure 4.2-4). Although the ES-1 location is not representative of any portions of the unit that are dominantly vitric (i.e., the southern portions of the area for the underground facilities), the location is considered to be representative by virtue of not being anomalous.

#### 4.2.4 Unit CHn3

The upper ash flows of the Prow Pass Member- those that are porous enough to have been zeolitized- comprise thermal/mechanical unit CHn3. The thickness of the unit above the water table is shown in Figure 4.2-6. Unit CHn3 is not above the water table at the ES-1 location; a thickness of zero is significantly lower than the mean value but is definitely not anomalous relative to the remainder of the data (Figure 4.2-7).

As is true for unit CHn2, unit CHn3 at the ES-1 location is dominated by zeolites. Although the unit will not be representative of any of the vitric material that is present in unit CHn3 in the southern and southwestern portions of the area for the underground facilities, the location is considered to be representative by virtue of not being anomalous.

 ZEOLITIZED

 TRANSITIONAL

 VITRIC

TZZ CONTACT (VERTICALLY) BETWEEN  
VITRIC-DOMINATED AND  
ZEOLITE-DOMINATED MINERALOGIES

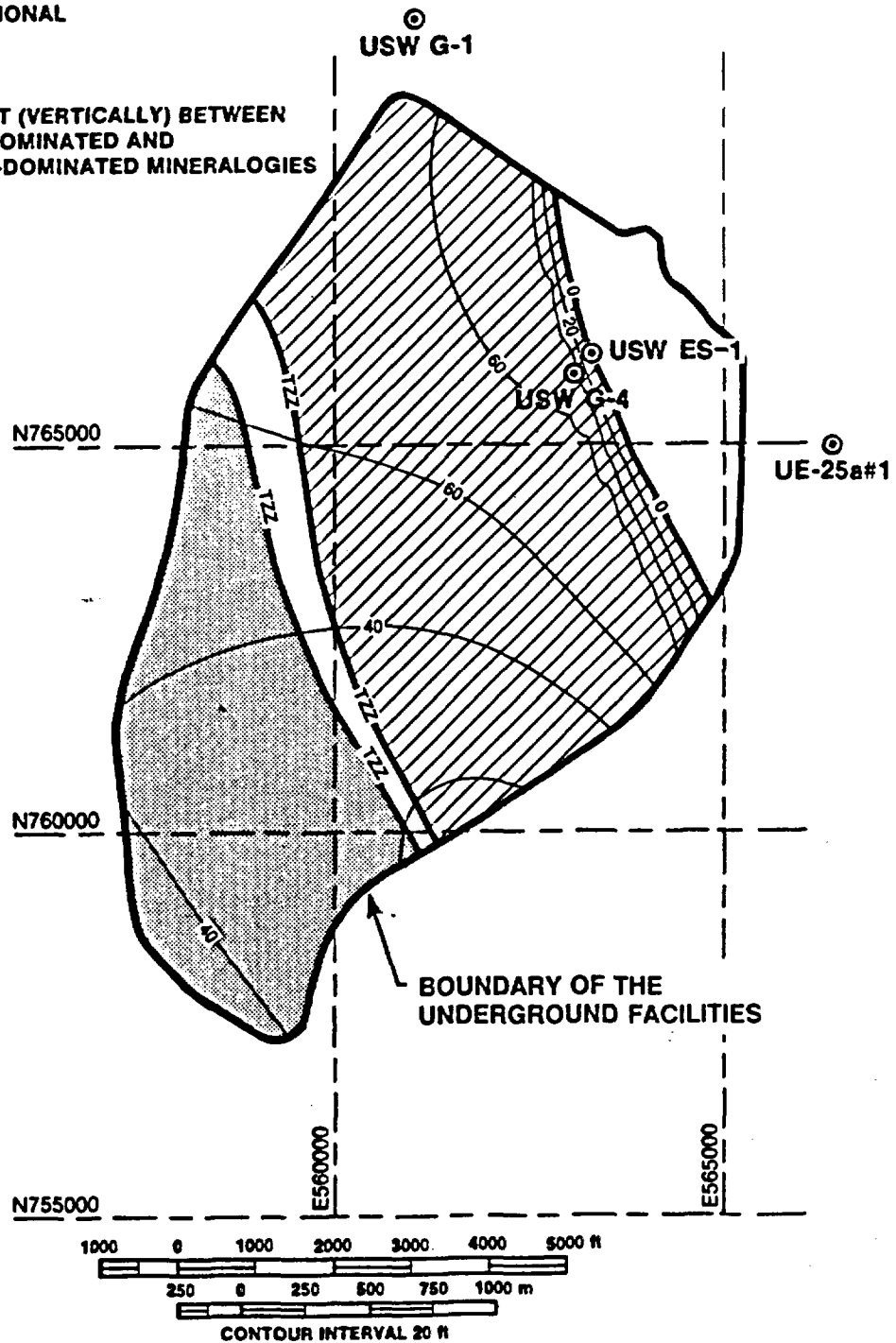


Figure 4.2-4. Isopach Map of Unit CHn2 Above the Water Table. Thickness (and location of TZZ) calculated using the three-dimensional modeling technique discussed by Ortiz et al. (1985).

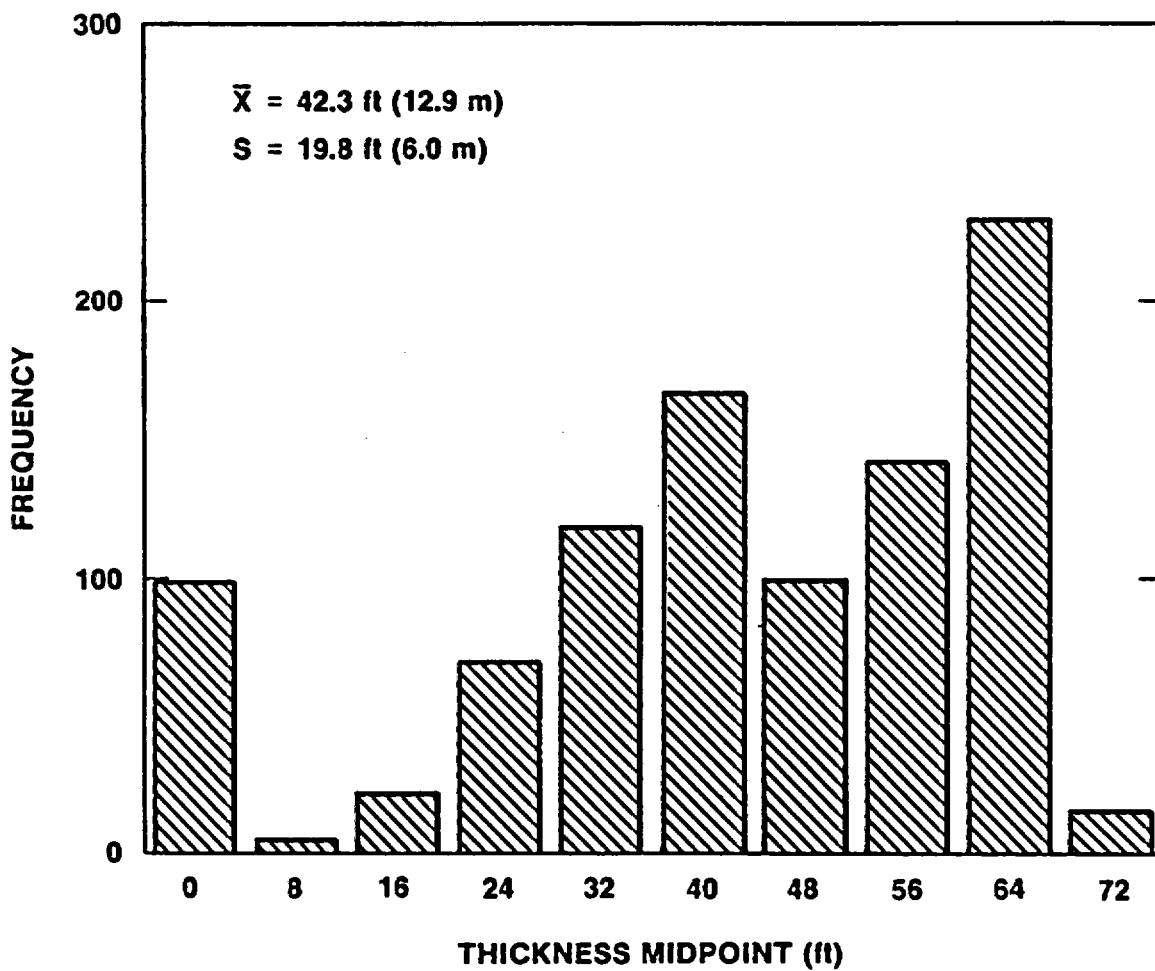


Figure 4.2-5. Histogram of Thicknesses of Unit CHn2 Above the Water Table. Note that distribution is non-normal, so that statistical parameters must be used with caution.

 ZEOLITIZED

 TRANSITIONAL

TZZ CONTACT (VERTICALLY) BETWEEN  
VITRIC-DOMINATED AND  
ZEOLITE-DOMINATED MINERALOGIES

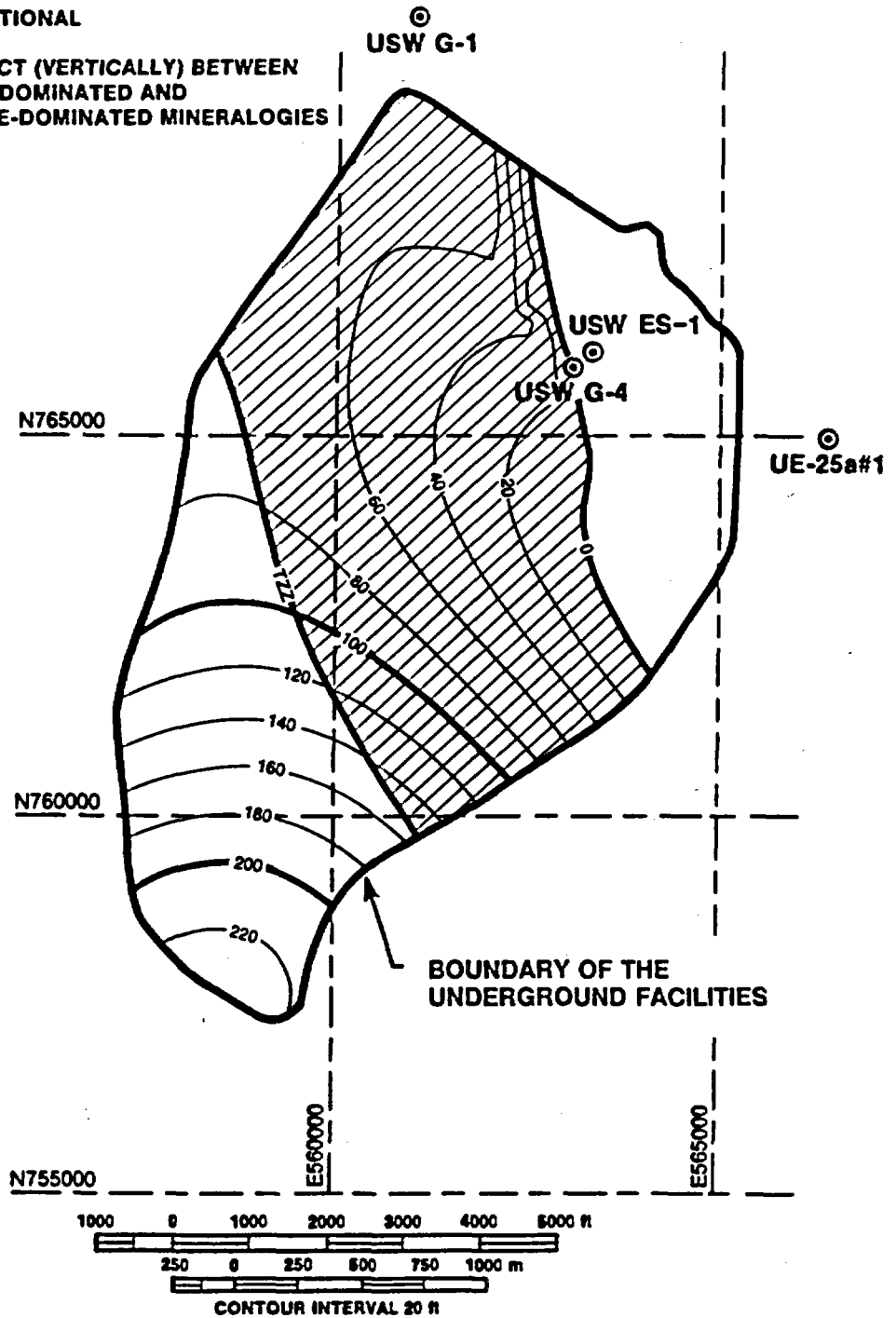


Figure 4.2-6. Isopach Map of Unit CHn3 Above the Water Table. Thickness (and location of TZZ) calculated using the three-dimensional modeling technique discussed by Ortiz et al. (1985).

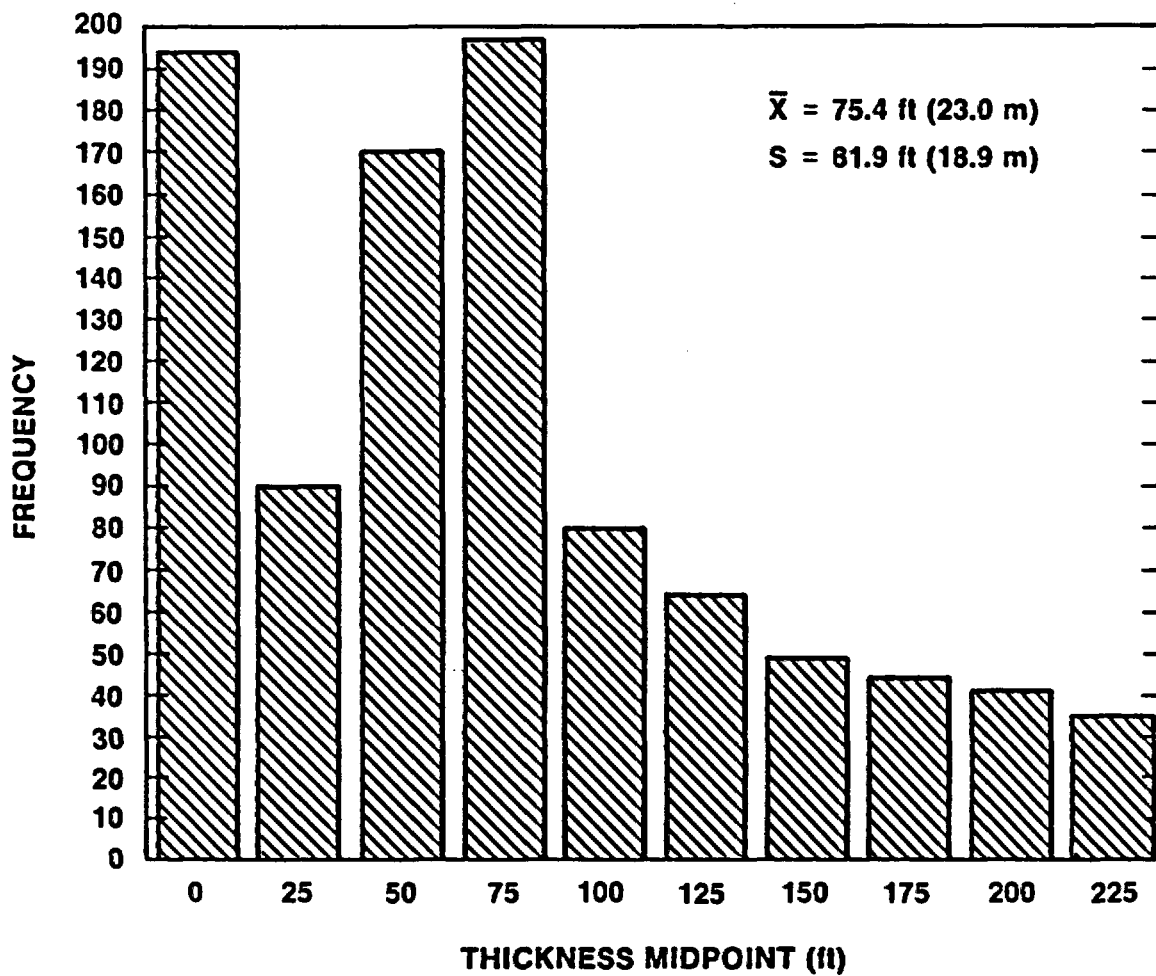


Figure 4.2-7. Histogram of Thicknesses of Unit CHn3 Above the Water Table. Note that distribution is non-normal, so that statistical parameters must be used with caution.

#### 4.3 Abundances of Lithophysal Cavities and Vapor-Phase Altered Material Within the Welded, Devitrified Topopah Spring Member

Lithophysal cavities contribute significantly to the total porosity of certain portions of the welded, devitrified Topopah Spring Member, and in doing so have an effect on material properties such as compressive strength, Young's modulus, thermal conductivity, heat capacity, and bulk density. Vapor-phase altered regions in the tuff [characterized by gray color, generally coarser crystal size, and generally higher porosity (Price et al., 1985)] also increase the total porosity relative to the surrounding matrix, although to a lesser extent than do the lithophysal cavities. Thus, the amounts of lithophysal cavities and vapor-phase altered material will affect the ranges in material properties to be expected in the proposed waste-emplacment unit.

##### 4.3.1 Lithophysal Cavities

The upper demonstration breakout room is designed to be excavated in the portion of the Topopah Spring Member containing the greatest abundance of lithophysal cavities. One of the reasons for placement of the room in such material is to examine stability of underground openings in material containing large concentrations of lithophysal cavities. As such, the representativeness of the material surrounding the room must be assessed relative to the upper end of the total range of cavity abundance for the member.

The depth at which the breakout room is to be excavated is estimated to be equivalent to a depth of approximately 494 ft (150 m) in USW G 4. Assuming this depth to be the center of a 15 ft (5 m) opening, the equivalent depth range in USW G-4 would be approximately 486 to 502 ft (148 to 153 m).

Figure 4.3-1 is a plot of cavity abundance as a function of depth for the welded, devitrified portion of the Topopah Spring Member in USW G-4. Assuming that the upper demonstration breakout room will be excavated in material similar to the interval marked as "Equivalent Depth of Breakout

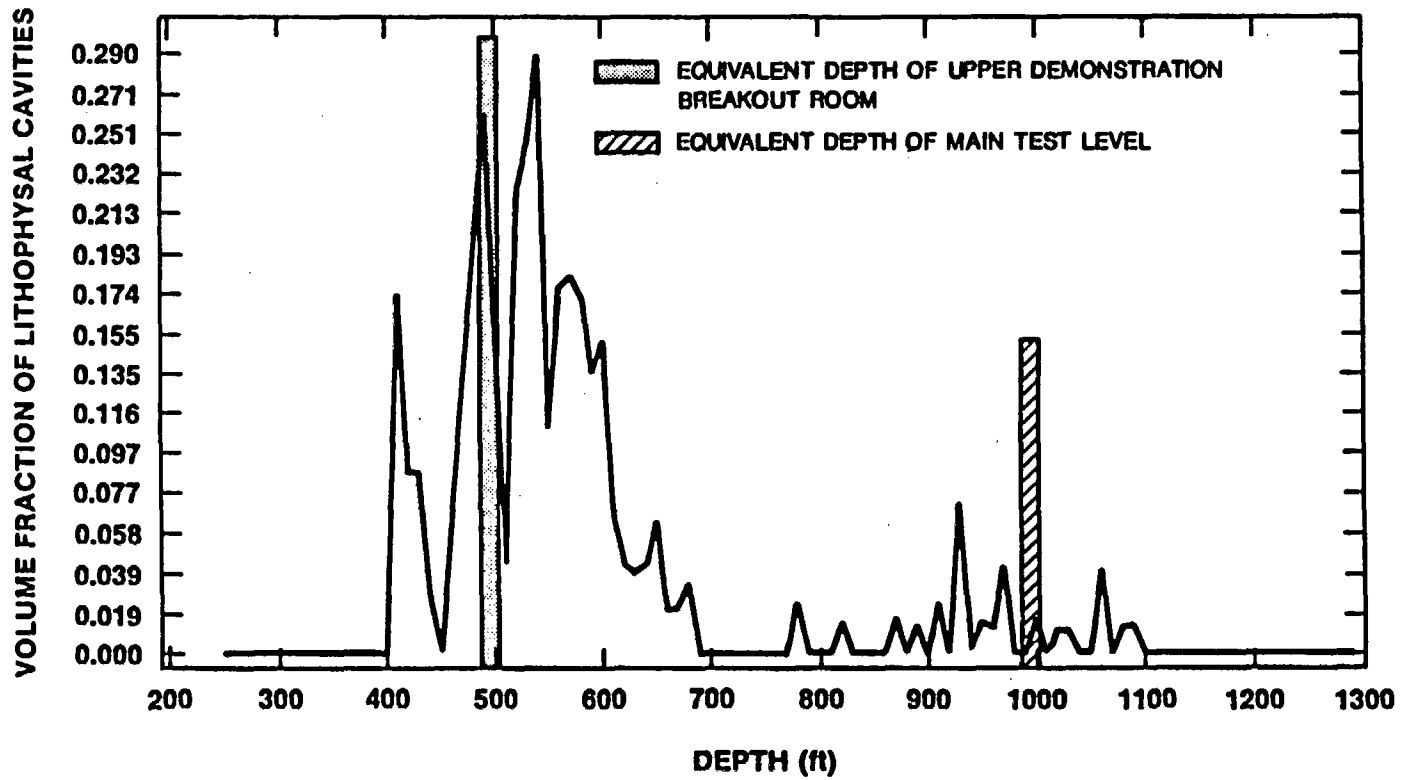


Figure 4.3-1. Abundance of Lithophysal Cavities in the Welded, Devitrified Topopah Spring Member as a Function of Depth in USW G-4. Data from Spengler and Chornack (1984).

Room" on Figure 4.3-1, lithophysal cavity abundance should range from 15 to 26 volume percent in the material surrounding the room.

This range is compared with cavity abundance in the entire zone of material rich in lithophysal cavities in USW G-4 and in three other core holes in Figure 4.3-2. It is clear that the range that is expected to be encountered in the breakout room includes nearly all of the upper portion of the total range observed to date at Yucca Mountain. Thus, the abundance of lithophysal cavities in material around the breakout room will be representative.

The main test level is designed to be excavated in the portion of the Topopah Spring Member in which the subsurface portion of a repository would be located. The representativeness of such material must be assessed relative to the material that will be encountered in the rest of the area for the underground facilities during excavation. As a first approximation, a zone of 70 ft (21 m) both above and below the main test level (and equivalent portions of the welded, devitrified Topopah Spring Member in other core holes) is used to evaluate representativeness.

The depth at which the main test level is to be excavated is estimated to be equivalent to a depth of approximately 994 ft (303 m) in USW G-4. Assuming this depth to be the center of a 15 ft (5 m) opening, the equivalent depth range in USW G-4 would be approximately 986 to 1002 ft (300 to 305 m). Assuming that the main test level will be excavated in material similar to the interval marked as "Equivalent Depth of Main Test Level" on Figure 4.3-1, the lithophysal cavity abundance should range from 0 to 1.7 volume percent.

This range is compared in Figure 4.3-3 with cavity abundance in the entire zone defined by the 15 ft (5 m) room plus the 140 ft (43 m) of additional rock discussed previously for USW G-4 and three other core holes. The range that is expected to be encountered in the main test level is only a small portion of the total ranges shown in Figure 4.3-3. However, in three of the four core holes more than 70 percent of the observed abundances are less than or equal to 2.5 volume percent. Thus, the expected range will be representative of a large proportion of the

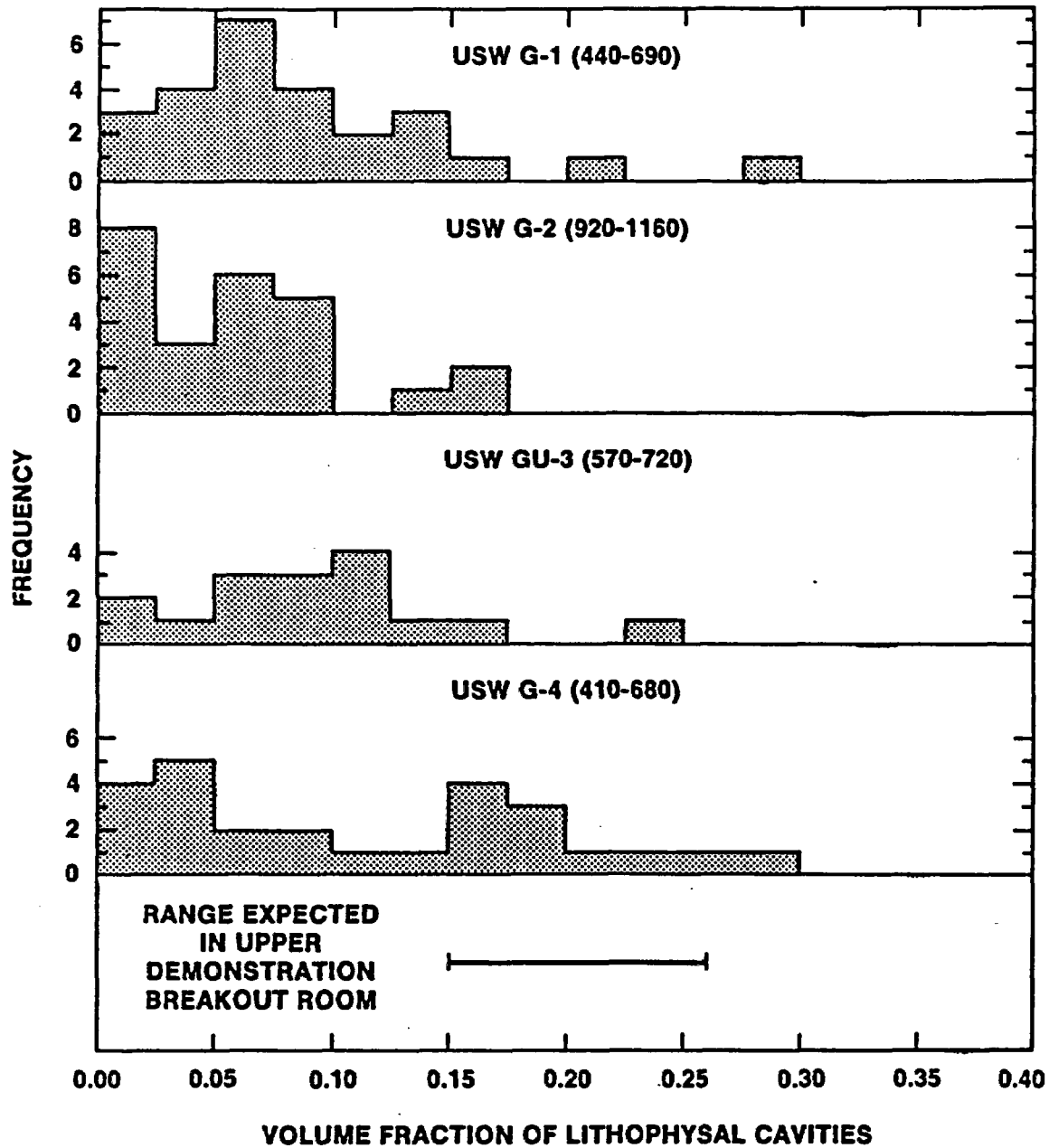


Figure 4.3-2. Comparison of Abundances of Lithophysal Cavities in the Upper Lithophysal Zone of the Topopah Spring Member. Data from Spengler and Chornack (1984).

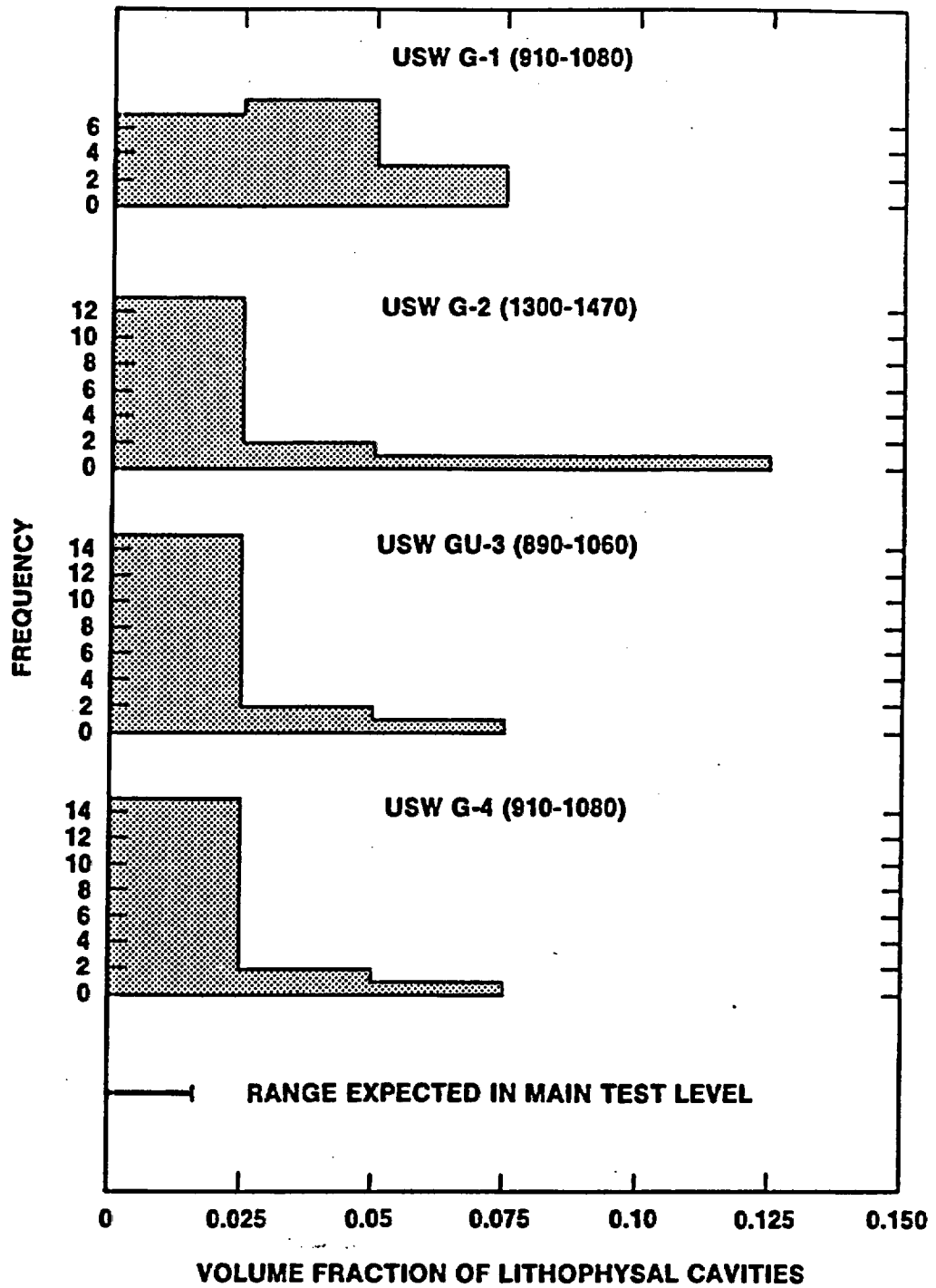


Figure 4.3-3. Comparison of Abundances of Lithophysal Cavities in the Zone Equivalent to the Main Test Level in the ES. Data from Spengler and Chornack (1984).

material in which the subsurface portion of a repository would be excavated.

A possible exception to the preceding statement is material located in the vicinity of USW G-1. As shown in Figure 4.3-3, only about 40 percent of observed cavity abundances are as low as the expected range in the main test level. The lateral drifting at the main test level in ES-1 should allow examination of the spatial extent of material containing the greater cavity abundance seen in the core from USW G-1.

#### 4.3.2 Vapor-Phase Altered Material

Existing data on the abundance of vapor-phase altered material are insufficient to assess representativeness throughout the area for the underground facilities. Data are available only for USW G-4 (Figure 4.3-4). A comparison of the ranges in abundance for depths equivalent to ESF excavations and accompanying wider depth zones (see Section 4.3.1 for definitions of these zones) is given in Table 4.3-1.

Table 4.3-1. Comparison of Range in Abundance of Vapor-Phase Altered Material in the Depth Intervals Coinciding With the Upper Breakout and Main Test Level and in Wider Depth Intervals Bounding These Levels

Level	Depth Interval [ft (m)]	Abundance (%)
Upper demonstration breakout room	486-502 (148-153)	0.0 - 14.6
Wider interval	410-680 (125-207)	0.0 - 16.6
Main test level	986-1002 (300-305)	5.7 - 7.6
Wider interval	910-1080 (277-329)	4.5 - 24.7

Based on these limited data, the upper demonstration breakout room can be expected to be surrounded by representative material. In contrast, the material in which the main test level is to be excavated may well be nonrepresentative because the excavation will sample a very small portion

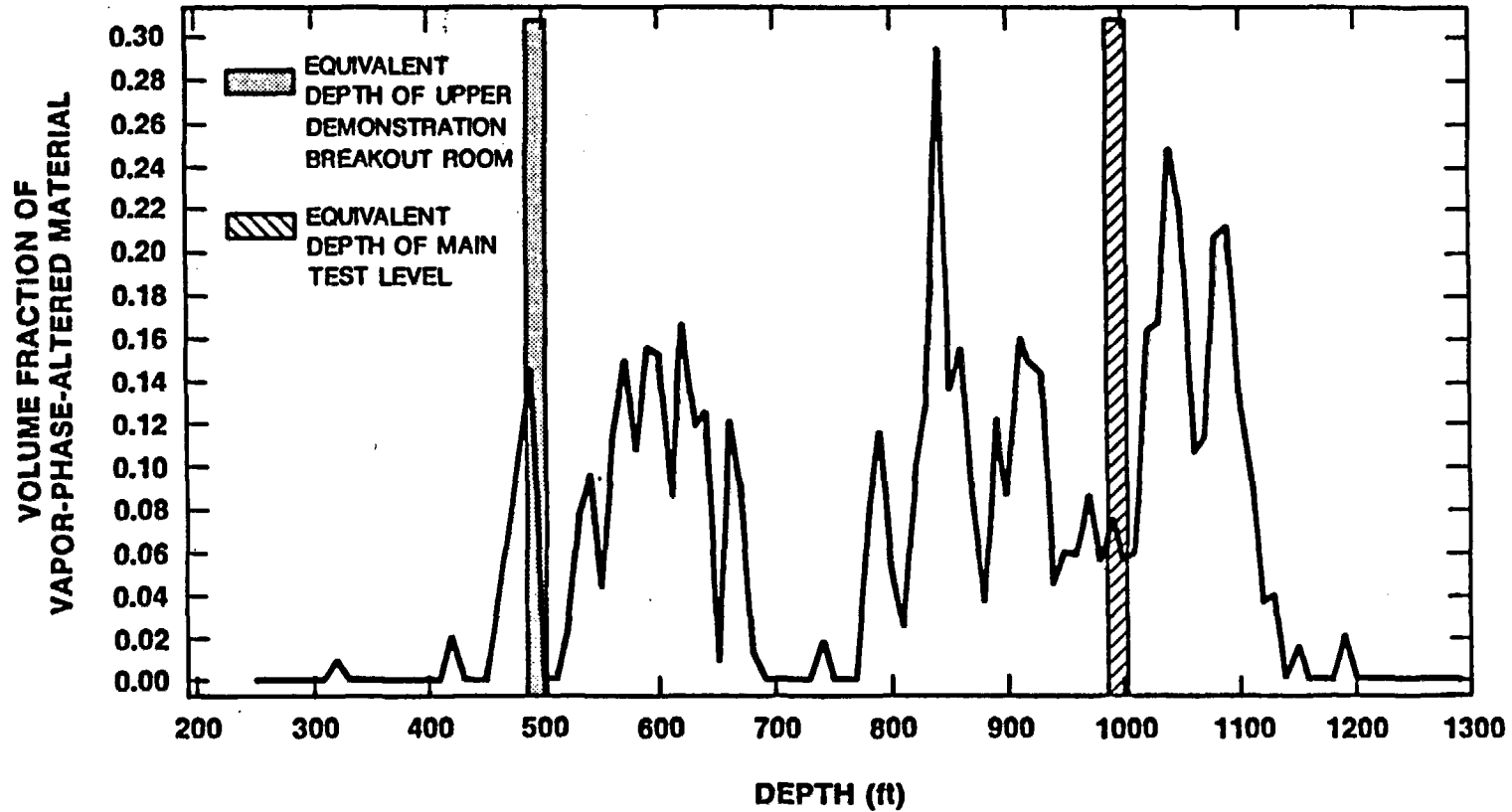


Figure 4.3-4. Abundance of Vapor-Phase-Altered Material in the Welded, Devitrified Topopah Spring Member as a Function of Depth in USW G-4. Data from Spengler and Chornack (1984).

of the total range in abundance of vapor-phase-altered material. This situation may be ameliorated by the excavation of the lateral drifts which should encounter material with a higher content of vapor-phase-altered material.

## 5.0 MINERALOGICAL CHARACTERISTICS

### 5.1 Distribution of $\text{SiO}_2$ Phases Within the Welded, Devitrified Portion of the Topopah Spring Member

Three phases of  $\text{SiO}_2$  are found in the welded, devitrified portion of the Topopah Spring Member: quartz, cristobalite, and tridymite. These phases all have different polymorphs that are stable in different temperature ranges. Some of the inversions from one polymorph of cristobalite and tridymite to another occur at temperatures within the range of temperatures expected in the vicinity of waste canisters after emplacement. These inversions have associated heats of transition and volume changes which may impact the calculated temperature and thermal-stress responses of the rock in the presence of heat-producing waste.

#### 5.1.1 Tridymite

Figure 5.1-1 is a plot of tridymite content in weight percent as a function of depth in USW G-4 (data from Bish and Vaniman, 1985). The two curves represent upper and lower bounds on the amount of tridymite based on experimental uncertainty. The equivalent depths of the upper demonstration breakout room and of the main test level also are plotted on the figure.

The expected tridymite content in the material around the upper demonstration breakout room is between 2 and 10 weight percent. Figure 5.1-2 compares this bracket of tridymite content with similar brackets for samples from equivalent depth zones in USW G-4 and three other core holes. The bracket for the expected tridymite content overlaps a large proportion of the brackets for two of the four samples from USW GU-3 and two of the four samples from USW G-1. (No tridymite was found in the six samples from USW G-2, so that there is no overlap of data between USW G-2 and USW G-4. There is significant overlap for 50 percent of samples from equivalent zones if USW G-2 samples are ignored, or for 29 percent of the

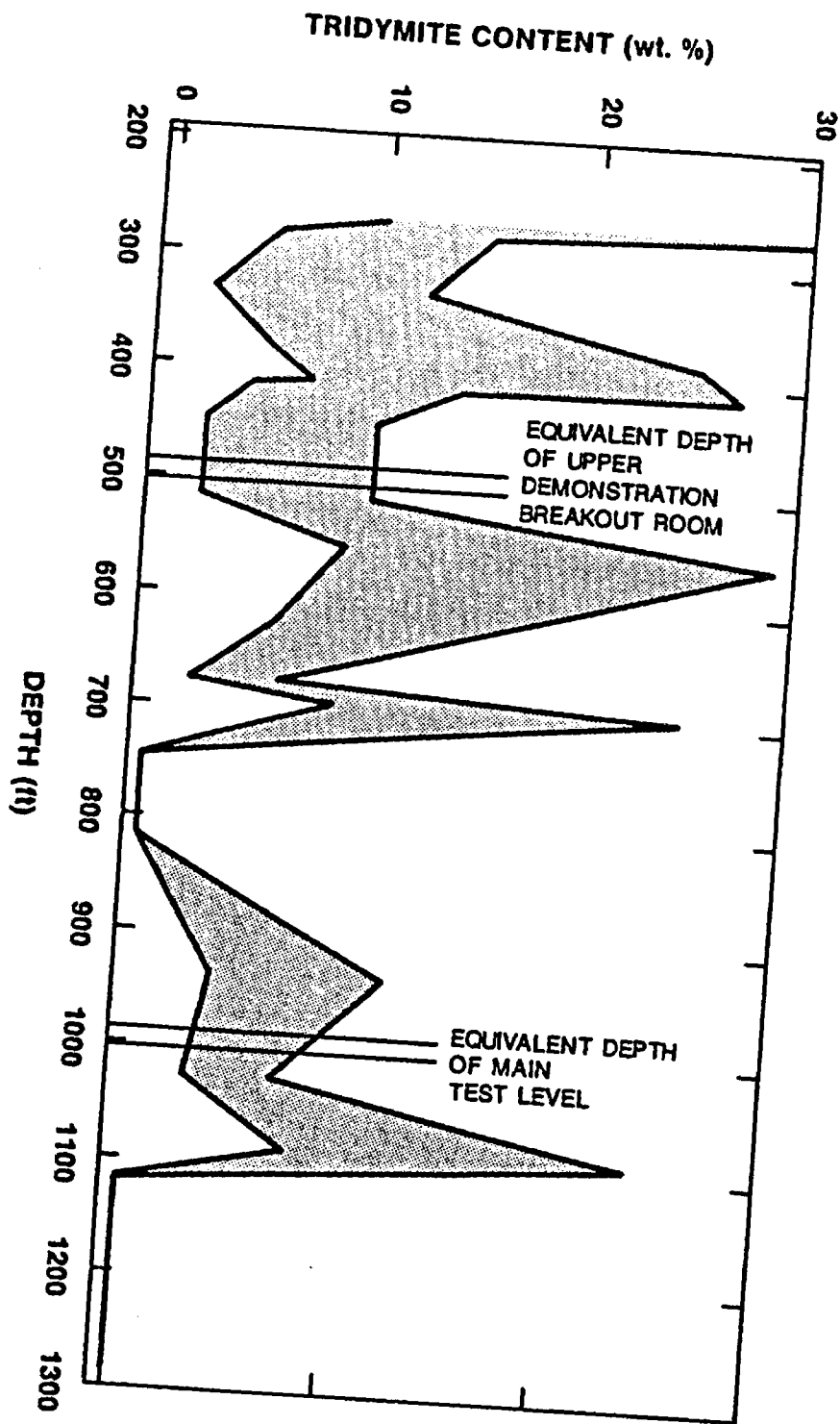


Figure 5.1-1. Abundance of Tridymite in the Welded, Devitrified Topopah Spring Member as a Function of Depth in USW G-4. Ranges are indicative of measured values  $\pm$  analytical uncertainty. Data from Bish and Vaniman (1985).

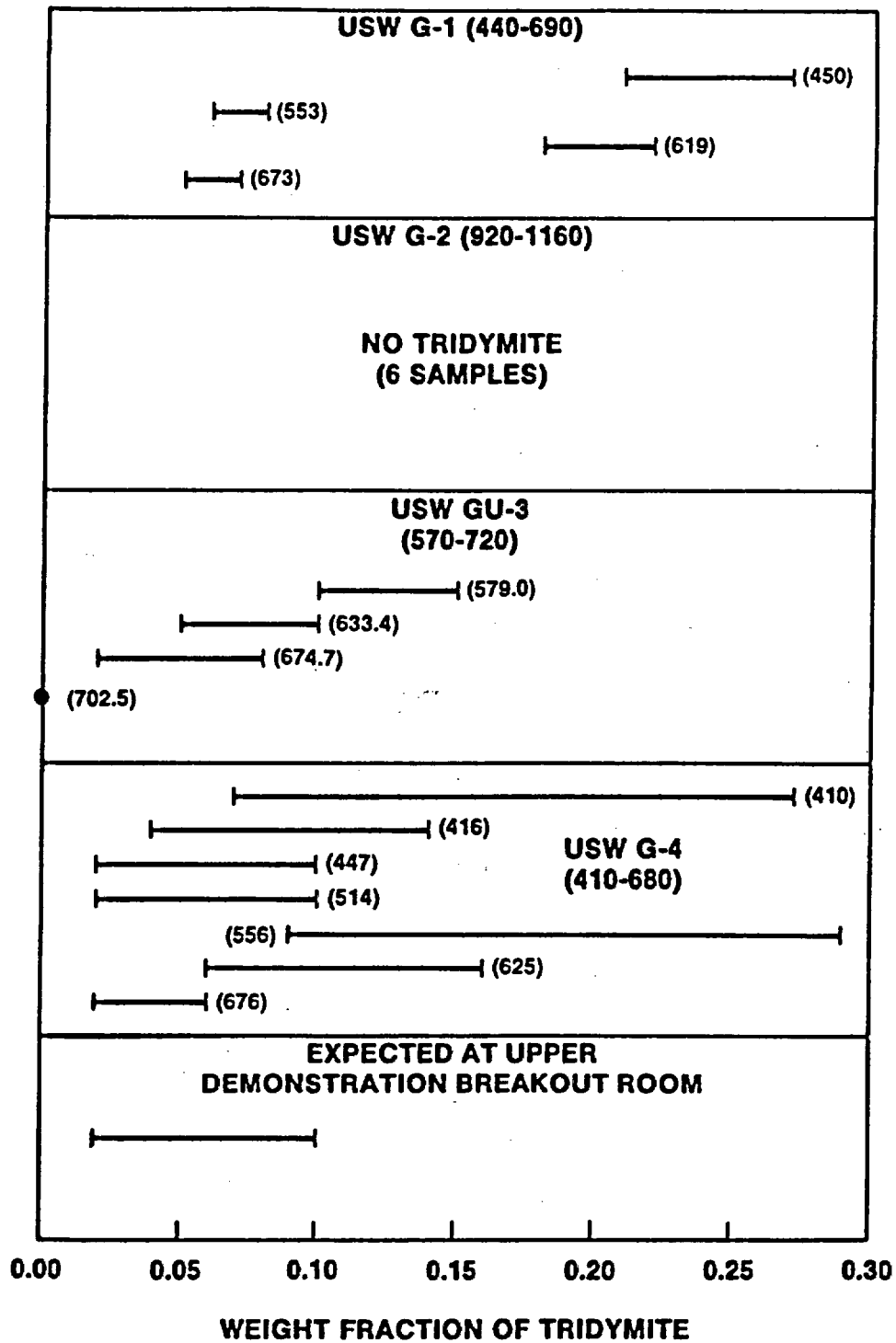


Figure 5.1-2. Comparison of Abundances of Tridymite in the Upper Lithophysal Zone of the Topopah Spring Member. Numbers in parentheses are depths in feet. Ranges are indicative of measured values  $\pm$  analytical uncertainty. Data from Bish and Vaniman (1985), Bish and Chipera (1986).

samples if USW G-2 samples are included. Thus, the tridymite content is expected to be representative (in the sense of not being anomalous) for the material surrounding the upper demonstration breakout room.

For the main test level, the bracket for the expected tridymite content is 3.3 to 9.2 percent (Figure 5.1-1). Figure 5.1-3 compares this bracket with similar brackets for the depth zones described in Section 4.3.1 in discussion of the main test level. The bracket for the expected tridymite content overlaps all or most of the brackets for three of the four samples (from core holes other than USW G-4) shown on Figure 5.1-3 (75 percent of samples from equivalent zones). If samples from USW G-2 are included, the percentage is 38 percent. Thus, the tridymite content is expected to be representative (in the sense of not being anomalous) for the material surrounding the main test level.

#### 5.1.2 Cristobalite

Figure 5.1-4 is a plot of cristobalite content in weight percent as a function of depth in USW G-4 (data from Bish and Vaniman, 1985). The two curves represent upper and lower bounds on the amount of cristobalite based on experimental uncertainty. The equivalent depths of the upper demonstration breakout room and of the main test level also are plotted on the figure.

The expected cristobalite content in the material around the upper demonstration breakout room is between 16 and 27 weight percent. Figure 5.1-5 compares this bracket with similar brackets for samples from equivalent depth zones in USW G-4 and three other core holes. The bracket for the expected cristobalite content overlaps a large proportion of the brackets for two of the four samples from USW G-1, two of the six samples from USW G-2, and all four samples from USW GU-3 (57 percent of samples from equivalent zones in core holes other than USW G-4). The expected cristobalite content in the material around the upper demonstration breakout room is representative (in the sense of being nonanomalous).

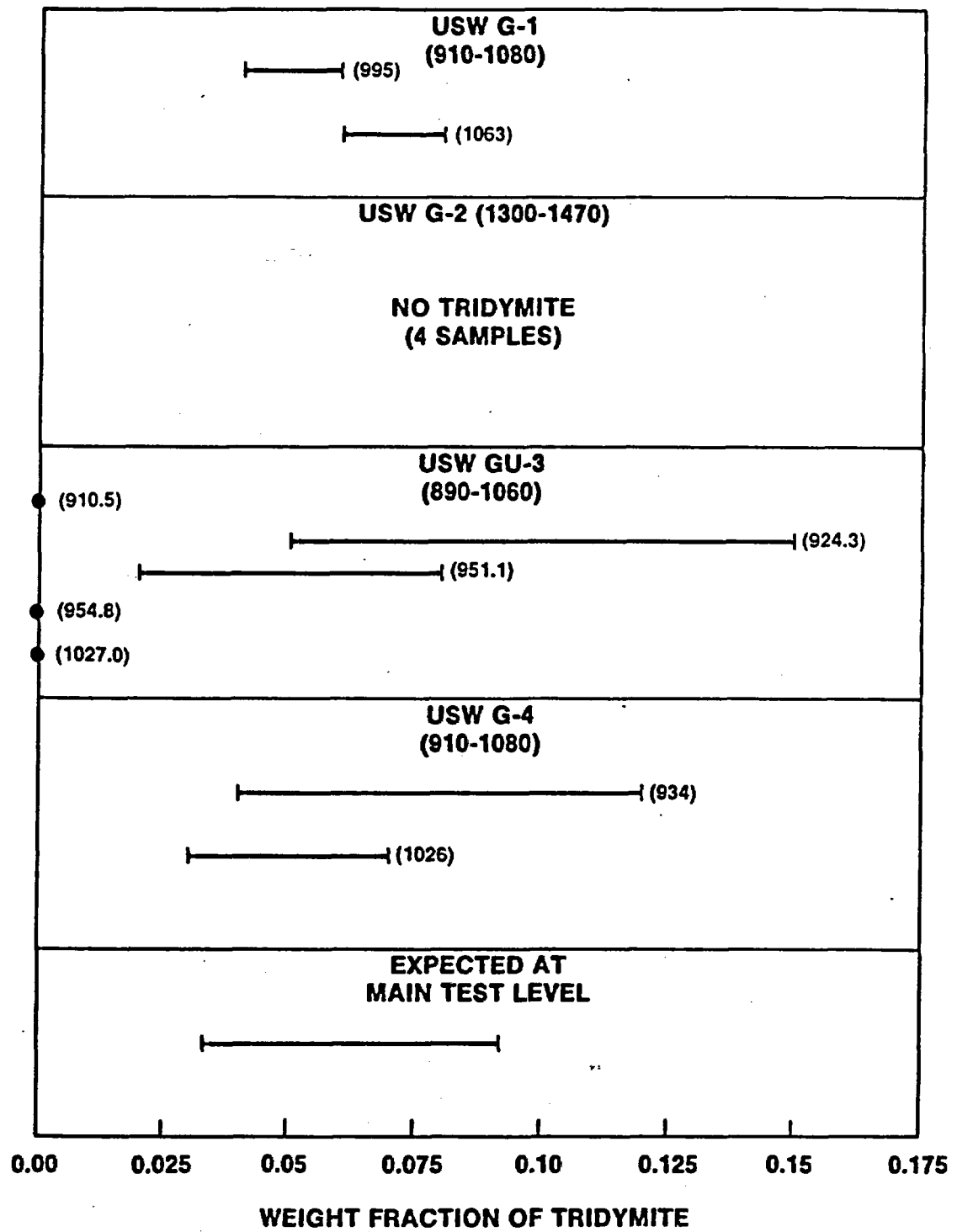


Figure 5.1-3. Comparison of Abundances of Tridymite in the Zone Equivalent to the Main Test Level in the ES. Numbers in parentheses are depths in feet. Ranges are indicative of measured values  $\pm$  analytical uncertainty. Data from Bish and Vaniman (1985), Bish and Chipera (1986).

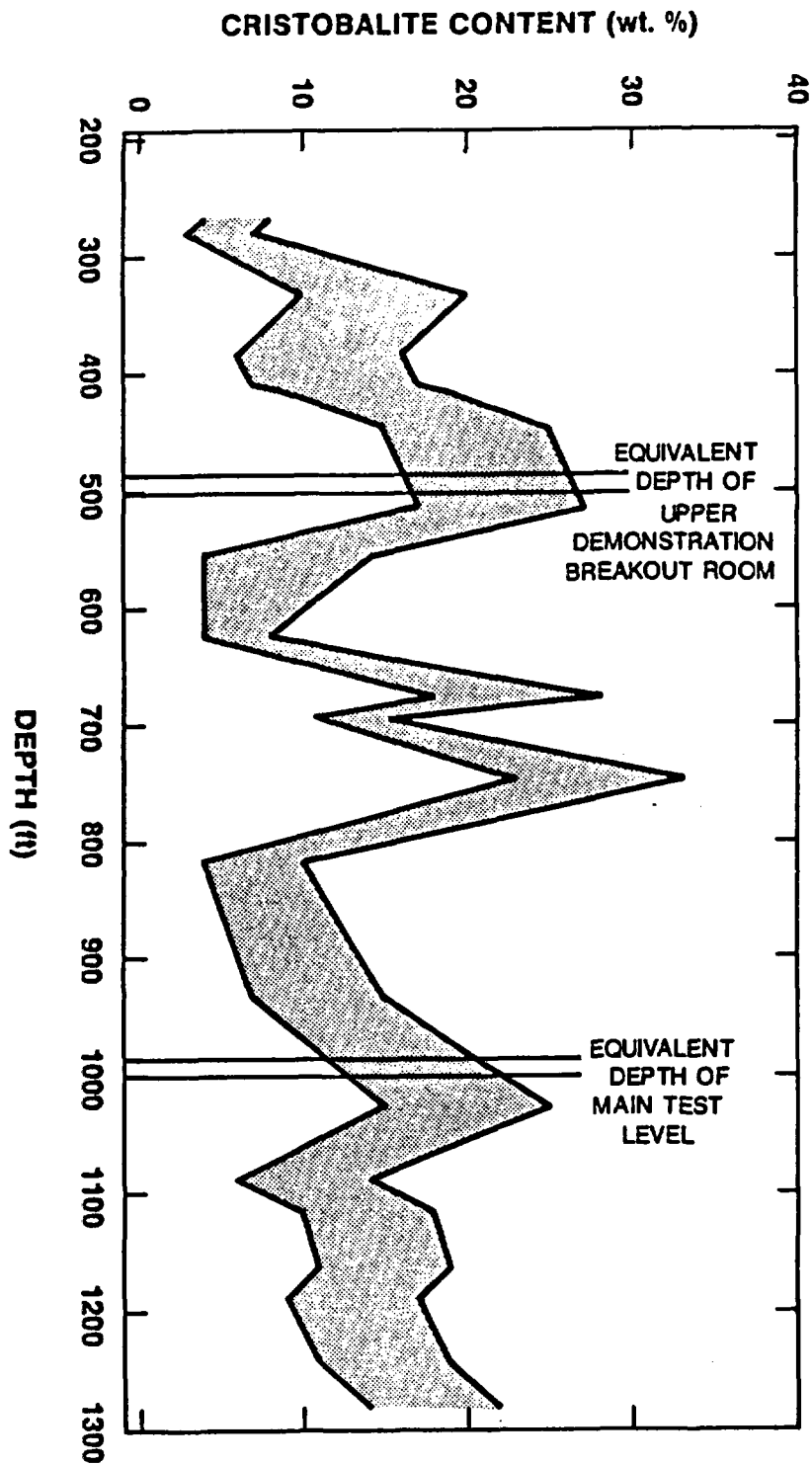


Figure 5.1-4. Abundance of Cristobalite in the Welded, Devitrified Topopah Spring Member as a Function of Depth in USW G-4. Ranges are indicative of measured values  $\pm$  analytical uncertainty. Data from Bish and Vaniman (1985).

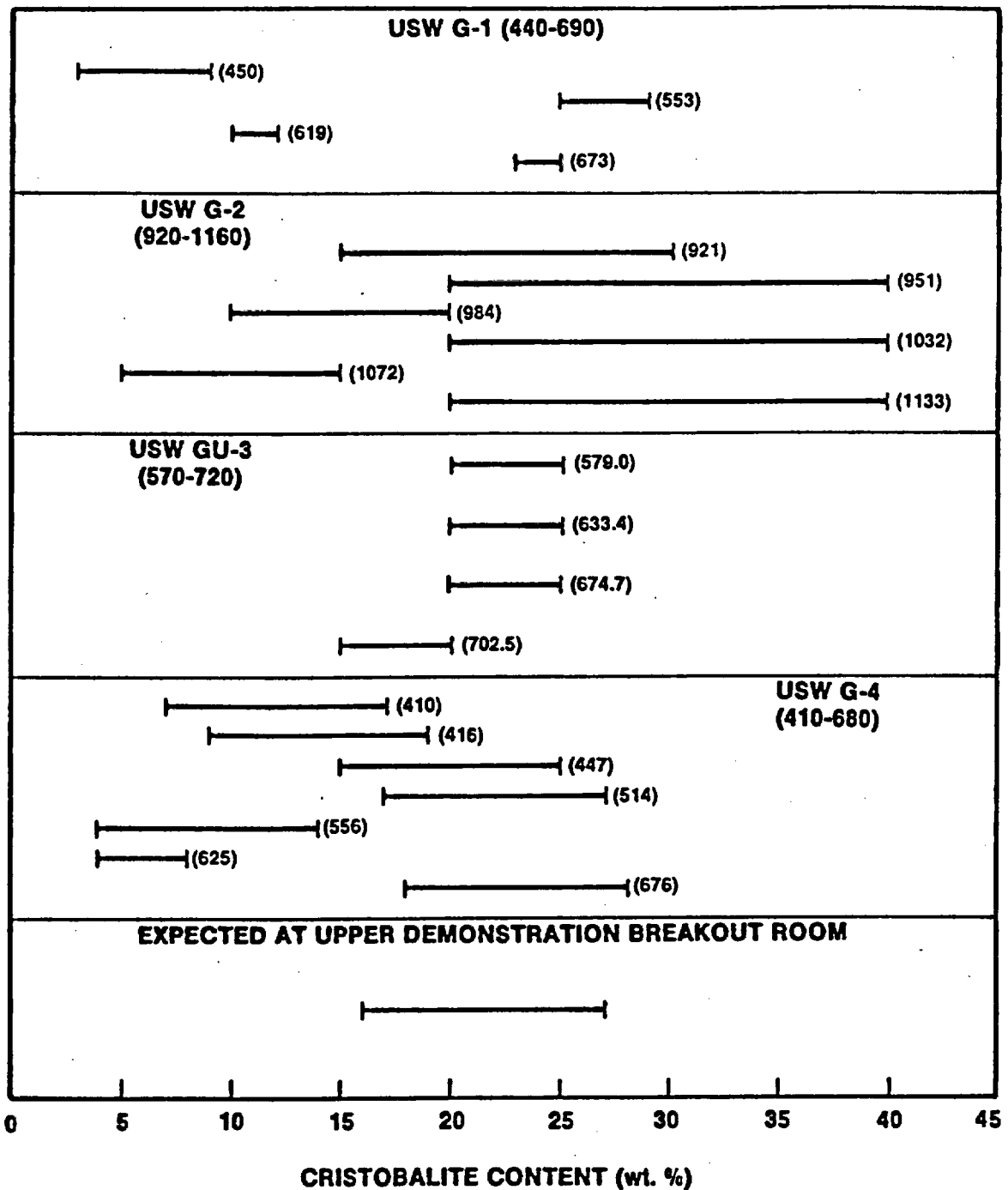


Figure 5.1-5. Comparison of Abundances of Cristobalite in the Upper Lithophysal Zone of the Topopah Spring Member. Numbers in parentheses are depths in feet. Ranges are indicative of measured values  $\pm$  analytical uncertainty. Data from Bish and Vaniman (1985), Bish and Chipera (1986).

The cristobalite content expected in the material surrounding the main test level is between 12 and 22 weight percent (Figure 5.1-4). Figure 5.1-6 compares this bracket with similar brackets for the depth zones described in Section 4.3.1 in discussion of the main test level. The bracket for the expected cristobalite content overlaps a large proportion of one of the two samples from USW G-1, one of the four samples from USW G-2, and four of the five samples from USW GU-3 (55 percent of samples from equivalent zones from core holes other than USW G-4). Thus, the cristobalite content in the material surrounding the main test level is expected to be representative in the sense of being nonanomalous.

## 5.2 Fracture Mineralogy

In scenarios involving groundwater flow through fractures, the minerals coating the fractures in the Topopah Spring Member and underlying units represent the first material to be encountered by radionuclides traveling from a waste container toward the water table. The extent to which this material removes radionuclides from solution will affect both rates and quantities of the radionuclides reaching the accessible environment. In addition, fracture coatings may have different hydrologic properties than does adjacent matrix material and thus may affect the hydrologic interaction between fractures and matrix porosity.

The fracture mineralogy has been studied in detail for USW G-4 only (Carlos, 1985). Fractures from material at depths in USW G-4 equivalent to the zone around the upper demonstration breakout room [410 to 680 ft (125 to 207 m)] have not been sampled because appropriate core has not been available. In contrast, six fractures from the depths of interest for the main test level [910 to 1080 ft (277 to 329 m)] have been examined. Two fractures from the approximate depth range equivalent to the main test level [986 to 1002 ft (301 to 305 m)] showed coatings with similar mineralogies but covering very different amounts of fracture surface. The sample from 984 ft (300 m) is entirely coated with secondary minerals, dominantly quartz and alkali feldspar. The fracture

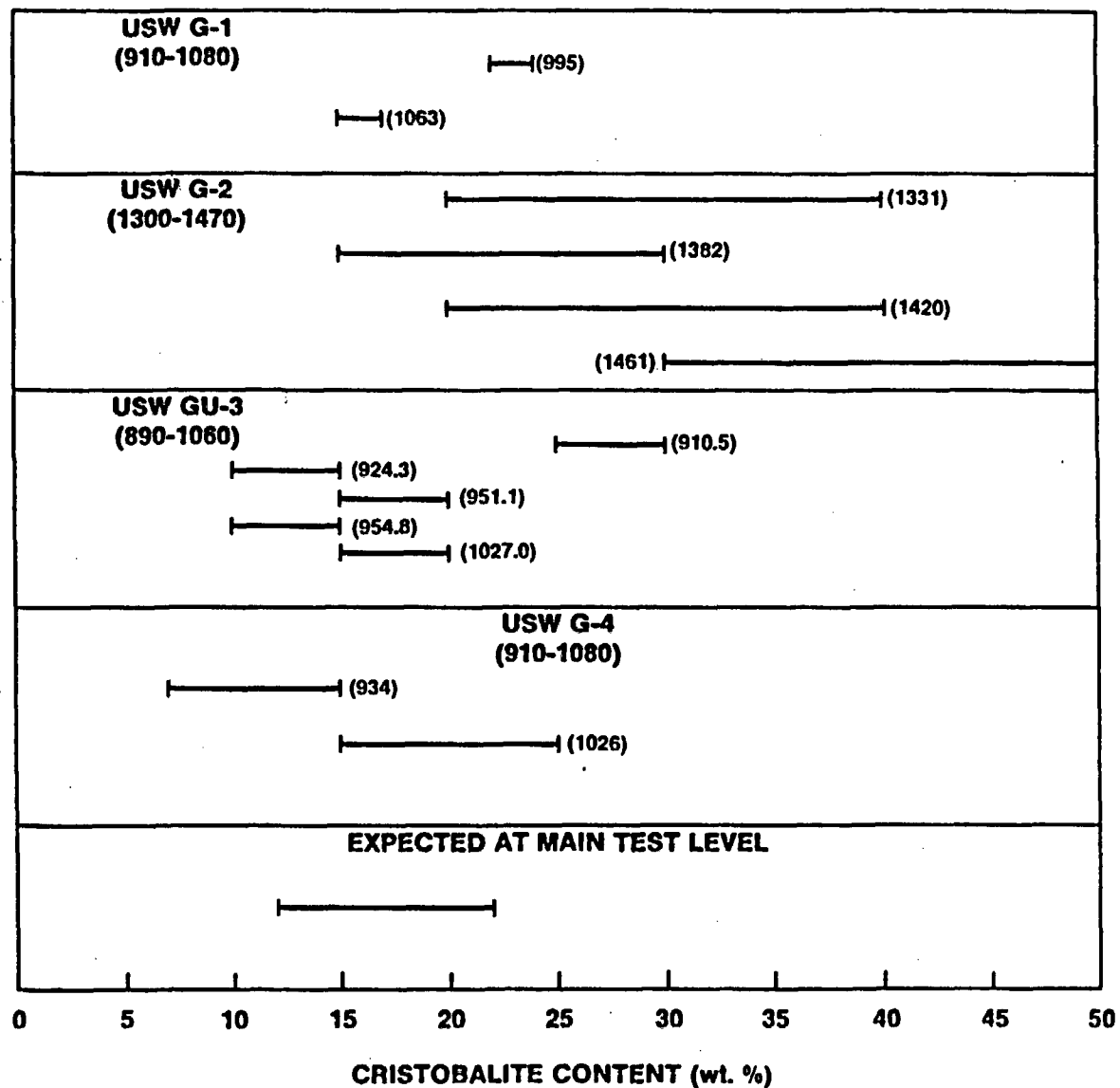


Figure 5.1-6. Comparison of Abundances of Cristobalite in the Zone Equivalent to the Main Test Level in the ES. Numbers in parentheses are depths in feet. Ranges are indicative of measured values  $\pm$  analytical uncertainty. Data from Bish and Vaniman (1985), Bish and Chipera (1986).

from 1001 ft (305 m) has secondary minerals on about 10 percent of the surface; the dominant minerals again were quartz and alkali feldspar. Three of the other four samples from the zone of interest contained either smectite or mordenite among the secondary minerals. The coatings covered from 30 to 100 percent of fracture surfaces on these samples.

Beginning at a depth of 1254 ft (382 m) and extending to 1763 ft (537 m), the mineralogy of sampled fractures was dominated by zeolites, clays, or both. Coatings covered from 20 to 100 percent of the fracture surfaces.

Preliminary examination of fractures from other core holes (Carlos, 1987) suggests that fractures in USW G-4 are representative of the northern part of the area for the underground facilities (USW G-1, UE-25a#1). Fractures in USW GU-3 contain more calcite than do fractures in the northern portion of the area. Other differences may exist as well, so that data on fracture mineralogy from USW G-4 may not be representative of the more southerly portions of the area. Additional study is required before a definitive conclusion about representativeness can be reached.

### 5.3 Clay Content of the Welded, Devitrified Portion of the Topopah Spring Member

Clay acts as functional porosity and as such affects the mechanical properties of tuff (cf., Price and Bauer, 1985). The clay content of the welded, devitrified portions of the Topopah Spring Member is plotted as a function of depth in USW G-4 in Figure 5.3-1 (data from Bish and Vaniman, 1985). The two curves represent upper and lower bounds on the amount of clay based on experimental uncertainty. The equivalent depths of the upper demonstration breakout room and of the main test level also are plotted on the figure.

The expected clay content in the material around the upper demonstration breakout room is between 1 and 3 weight percent. Figure 5.3-2A compares this bracket with similar brackets for samples from equivalent depth zones in USW G-4 and three other core holes. The

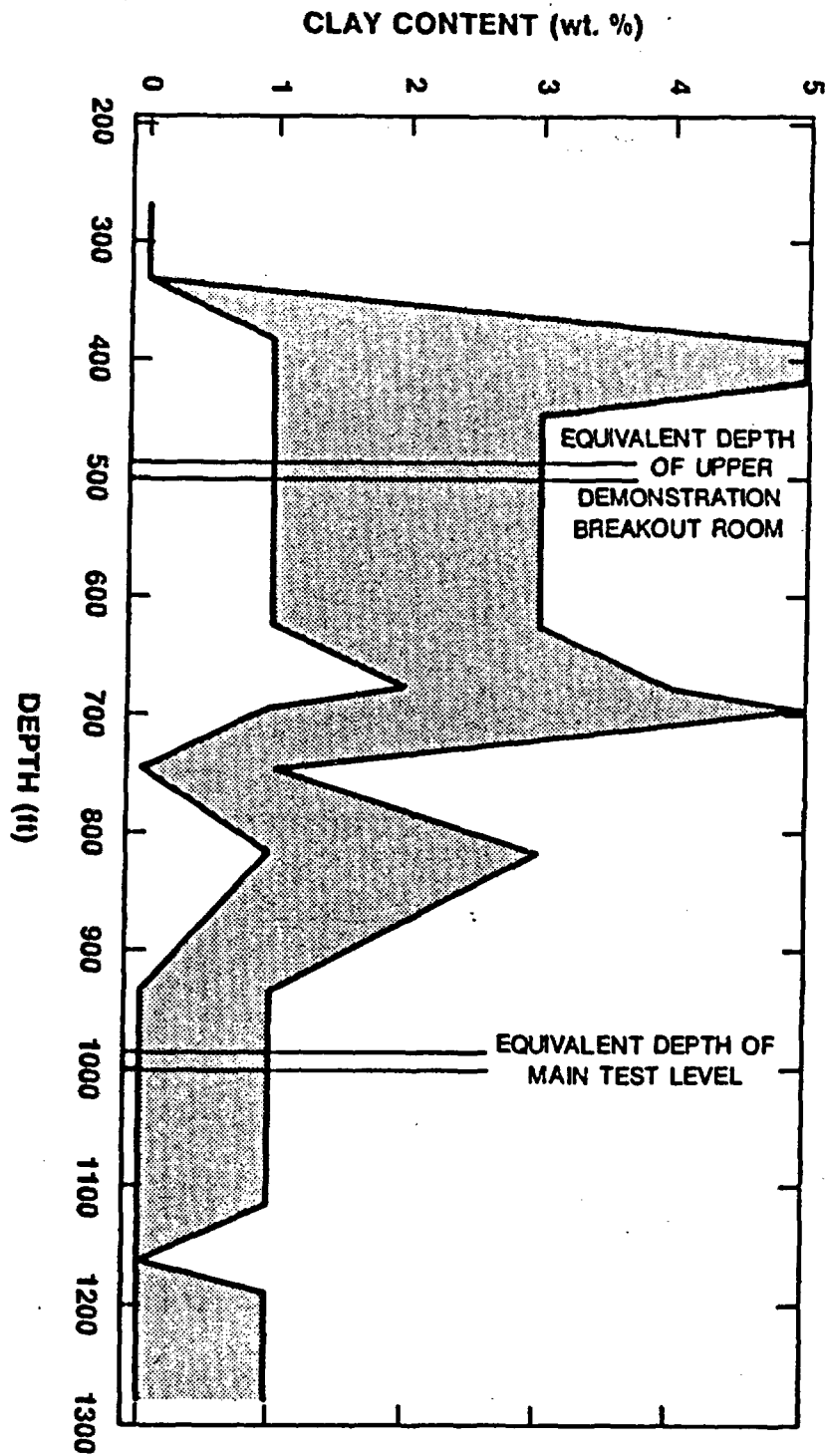


Figure 5.3-1. Abundance of Clay in the Welded, Devitrified Topopah Spring Member as a Function of Depth in USW G-4. Numbers in parentheses are depths in feet. Ranges are indicative of measured values  $\pm$  analytical uncertainty. Data from Bish and Vaniman (1985).

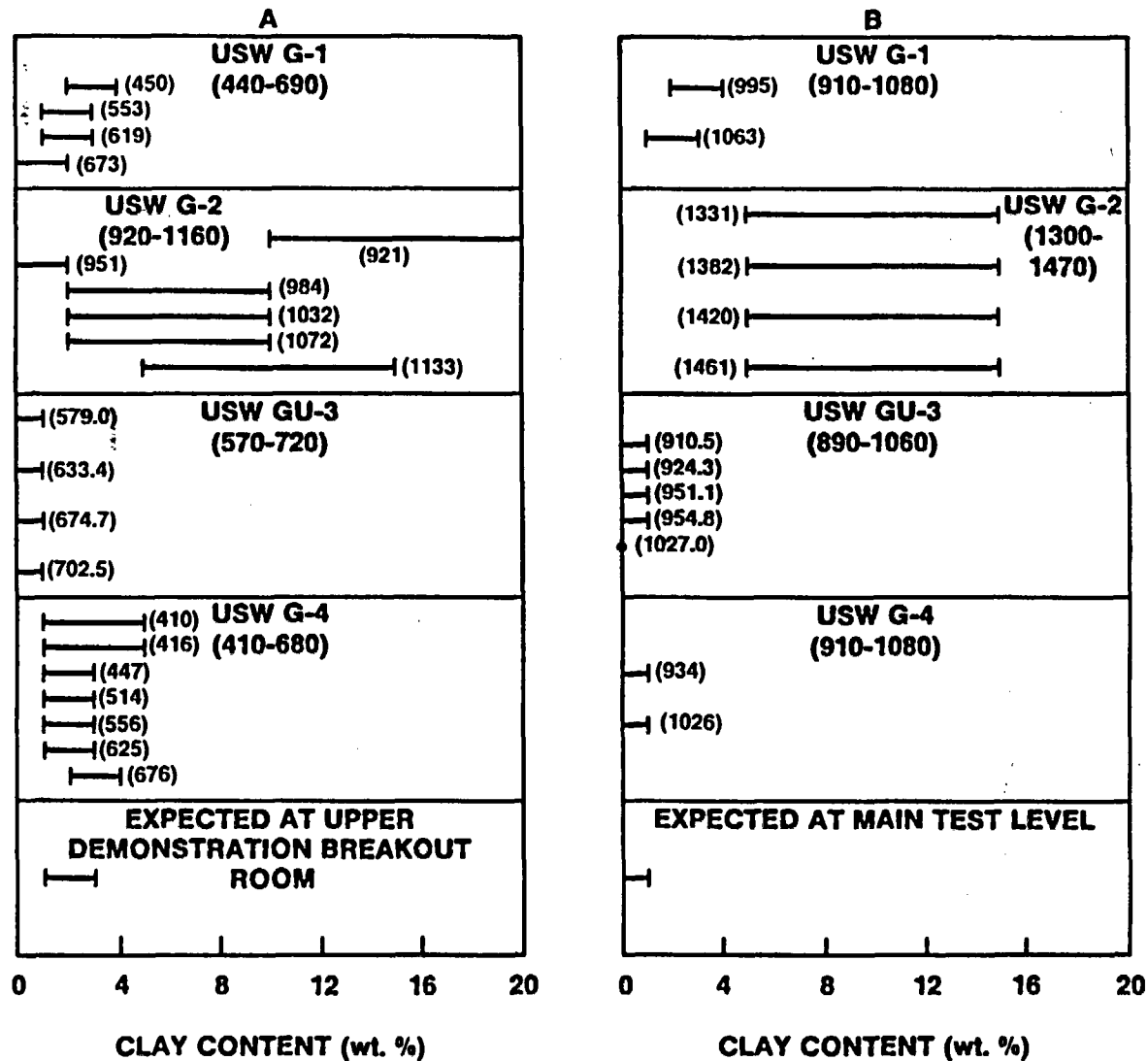


Figure 5.3-2. Comparison of Abundances of Clay in the Welded, Devitrified, Topopah Spring Member (A) Upper lithophysal zone (B) Zone equivalent to the main test level in the ES. Numbers in parentheses are depths in feet. Ranges are indicative of measured values  $\pm$  analytical uncertainty. Data from Bish and Vaniman (1985), Bish and Chipera (1986).

bracket for expected clay content in the vicinity of the breakout room overlaps a large proportion of brackets for samples from the equivalent zone in USW G-1. Less clay is present in samples from USW GU-3 and more is present in samples from USW G-2 than is expected at the location of the breakout room. Thus, the expected clay content in the material in which the breakout room is to be excavated will be representative of the northern part of the area for the underground facilities, but is expected to be higher than clay contents in the southern portion of the area. Clay contents north of the area for the underground facilities may be significantly higher than any found within the area.

Figure 5.3-2B compares the expected clay content in the vicinity of the main test level [zero to 1 weight percent (Figure 4.3-1)] with clay contents of samples from the depth zones associated with the main test level discussed in Section 4.3.1. The expected clay content is the same as that found in all samples for USW GU-3, but is less than the clay content of samples from USW G-1 and USW G-2. Representativeness of the expected clay content cannot be assessed beyond the statement that clay content of material at the main test level will be representative of some portion of the area for the underground facilities. As with clay content near the breakout room, more clay is expected in the region north of the area based on data from USW G-2.

Byers and Moore (1987) report the results of a comparison of the petrography of the welded devitrified portion of the Topopah Spring Member in the five core holes at Yucca Mountain. Although the analysis considered characteristics other than specific minerals, the conclusions were quite similar. Four petrographic zones were identified and found to be similar in the four core holes in and near the area for the underground facilities. The petrography of the material indicated a different zonation in USW G-2. This analysis reported by Byers and Moore (1987) supports a general conclusion that the welded, devitrified portion of the Topopah Spring Member at ES-1 should be representative of the material in the remainder of the area.

#### 5.4 Sorptive Mineralogy Between the Proposed Waste Emplacement Unit and the Water Table

The minerals encountered by radionuclides moving from the proposed waste emplacement unit to the water table through the rock matrix will affect the rates and quantities of radionuclides released to the accessible environment.

Most experimental data on radionuclide sorption have been obtained using tuff samples from USW G-1. Comparison of data on mineral abundances in other drill holes (Bish and Vaniman, 1985) to those from USW G-1 (Bish and Chipera, 1986) should give a good estimate of the sorptive ability of the tuffs from the other core holes. The discussion that follows focuses on potentially sorptive phases. The emphasis is on clinoptilolite, mordenite, and smectite clay, which have been determined to have excellent sorptive capabilities for  $^{90}\text{Sr}$  and  $^{137}\text{Cs}$  and good sorption of many actinide radionuclides (Daniels et al., 1982; DOE, 1986). Glass is included for completeness.

The method of comparison of sorptive mineralogy involves the estimation of the cumulative volume of a given phase within a column of rock extending vertically downward from the base of unit TSw2. Data on mineral abundances as reported in Bish and Vaniman (1985) and Bish and Chipera (1986) were integrated as a function of depth below the base of unit TSw2 using linear interpolation between successive samples. The units obtained for such an integration are weight percent-feet. In these tuffs, weight percentages are nearly equivalent to volume percentages. It is assumed that the samples are representative of a column of rock with a square unit cross-sectional area, and then the units resulting from the integration ( $\text{ft}^3$ ) have been converted to  $\text{m}^3$ . (These may be changed back to  $\text{ft}^3$  by multiplying by 35.3.)

##### 5.4.1 Clinoptilolite

Figure 5.4-1 compares the cumulative volumes of clinoptilolite present between the base of unit TSw2 and the water table in USW G-1,

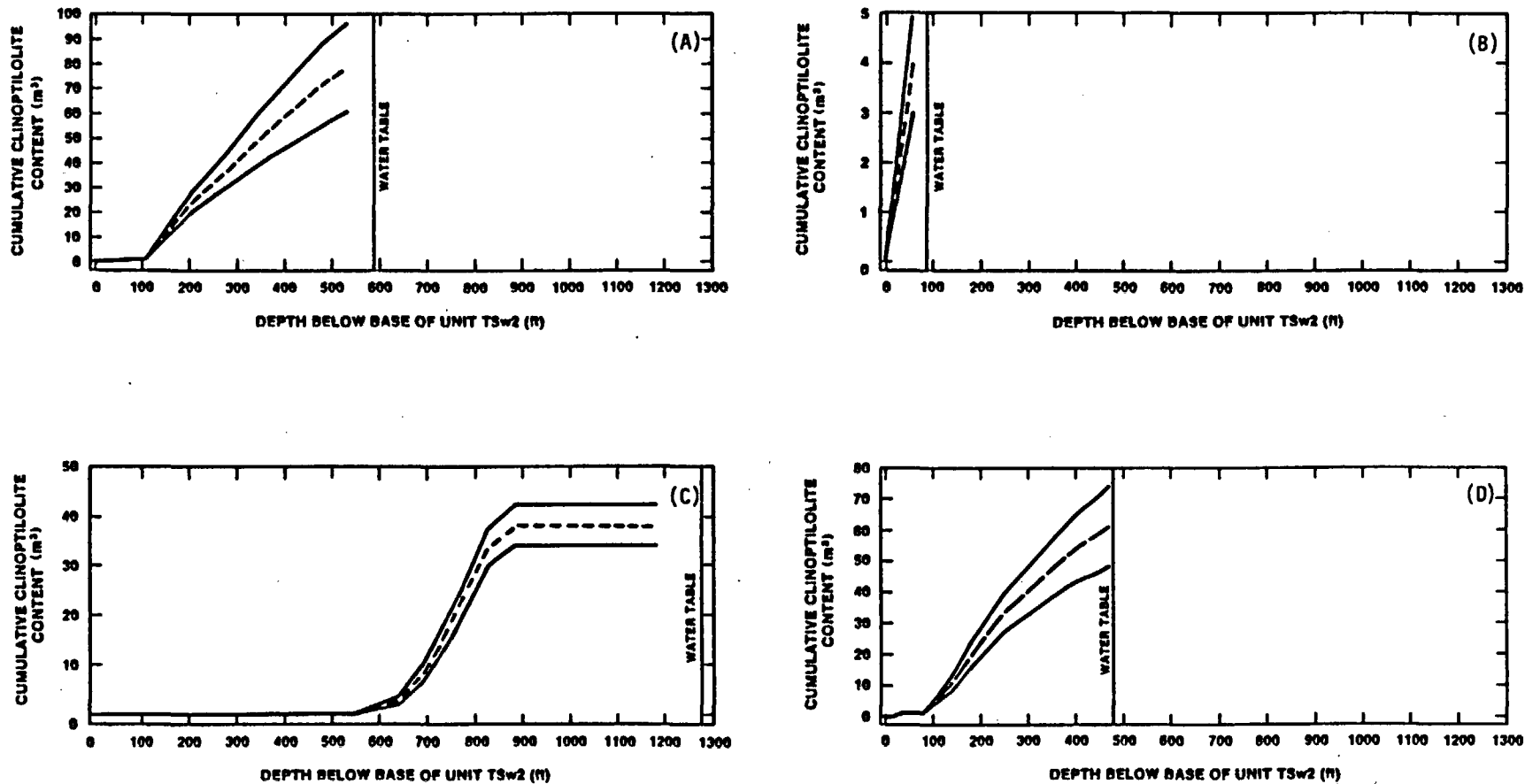


Figure 5.4-1. Comparison of Cumulative Contents of Clinoptilolite Between the Base of Unit TSw2 and the Water Table. Ranges are the result of accounting for analytical uncertainty. data from Bish and Vaniman (1985), Bish and Chipera (1986). (A) USW G-1. (B) USW G-2. (C) USW GU-3. (D) USW G-4. Note differences in ordinate scales.

USW G-2, USW GU-3, and USW G-4. The average volume in USW G-4 [Figure 5.4-1 (D)] is  $61.3 \text{ m}^3$  ( $2160 \text{ ft}^3$ ) whereas the average volumes in the other three core holes are  $78.4 \text{ m}^3$  ( $2770 \text{ ft}^3$ ) in USW G-1,  $4.0 \text{ m}^3$  ( $140 \text{ ft}^3$ ) in USW G-2, and  $38.2 \text{ m}^3$  ( $1350 \text{ ft}^3$ ) in USW GU-3. Assuming that sorption is a direct function of the volume of a sorptive phase, the comparison suggests that material between unit TSw2 and the water table will be most effective at removal of radionuclides near USW G-1, and almost comparable at USW G-4 (and at the ES-1 location by inference). In the vicinity of USW GU-3, clinoptilolite content is lower than is present in the northern portion of the area for the underground facilities. North of the area, the water table and the base of unit TSw2 are converging. Thus, although the fraction of clinoptilolite is high in samples from USW G-2, the total volume of the mineral is greatly reduced relative to the amounts in USW G-1 and USW G-4.

Figure 5.4-2 compares the expected ranges in the volume of clinoptilolite for the four core holes. Based on this comparison and on Figure 5.4-1, the ES-1 location (as represented by USW G-4) appears to be representative of the northern part of the area for the underground facilities in terms of clinoptilolite volume and nonrepresentative of the southern portion of the area and of the region north of the area for the underground facilities.

#### 5.4.2 Mordenite

The only zeolite other than clinoptilolite that is found in measurable quantities in the material between the base of unit TSw2 and the water table is mordenite. Figure 5.4-3 compares the cumulative volumes of this phase in USW G-1, USW G-2, and USW G-4. The average volume in USW G-4 [Figure 5.4-3(C)] is  $11.4 \text{ m}^3$  ( $400 \text{ ft}^3$ ), as compared with  $12.8 \text{ m}^3$  ( $450 \text{ ft}^3$ ) in USW G-1,  $0.3 \text{ m}^3$  ( $10 \text{ ft}^3$ ) in USW G-2, and no mordenite in USW GU-3.

The ranges in expected volume of mordenite for USW G-1, USW G-2, and USW G-4 are compared in Figure 5.4-4. Based on this comparison and on Figure 5.4-3, the ES-1 location (as represented by USW G-4) appears to be representative of the northern part of the area for the underground

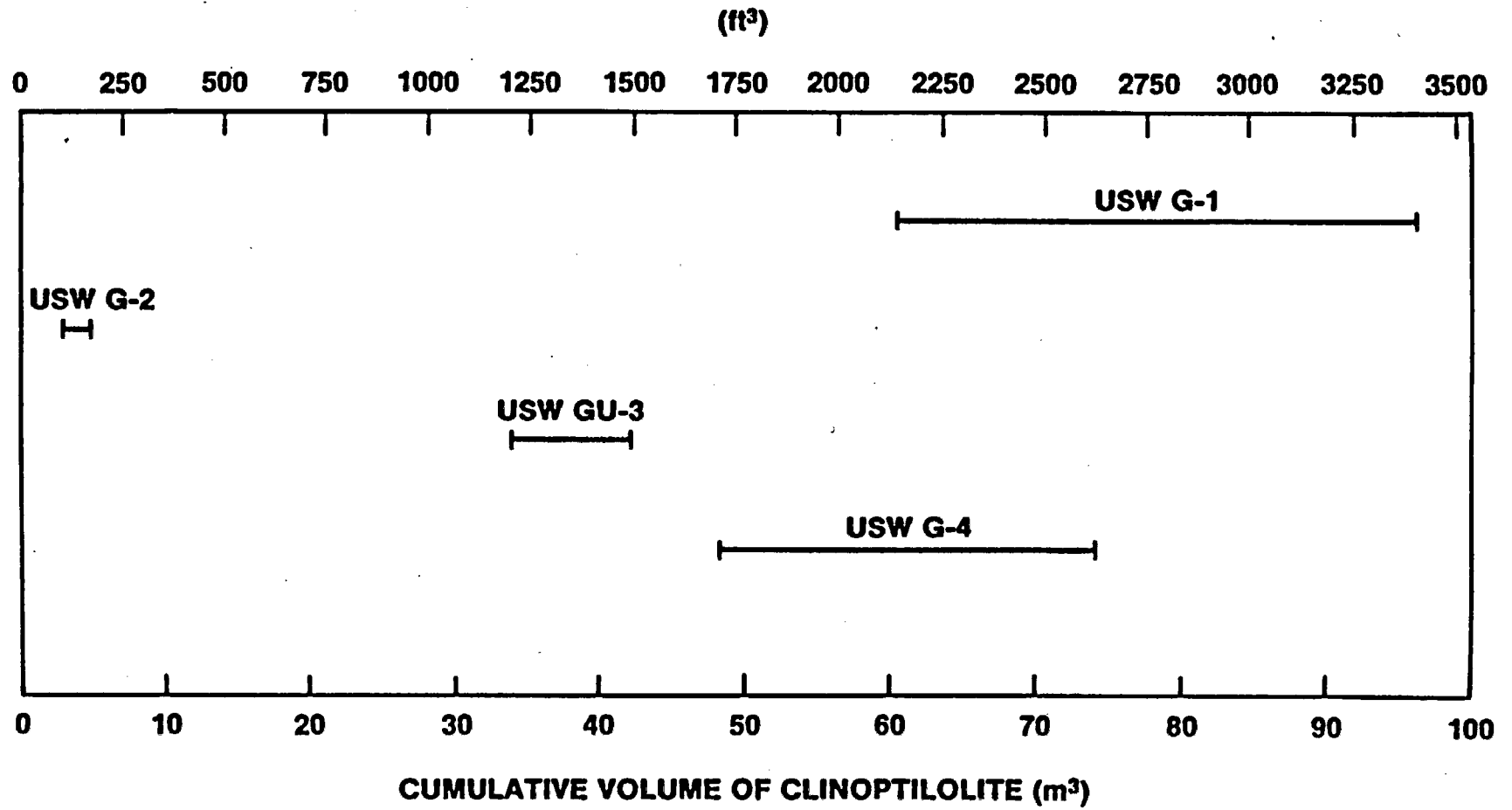


Figure 5.4-2. Comparison of Expected Ranges in Cumulative Content of Clinoptilolite. Data from Bish and Vaniman (1985), Bish and Chipera (1986).

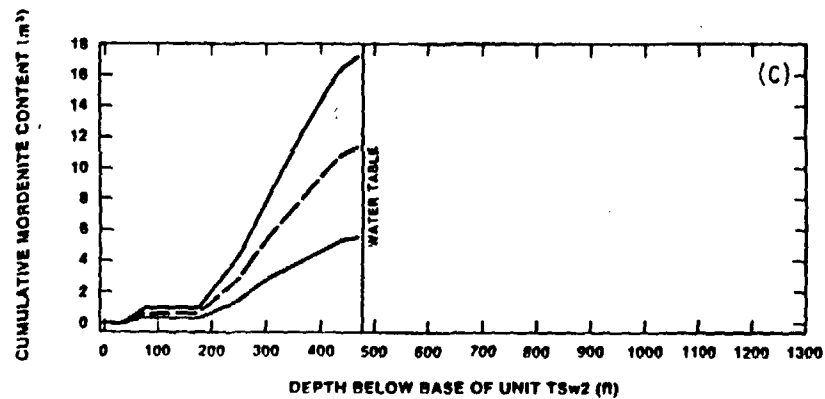
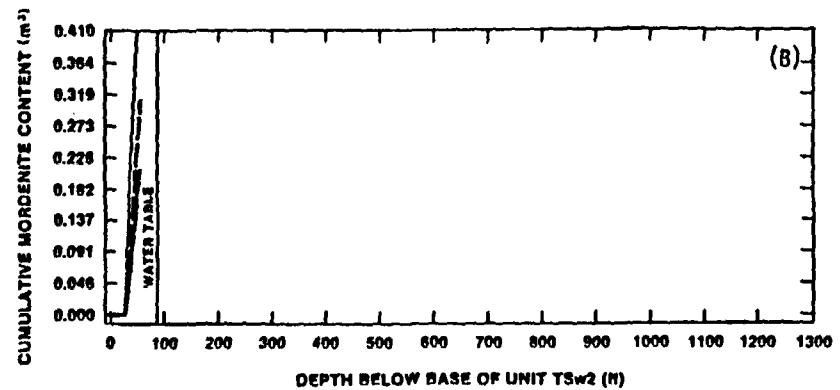
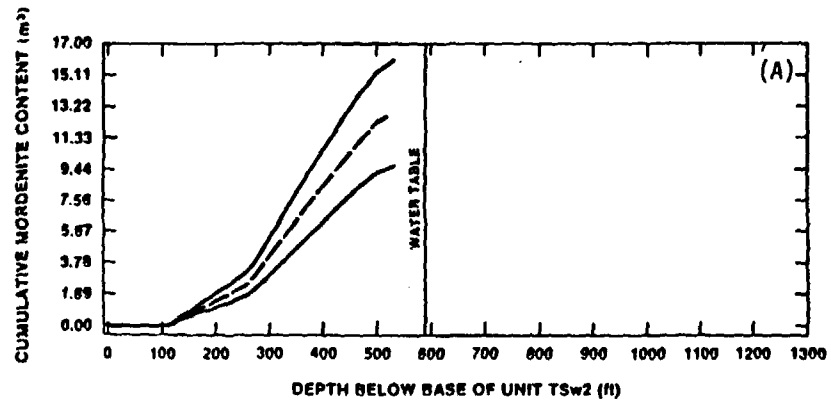


Figure 5.A.3. Comparison of Cumulative Contents of Mordenite Between the Base of Unit TSw2 and the Water Table. Ranges are the result of accounting for analytical uncertainty. Data from Bish and Vaniman (1985), Bish and Chipera (1986). (A) USW G-1. (B) USW G-2. (C) USW G-4. Note differences in ordinate scales.

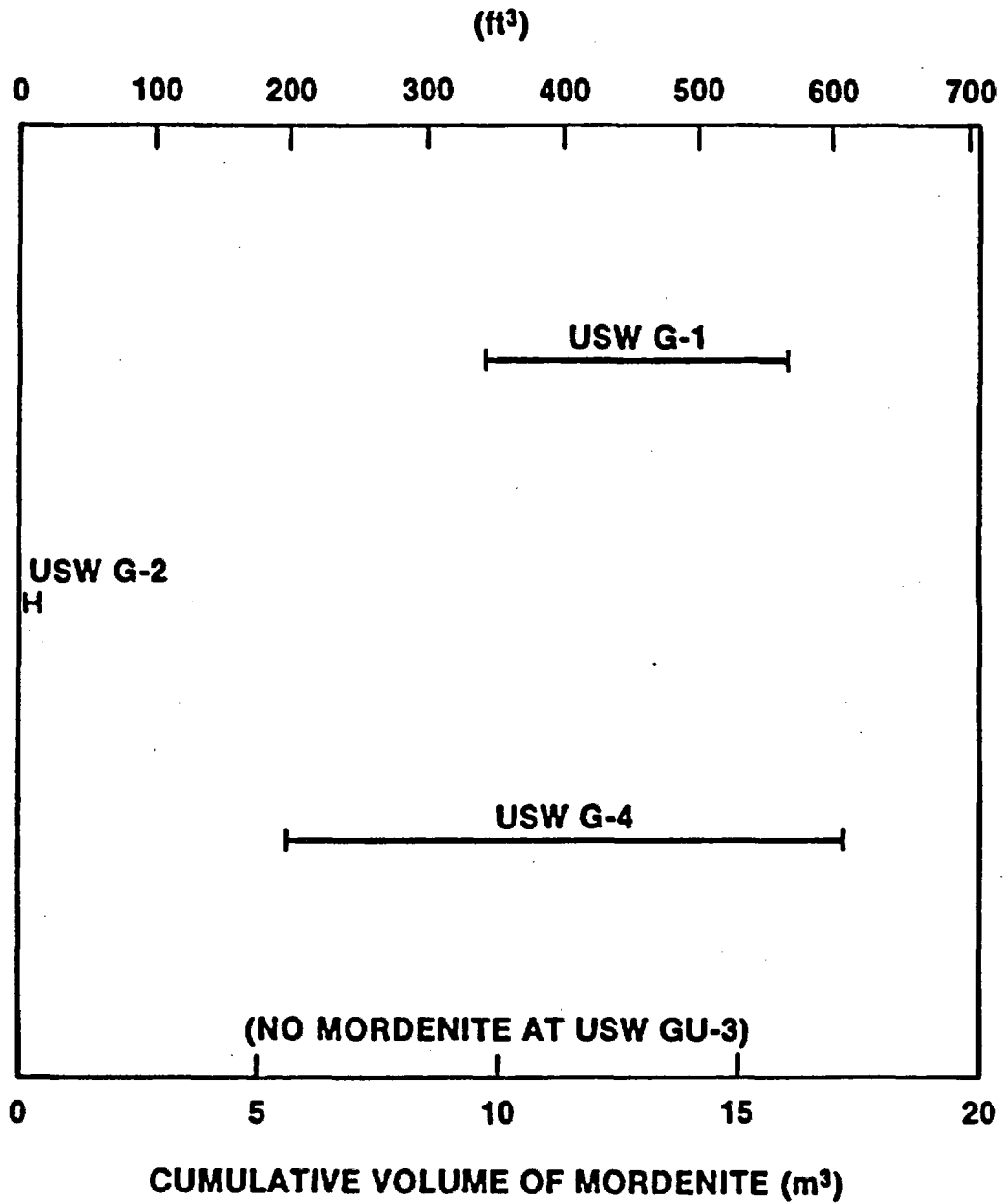


Figure 5.4-4. Comparison of Expected Ranges in Cumulative Content of Mordenite. Data from Bish and Vaniman (1985), Bish and Chipera (1986).

facilities in terms of mordenite volume and nonrepresentative of the southern portion of the area and of the region north of the area for the underground facilities.

#### 5.4.3 Smectite Clay

Figure 5.4-5 compares the cumulative volumes of smectite clay in USW G-1, USW G-2, USW GU-3, and USW G-4. The average volume in USW G-4 [Figure 5.4-5(D)] is  $3.8 \text{ m}^3$  ( $140 \text{ ft}^3$ ), as compared with  $3.0 \text{ m}^3$  ( $110 \text{ ft}^3$ ) in USW G-1,  $2.3 \text{ m}^3$  ( $80 \text{ ft}^3$ ) in USW G-2, and  $8.1 \text{ m}^3$  ( $280 \text{ ft}^3$ ) in USW GU-3.

The ranges in expected volume of clay in the four core holes are compared in Figure 5.4-6. Based on this comparison and on Figure 5.4-5, the ES-1 location (as represented by USW G-4) appears to be representative of the northern portion of the area for the underground facilities and of regions north of the area. Material between the base of unit TSw2 and the water table in the southern portion of the area apparently contains a greater volume of clay.

#### 5.4.4 Glass

Figure 5.4-7 compares the cumulative volume of glass in USW G-1, USW G-2, USW GU-3, and USW G-4. The average volume in USW G-4 [Figure 5.4-7(D)] is  $5.3 \text{ m}^3$  ( $190 \text{ ft}^3$ ), as compared with  $23.9 \text{ m}^3$  ( $840 \text{ ft}^3$ ) in USW G-1,  $5.2 \text{ m}^3$  ( $180 \text{ ft}^3$ ) in USW G-2, and  $62.4 \text{ m}^3$  ( $2200 \text{ ft}^3$ ) in USW GU-3.

The range in expected volume of glass in the four core holes are compared in Figure 5.4-8. Based on this comparison and on Figure 5.4-7, the ES-1 location (as represented by USW G-4) appears to be nonrepresentative of the area for the underground facilities in terms of the volume of glass in the material between the base of unit TSw2 and the water table.

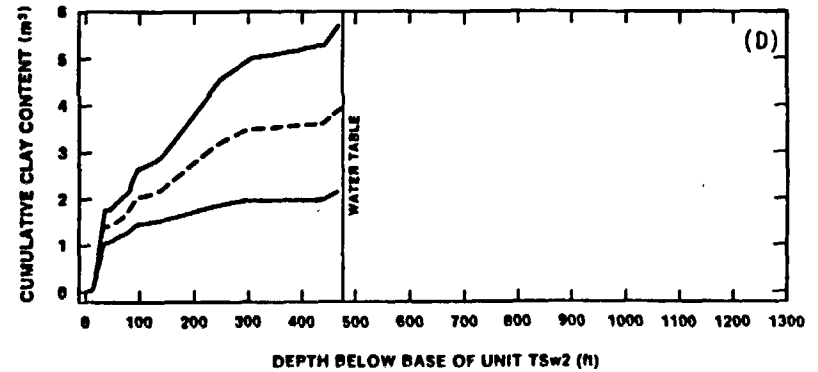
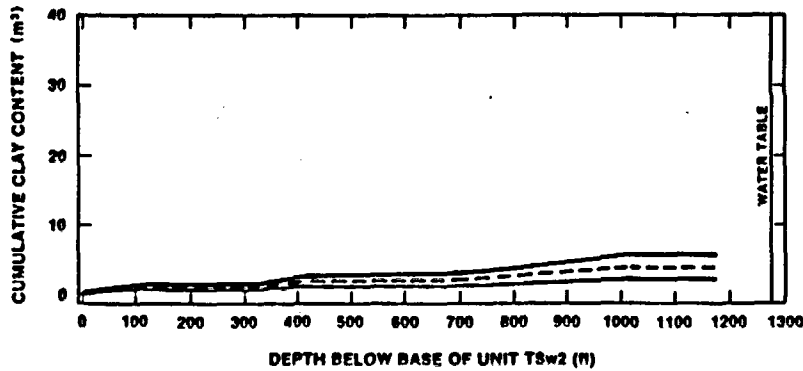
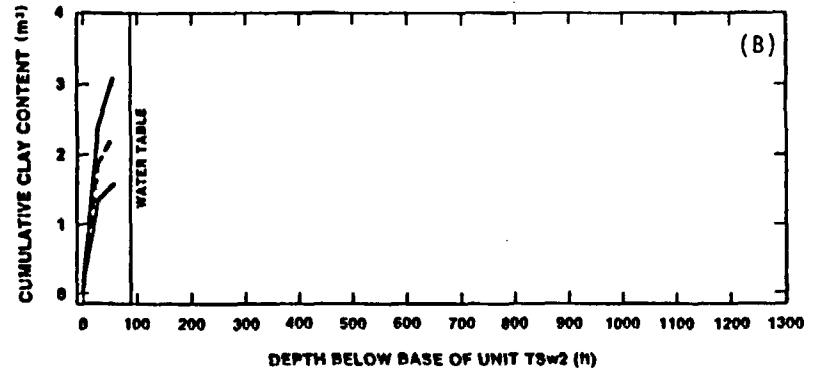
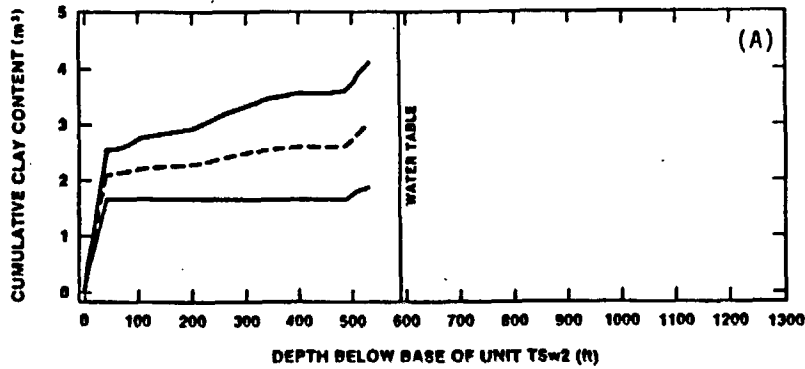


Figure 5.4-5. Comparison of Cumulative Contents of Clay Between the Base of Unit TSw2 and the Water Table. Ranges are the result of accounting for analytical uncertainty. Data from Bish and Vaniman (1985), Bish and Chipera (1986). (A) USW G-1. (B) USW G 2. (C) USW GU-3. (D) USW G-4. Note differences in ordinate scales.

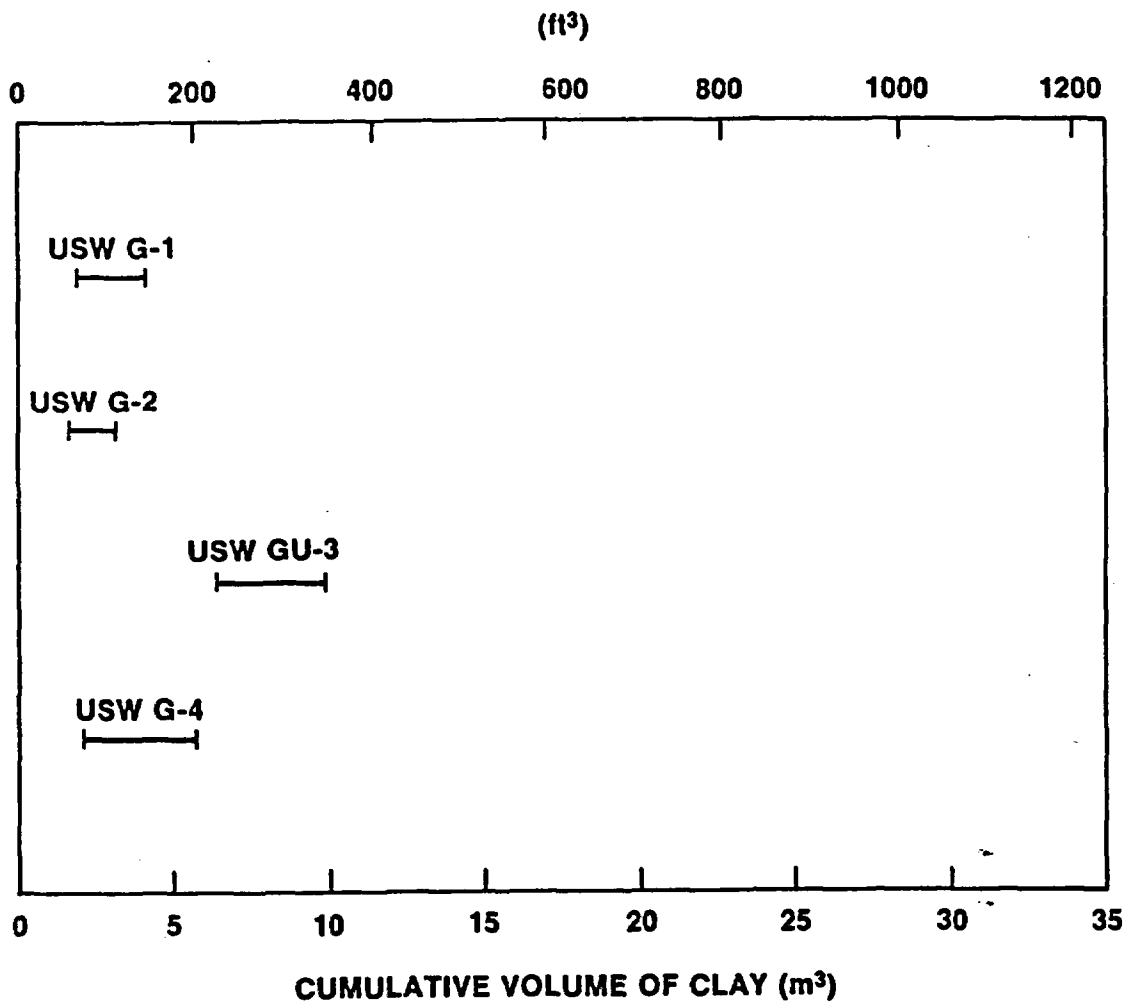


Figure 5.4-6. Comparison of Expected Ranges in Cumulative Content of Clay. Data from Bish and Vaniman (1985), Bish and Chipera (1986).

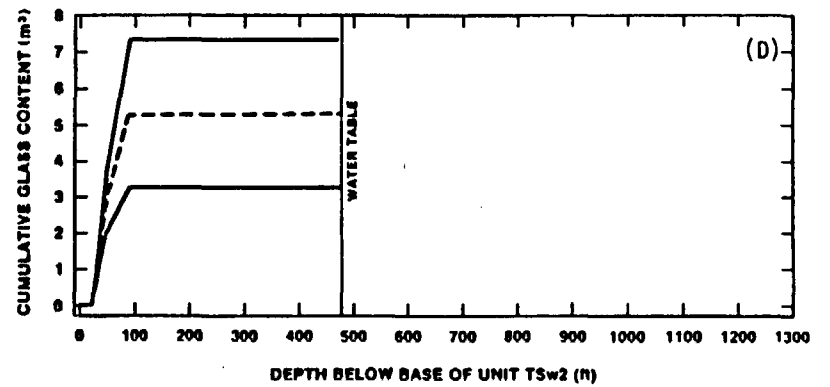
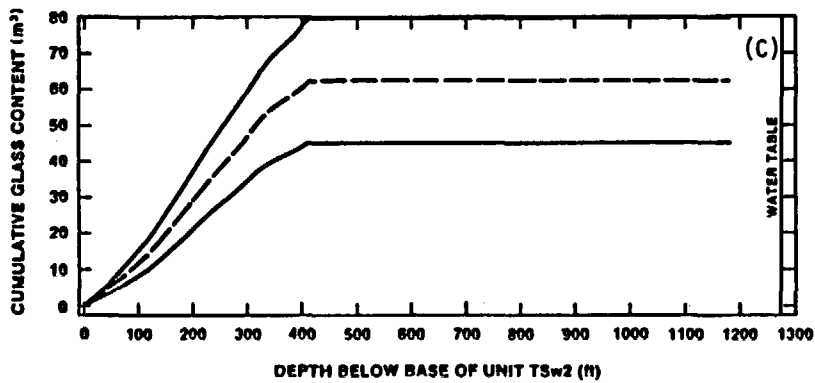
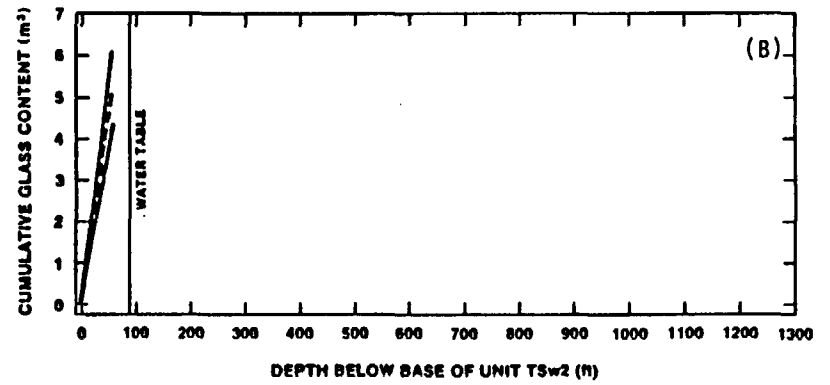
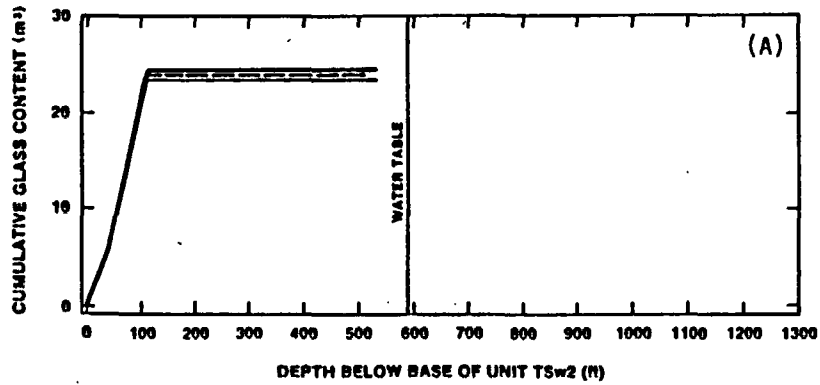


Figure 5.4-7. Comparison of Cumulative Contents of Glass Between the Base of Unit TS<sub>w</sub>2 and the Water Table. Ranges are the result of accounting for analytical uncertainty. Data from Bish and Vaniman (1985), Bish and Chipera (1986). (A) USW G-1. (B) USW G-2. (C) USW GU-3. (D) USW G-4. Note differences in ordinate scales.

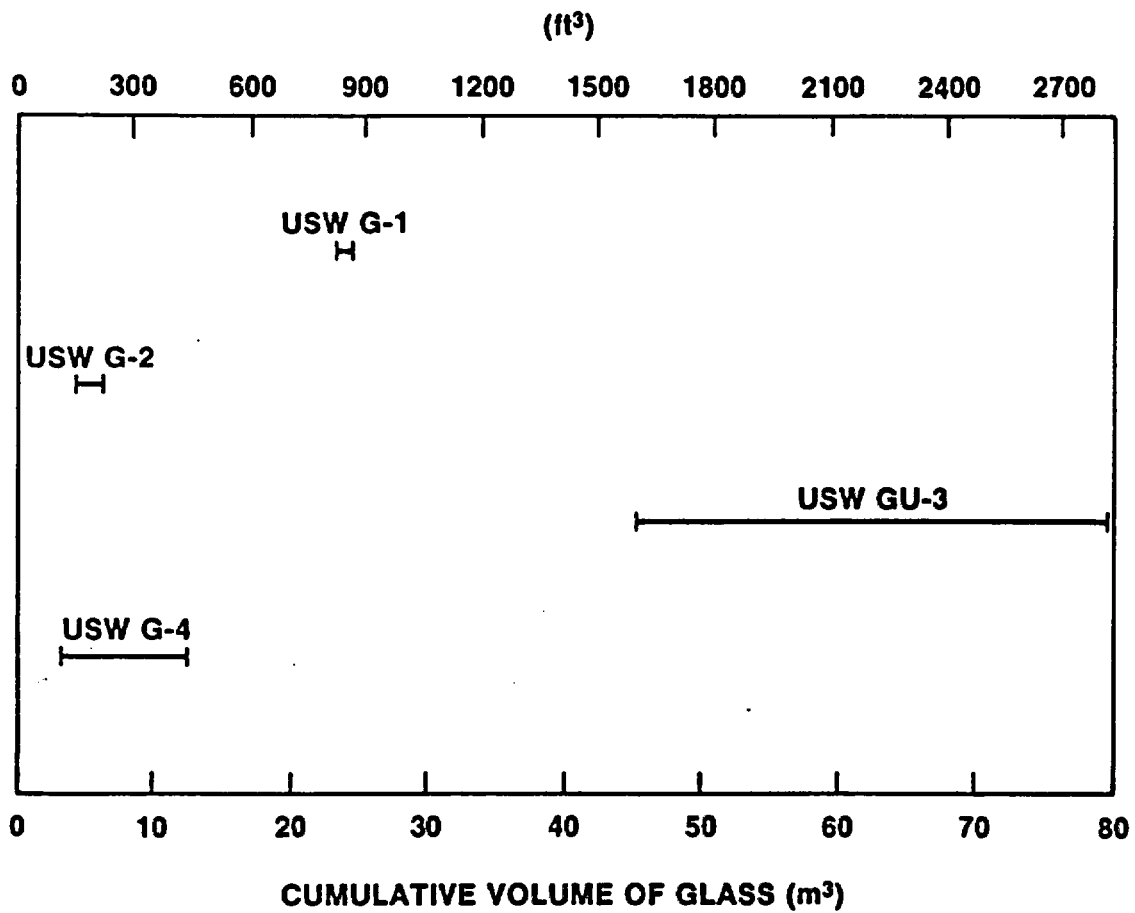


Figure 5.4-8. Comparison of Expected Ranges in Cumulative Content of Glass. Data from Bish and Vaniman (1985), Bish and Chipera (1986).

## 6.0 ROCK MECHANICS CHARACTERISTICS

In this section, evaluations of representativeness are made based on the entire thicknesses of units TSw1 and TSw2 rather than on the smaller depth intervals used in Section 4.3 and Chapter 5. This difference is necessary because for many of the rock mechanics characteristics, data for the smaller intervals are insufficient for an adequate evaluation.

### 6.1 In Situ Stress State at the ES-1 Location

The state of in situ stress that exists within the boundary of the underground facilities prior to the presence of underground excavations will affect the stability of such excavations as well as the response of the rock units to the presence of the excavations and heat-producing waste. The three principal stresses are assumed to be equivalent to the vertical, maximum horizontal, and minimum horizontal stresses.

#### 6.1.1 Vertical Stress

As is normal practice in the analysis of in situ stress, the vertical stress has been estimated as  $\rho gh$ , where  $\rho$  is the density of the rock,  $g$  is gravitational acceleration, and  $h$  is the thickness of the overlying material. (This was actually done as  $g\sum\rho_i h_i$  for all units above the datum of interest.) We realize that topography can influence the vertical stress beyond a simple change in  $h$ . However, the calculations of Savage et al. (1985) indicate that neglecting other effects and using  $\rho gh$  alone is a good first approximation.

The vertical stress has been calculated on a 250-ft (76-m) grid over the entire area for the underground facilities by combining estimated thicknesses of thermal/mechanical units (obtained from the three dimensional model of Ortiz et al., 1985) with estimated mean values for the in situ bulk densities of the units (Nimick and Schwartz, 1987). Stress has been calculated for three datums: the base of unit TSw1, the floor of the design subsurface facilities, and the base of unit TSw2.

The contact between units TSw1 and TSw2 has been corrected since the vertical stress calculations were performed, and the bulk densities of these two units have been revised slightly as well. The net effect of these changes is estimated to be a maximum increase of 0.1 MPa (15 psi) in the vertical stresses discussed in the remainder of this section.

Figure 6.1-1 is a contour map of the estimated vertical stresses within the boundary of the underground facilities at the bottom of unit TSw1 (top of unit TSw2). The vertical stress at the ES-1 location is expected to be approximately 3.8 MPa (550 psi). The approximate range of vertical stresses for this datum is 0 to 6 MPa (0 to 870 psi) for the area for the underground facilities, with most of the area having vertical stresses of 4 to 5 MPa (580 to 730 psi) on the contact. Thus, the stress on the base of TSW1 at the ES-1 location is slightly lower than average for the area.

At the floor of the design subsurface facilities, the vertical stress ranges from 4 to 9 MPa (580 to 1310 psi) within the boundary of the underground facilities (Figure 6.1-2), with most stresses between 7 and 8 MPa (1020 and 1160 psi). At the ES-1 location, the stress is estimated to be approximately 6.5 MPa (940 psi), again slightly lower than average.

The vertical stress at the base of unit TSw2 ranges from 5 to 10 MPa (730 to 1450 psi) within the boundary of the underground facilities (Figure 6.1-3). For most of the area, the stress is 8 to 9 MPa (1160 to 1310 psi). At the ES-1 location, a vertical stress of approximately 8 MPa (1160 psi) is expected. As is the case for the other datums, the stress at the ES-1 location is at the lower side of the expected stress range for a large part of the area for the underground facilities.

Although vertical stress at the ES-1 location itself is expected to be somewhat lower than average for the area for the underground facilities, lateral drifts excavated from the main test level in ES-1 should encounter a wider range of in situ stress conditions. Based on Figure 6.1-2, vertical stresses should be lower in a north- to northeast-trending drift and higher in drifts trending west or

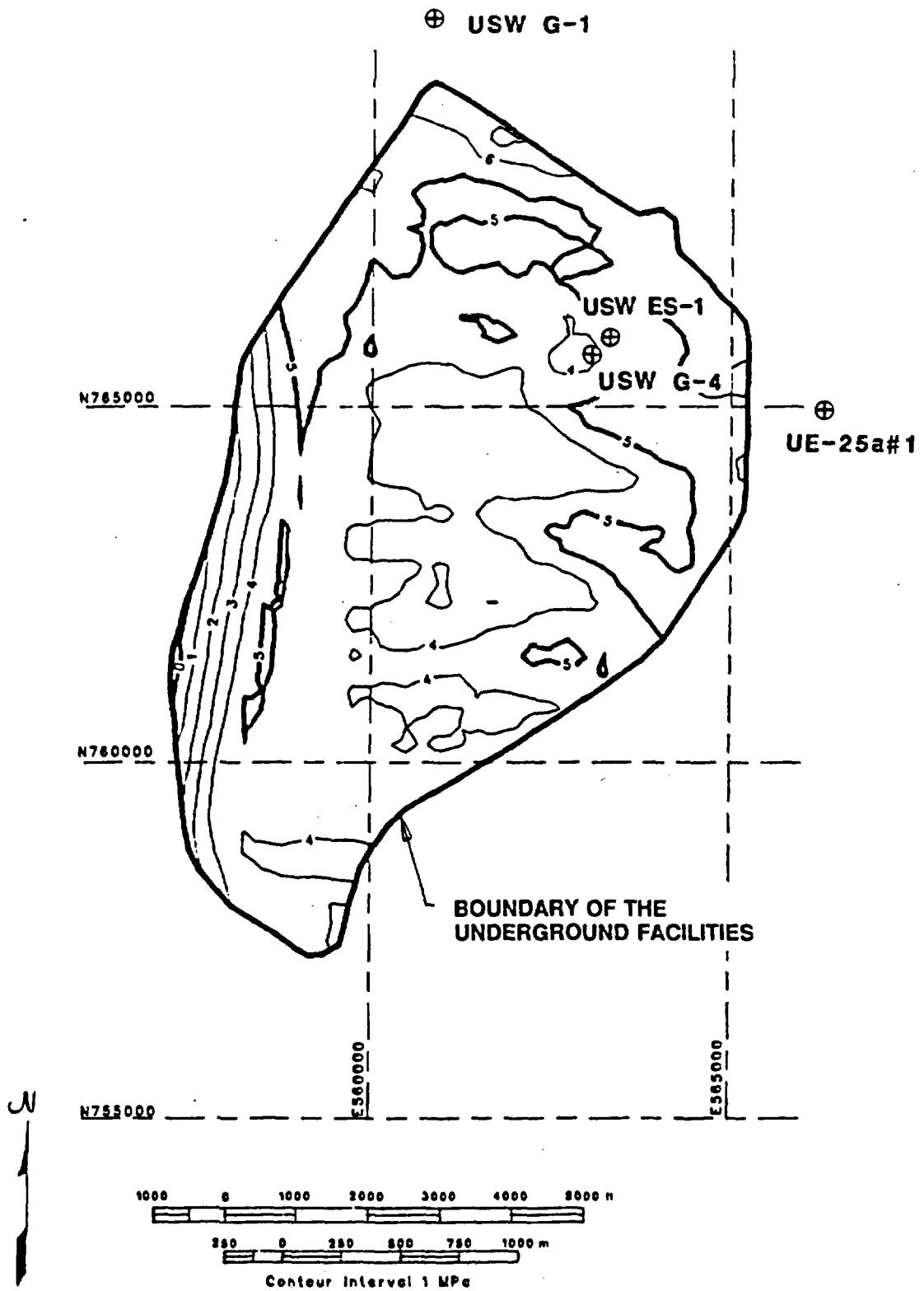


Figure 6.1-1. Estimated Vertical Stresses at the Base of Unit TSw1 (Nimick and Schwartz, 1987)

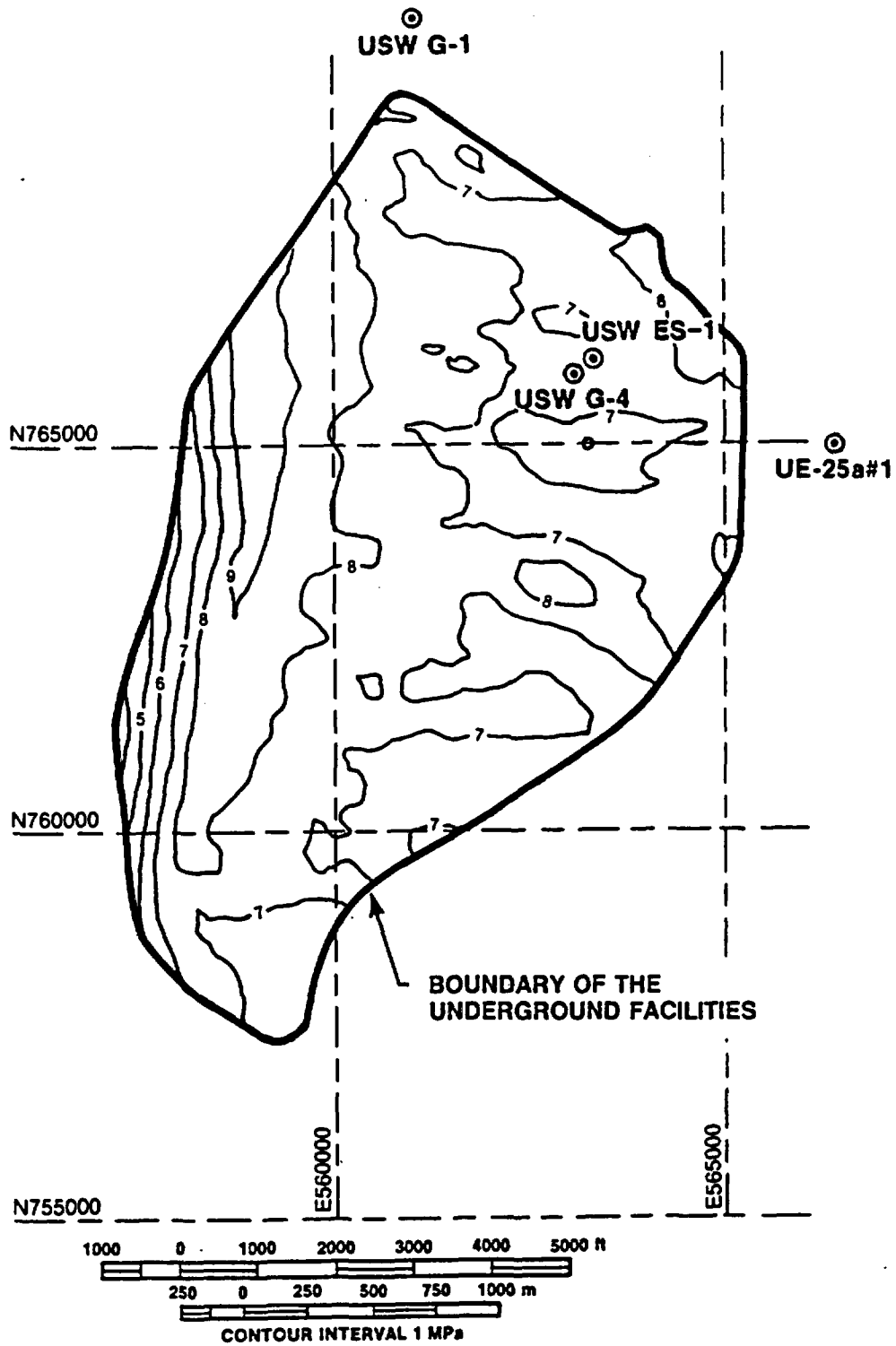


Figure 6.1-2. Estimated Vertical Stresses at the Floor of the Design Subsurface Facilities (Nimick and Schwartz, 1987)

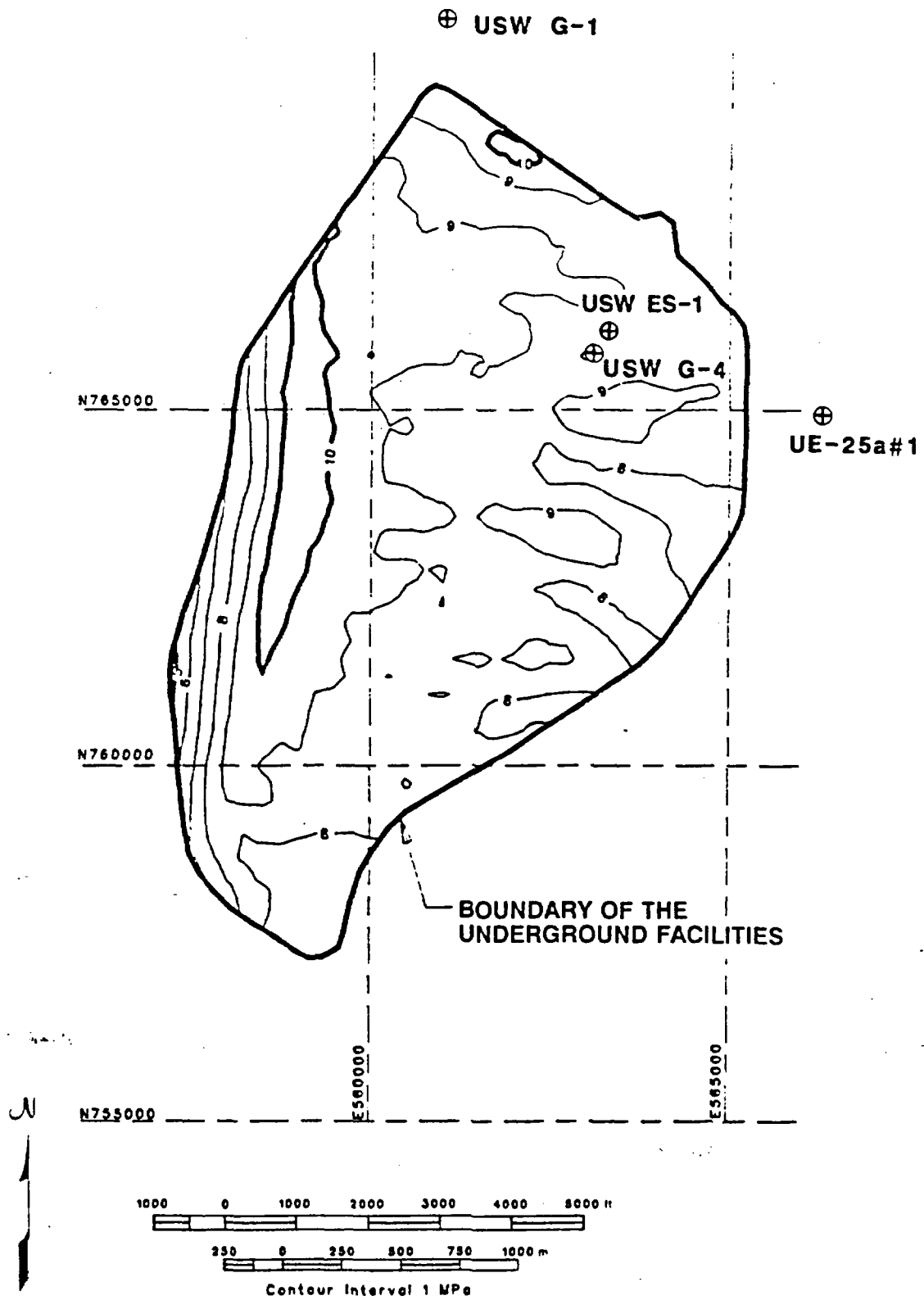


Figure 6.1-3. Estimated Vertical Stresses at the Base of Unit TSw2 (Nimick and Schwartz, 1987)

southwest. These results indicate that the estimated vertical stress conditions within the main test level and lateral drifts will sample a large portion of the overall range in vertical stresses to be expected in the subsurface facilities. In addition, the upper demonstration breakout room in unit TSW1 will encounter lower vertical stress values than those at the main test level, further extending the ranges of stresses encountered. Thus, the ES-1 location is considered to be representative in terms of vertical in situ stress.

#### 6.1.2 Horizontal Stresses

Although measurements of the in situ horizontal stresses at Yucca Mountain are limited, especially in the unsaturated zone, the existing data are in reasonable agreement within themselves and with regional data (Stock et al., 1985). The minimum horizontal stress has been inferred to trend NW to WNW from observation of hydraulic fractures in USW G-1 and USW G-2. The relative magnitudes of the three stresses are vertical > maximum horizontal > minimum horizontal, indicative of a normal-faulting stress regime. The uniformity of the stress indications both at the site and regionally suggest that results for horizontal stresses that will be obtained in the ESF should be representative of the entire area for the underground facilities.

### 6.2 Physical Properties of the Welded, Devitrified Portion of the Topopah Spring Member

#### 6.2.1 Grain Density

The bulk density of the welded, devitrified portion of the Topopah Spring Member is used to predict temperatures resulting from waste emplacement and to estimate vertical stresses resulting from overburden loads. Because of the variable in situ saturation state in these tuffs, both initially and as a result of temperature changes resulting from the presence of heat-producing waste, the components of the bulk density (grain density, porosity, and saturation) must be known.

Statistical analysis of available data for thermal/mechanical unit TSw2 indicates that the mean value for grain density of this unit from a given core hole is indistinguishable from that for any other core hole (Nimick and Schwartz, 1987). This conclusion is supported by comparison of the ranges of grain density for unit TSw2 in the individual coreholes (Figure 6.2-1). Thus, material at the ES location should be representative of unit TSw2 throughout the area for the underground facilities.

In unit TSw1, statistical analysis indicates that the mean value for grain density for core hole UE-25a#1 is higher than the grain density for other core holes. The difference is attributed to variations in tridymite content (Nimick and Schwartz, 1987). However, comparison of the ranges of grain density found for unit TSw1 in the individual core holes (Figure 6.2-2) indicates that grain densities measured on samples of unit TSw1 from ES-1 (as represented by USW G-4) should be representative of the majority of unit TSw1 within the boundary of the underground facilities.

#### 6.2.2 Matrix Porosity

The porosity of the welded, devitrified portion of the Topopah Spring Member must be known in order to calculate the bulk density as a function of its components (grain density, porosity, and saturation). In addition, a number of other thermal and mechanical properties are functions of porosity, including unconfined compressive strength and Young's modulus (Price and Bauer, 1985); cohesion and angle of internal friction (Nimick and Schwartz, 1987); thermal conductivity (Lappin, 1980); and heat capacity (Tillerson and Nimick, 1984).

Statistical analysis of available porosity data has been performed for thermal/mechanical units TSw1 and TSw2 (Nimick and Schwartz, 1987). The results for unit TSw2 indicate the following:

- mean porosity in USW G-1 is greater than mean porosities in USW GU-3 and USW G-4; and

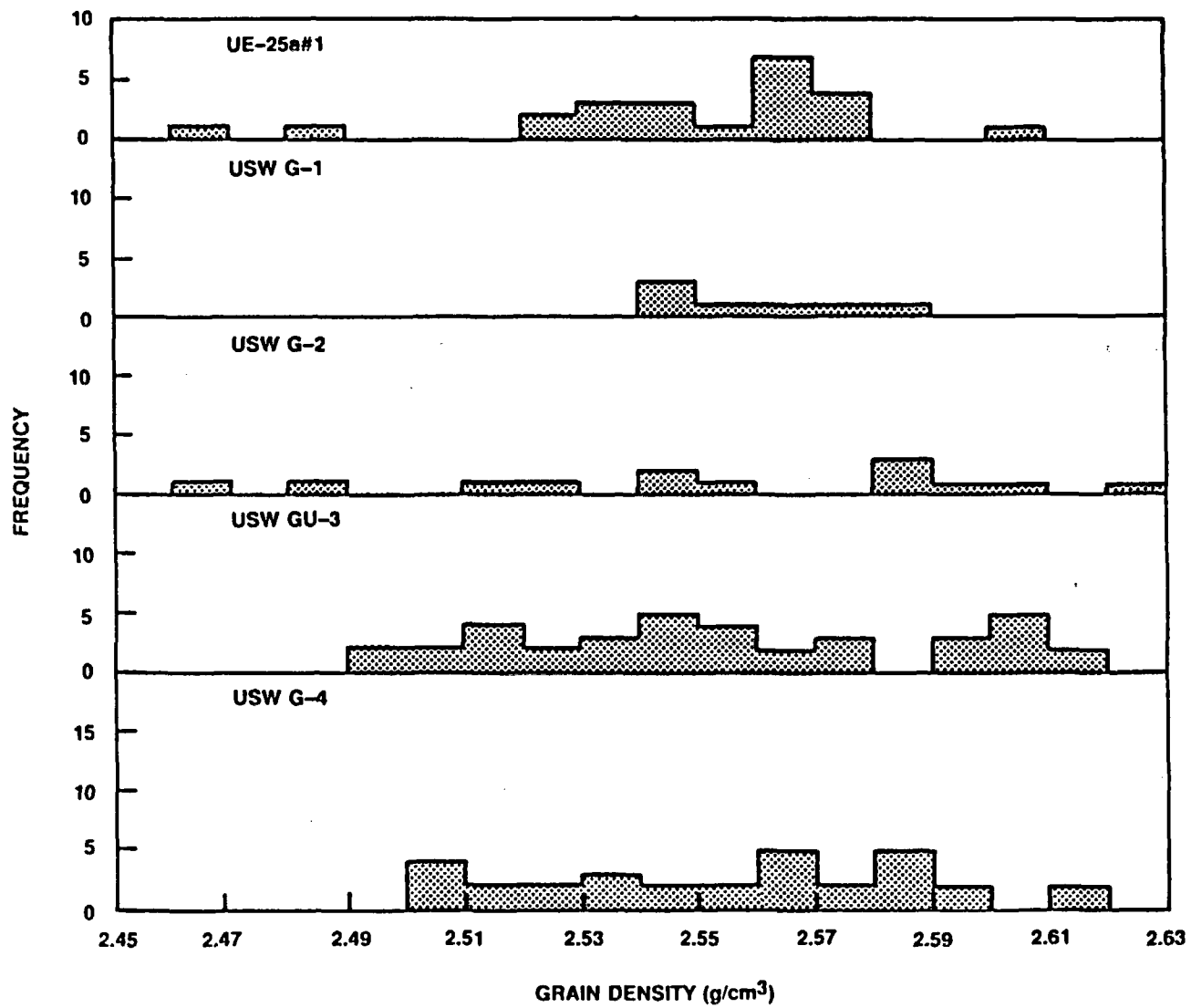


Figure 6.2-1. Comparison of Ranges of Grain Density for Unit TSw2. Data from Nimick and Schwartz' (1987).

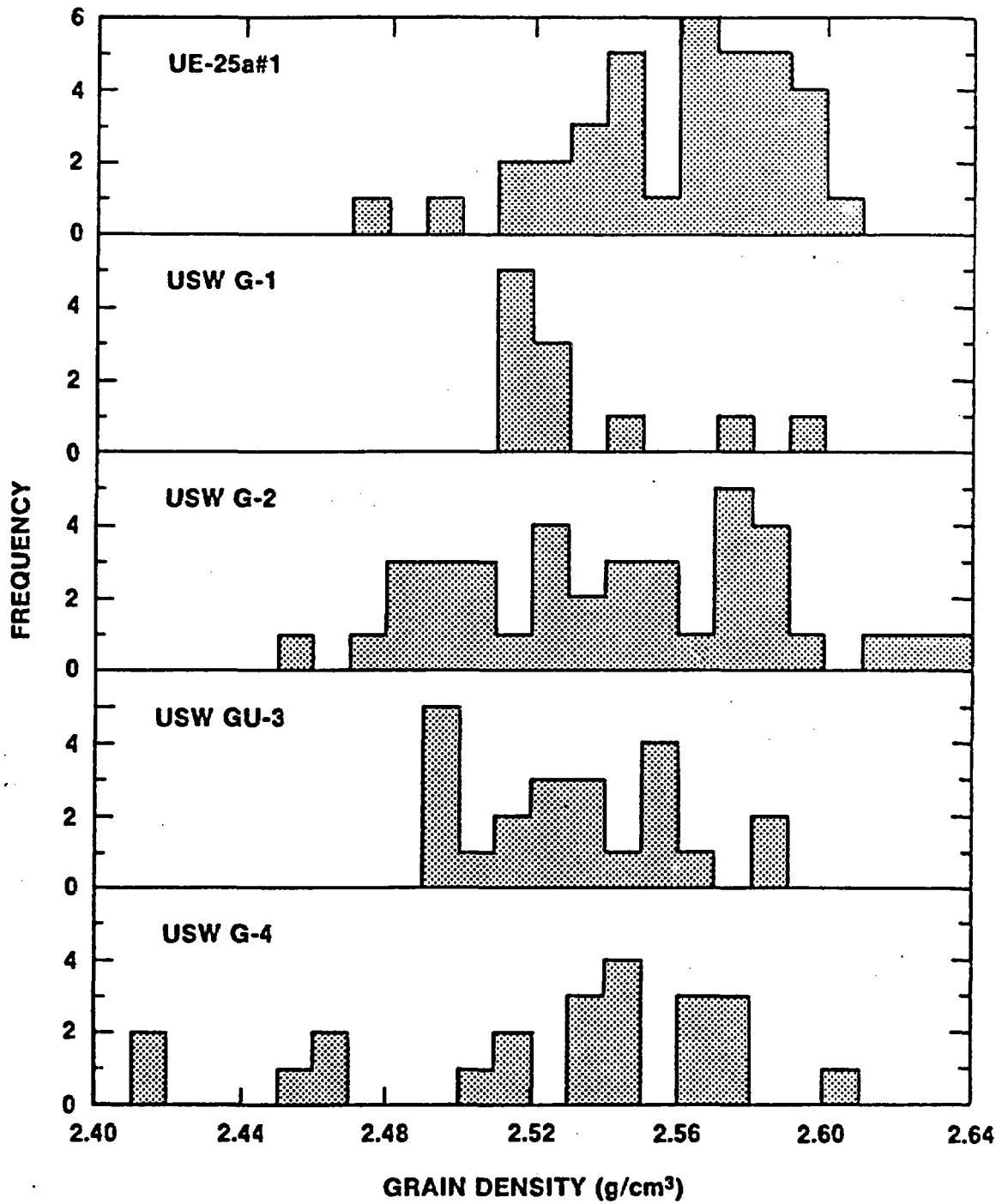


Figure 6.2-2. Comparison of Ranges of Grain Density for Unit TSw1. Data from Nimick and Schwartz (1987).

- mean porosity in USW G-2 is greater than mean porosity in USW GU-3.

Comparison of the ranges in matrix porosity (Figure 6.2-3) indicates that the material sampled at the ES-1 location (as represented by USW G-4) will have a range in matrix porosity covering most, if not all, of the range to be expected in other core holes. Thus, the ES-1 location should be representative of the entire area for the underground facilities.

Statistical comparison also indicated differences in mean values of matrix porosity between core holes for unit TSw1. The mean matrix porosity from USW GU-3 was greater than all other mean porosities, and the mean porosity in USW G-4 was greater than that in USW G-2. However, comparison of the ranges in matrix porosity (Figure 6.2-4) leads to the same conclusion stated in the preceding paragraph: the ES-1 location (as represented by USW G-4) should be representative of the entire area for the underground facilities.

### 6.3 Mechanical Properties of the Welded, Devitrified Portion of the Topopah Spring Member

#### 6.3.1 Poisson's Ratio

Poisson's ratio is an elastic parameter used in the calculation of the two- or three-dimensional deformational response to imposed stresses. Thus, the parameter is required in order to calculate the deformations induced by the presence of underground openings, heat-producing waste, or both.

Statistical analysis of Poisson's ratio data, for unit TSw2 devitrified portion of the Topopah Spring Member indicates a significant differences in mean values between core holes USW GU-3 and USW G-4 (Nimick and Schwartz, 1987). Comparison of the ranges of Poisson's ratio for the individual core holes (Figure 6.3-1) substantiates this conclusion. Therefore, data for Poisson's ratio from samples from ES-1 may not be representative.

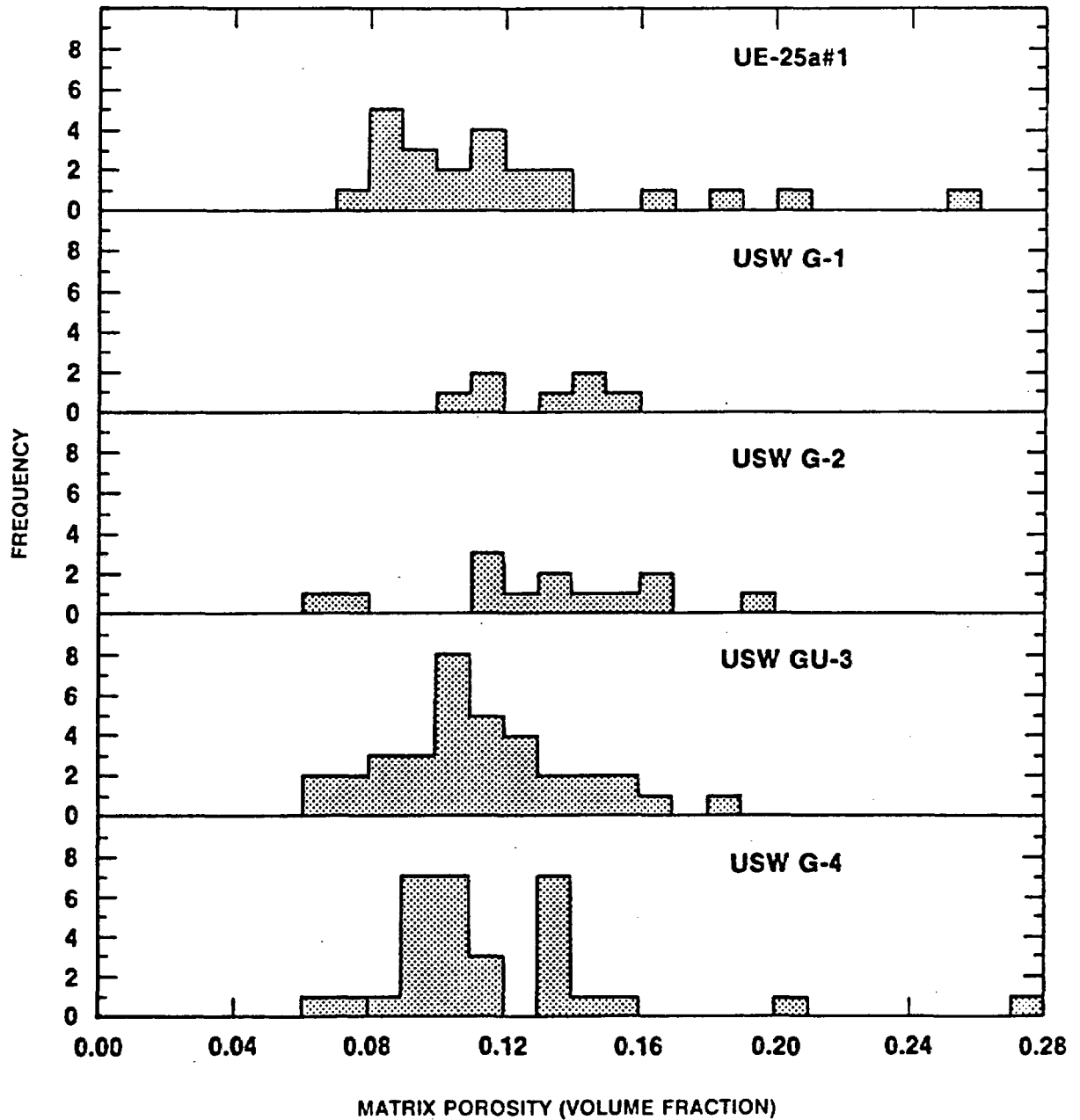


Figure 6.2-3. Comparison of Ranges of Matrix Porosity for Unit TSw2. Data from Nimick and Schwartz (1987).

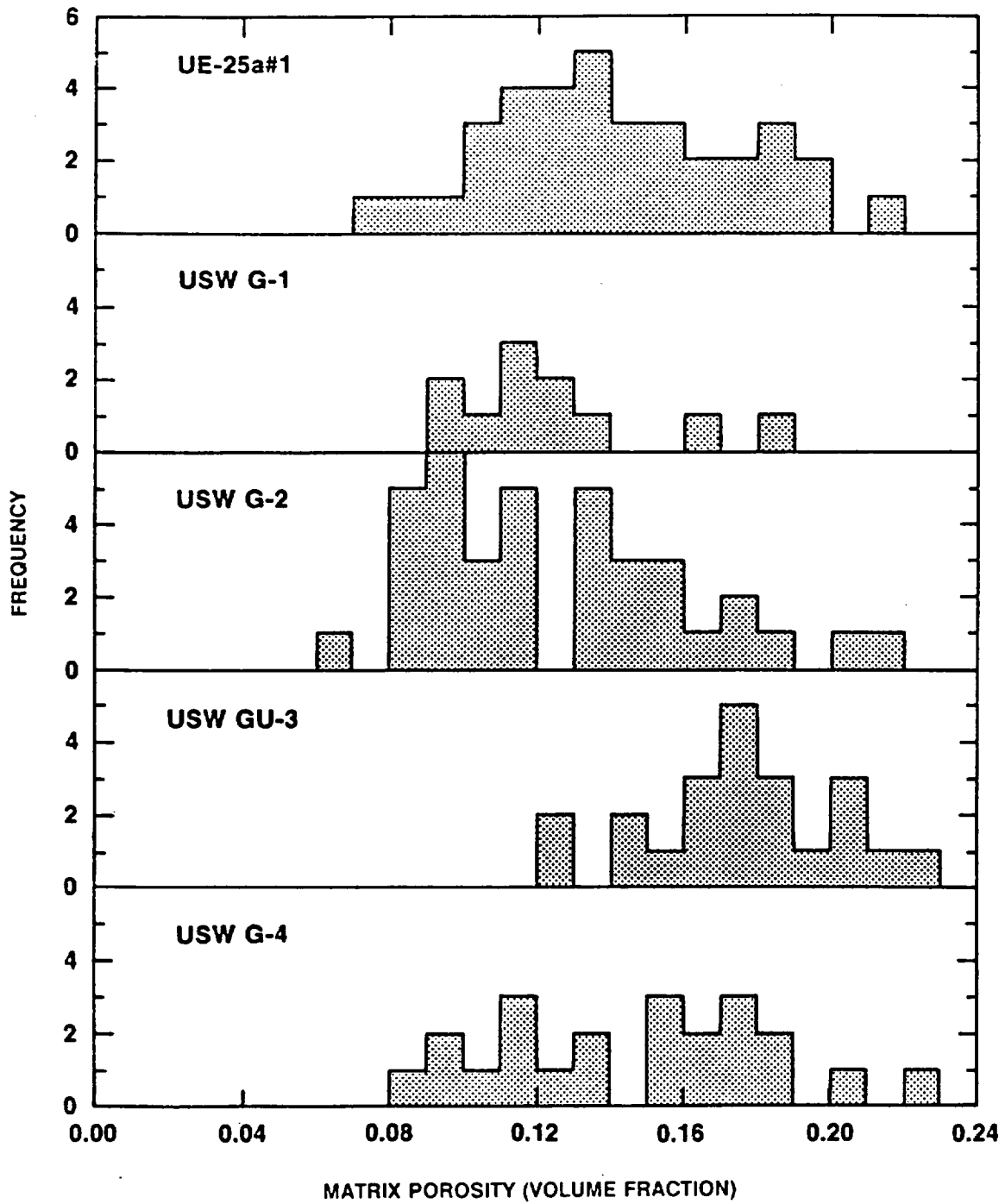


Figure 6.2-4. Comparison of Ranges of Matrix Porosity for Unit TSw1. Data from Nimick and Schwartz (1987).

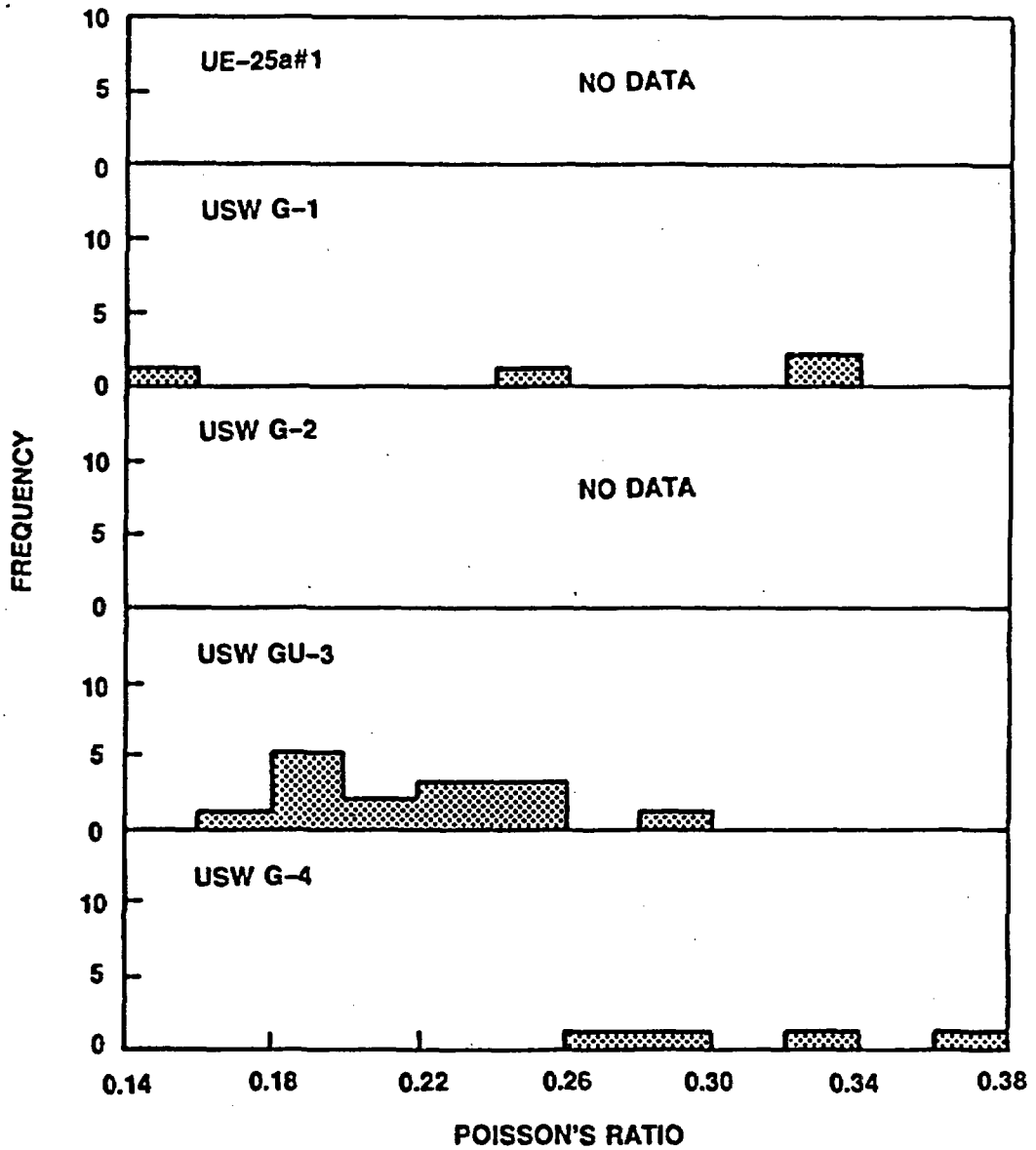


Figure 6.3-1. Comparison of Ranges of Poisson's Ratio for Unit TSw2. Data from Nimick and Schwartz (1987).

Data for Poisson's ratio are available for unit TSw1 only in USW GU-3, so no conclusions can be made about the representativeness of the ES-1 location for the Poisson's ratio of unit TSw1.

### 6.3.2 Unconfined Compressive Strength

Unconfined compressive strength serves as an index in empirical rock classification schemes that assess opening stability. In addition, the strength is used in the evaluation of the results of numerical calculations of the mechanical response of the tuff to the presence of underground openings.

Few data are available for the unconfined compressive strength of unit TSw1. Comparison of the ranges obtained for individual coreholes (Figure 6.3-2) does not justify drawing conclusions about the representativeness of the ES-1 location.

Statistical analysis of data for the unconfined compressive strength of unit TSw2 indicates a difference in mean values only between USW G-1 and USW G-4 (Nimick and Schwartz, 1987). Figure 6.3-3 provides a comparison of the ranges of data for each core hole. Based on this comparison, the preliminary conclusion is made that the ES-1 location (as represented by USW G-4) will be representative of the area for the underground facilities in terms of unconfined compressive strength.

The preceding paragraphs are relevant to material without lithophysal cavities. The unconfined compressive strength of material containing lithophysal cavities is related to the volume percentage of cavities and associated vapor-phase-altered material and clay content because of the relationship between strength and functional porosity (e.g., Price et al., 1985). This relationship could be used to make inferences about representativeness. However, in the absence of experimental data, we cannot draw firm conclusions about the representativeness of the compressive strength of this material.

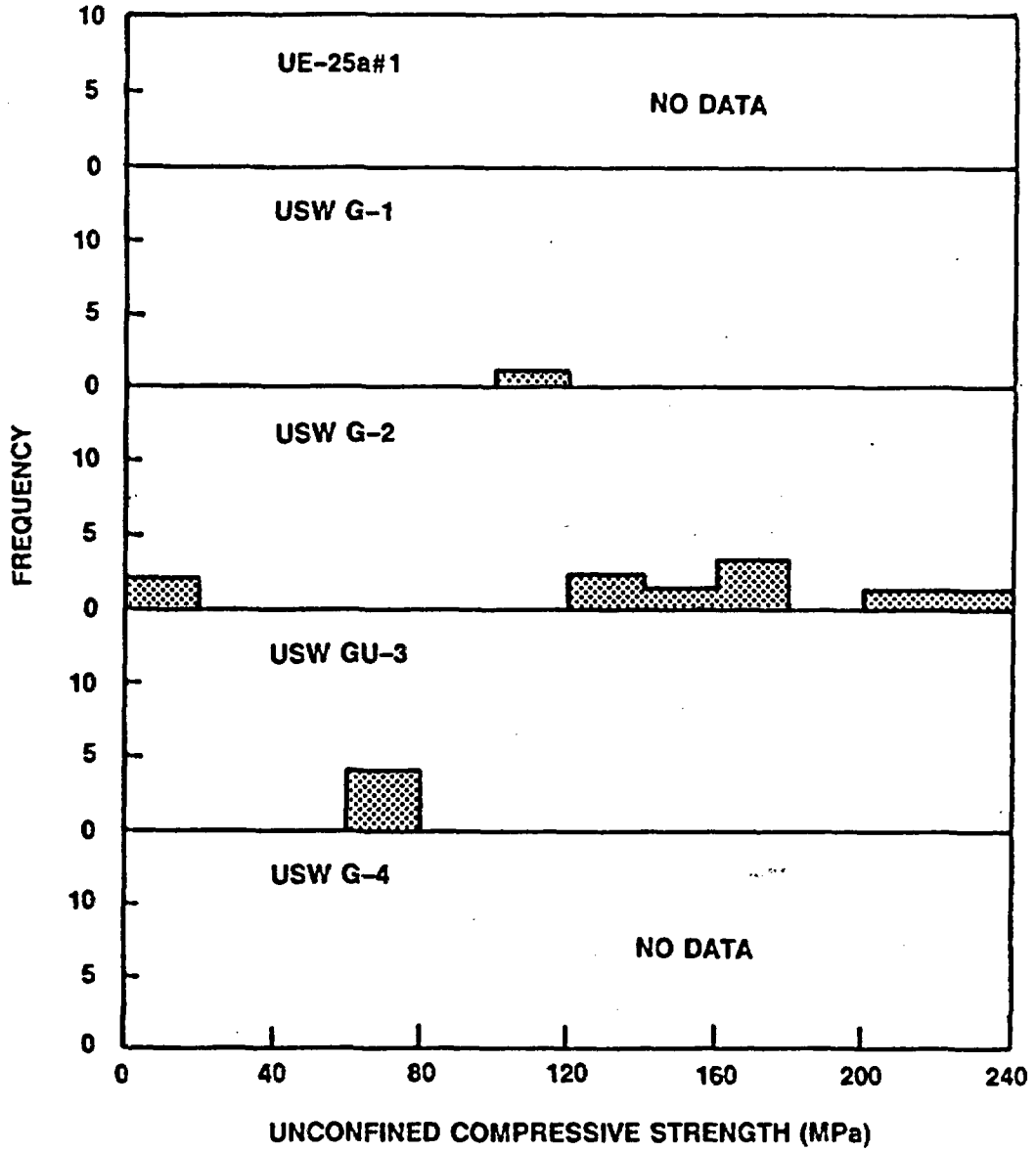


Figure 6.3-2. Comparison of Ranges of Unconfined Compressive Strength for Unit TSw1. Data from Nimick and Schwartz (1987).

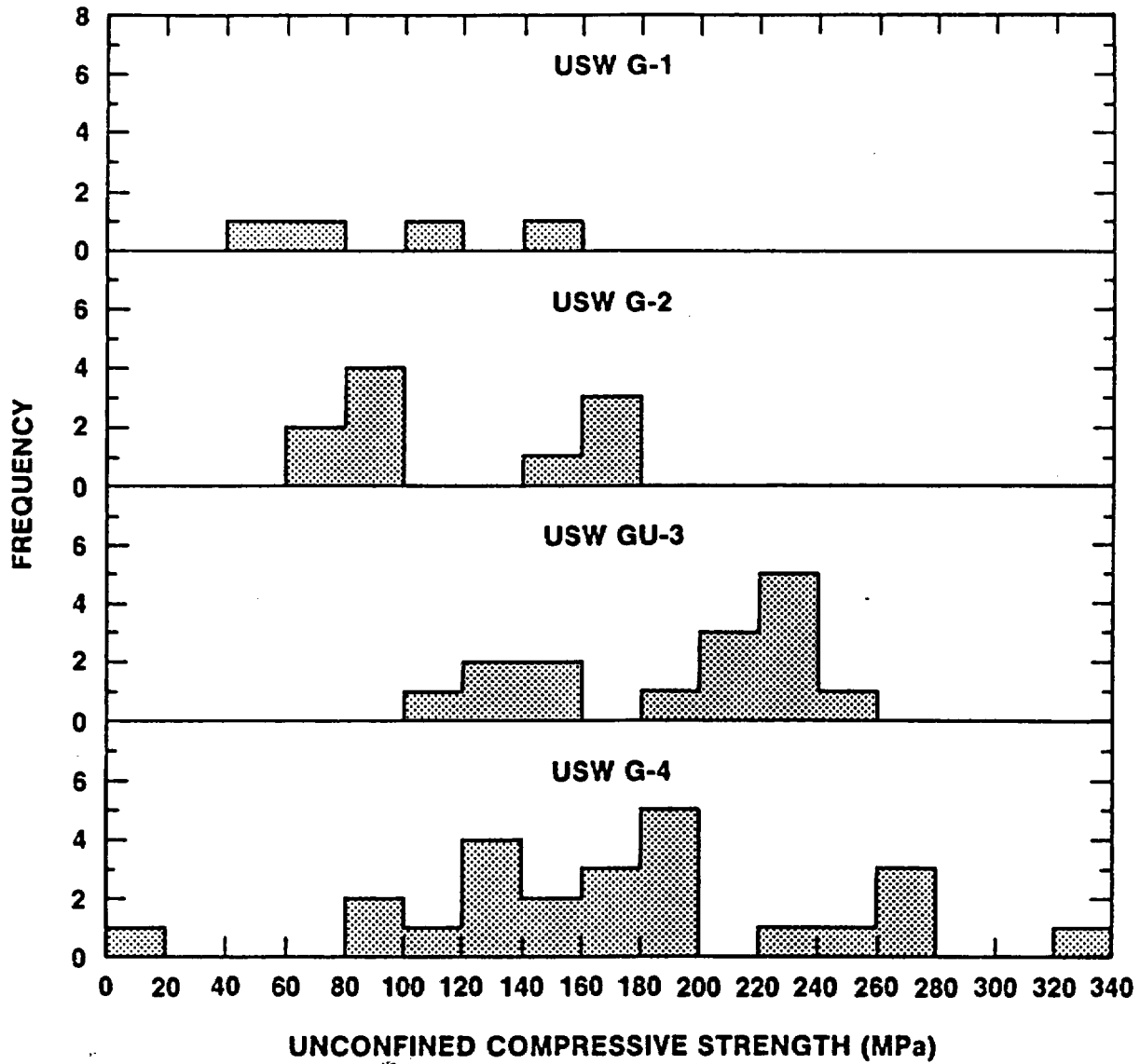


Figure 6.3-3. Comparison of Ranges of Unconfined Compressive Strength for Unit TSw2. Data from Nimick and Schwartz (1987).

### 6.3.3 Young's Modulus

Young's modulus is an elastic parameter used in the calculation of the deformational response to imposed stresses. In addition, the modulus is used with the thermal expansion coefficient to estimate stresses induced by temperature changes. Thus, this parameter is required in order to calculate the elastic deformation around underground openings as well as the stress and deformation resulting from the presence of heat-producing wastes.

Few data are available for the Young's modulus of unit TSw1. Comparison of ranges of Young's modulus for individual coreholes (Figure 6.3-4) does not justify drawing conclusions about the representativeness of unit TSw1 at the ES-1 location.

Statistical analysis of the data for the Young's modulus of unit TSw2 shows no differences in mean values resulting from a comparison of data from different core holes (Nimick and Schwartz, 1987). This conclusion is supported by comparison of ranges for the individual coreholes (Figure 6.3-5). Thus, material at the ES-1 location should be representative of unit TSw2 throughout the area for the underground facilities.

The preceding paragraphs are relevant to material without lithophysal cavities. The Young's modulus of material containing lithophysal activities is related to the volume percentage of cavities and associated vapor phase altered material and clay content because of the relationship between Young's modulus and functional porosity (e.g., Price et al., 1985). This relationship could be used to make inferences about representativeness. However, in the absence of experimental data, we cannot draw firm conclusions about the representativeness of the Young's modulus of this material.

### 6.3.4 Mohr-Coulomb Parameters

The two Mohr-Coulomb parameters, cohesion and the angle of internal friction, combine to give a failure criterion for the intact-rock portion of the units that will be encountered in ES-1. This failure criterion,

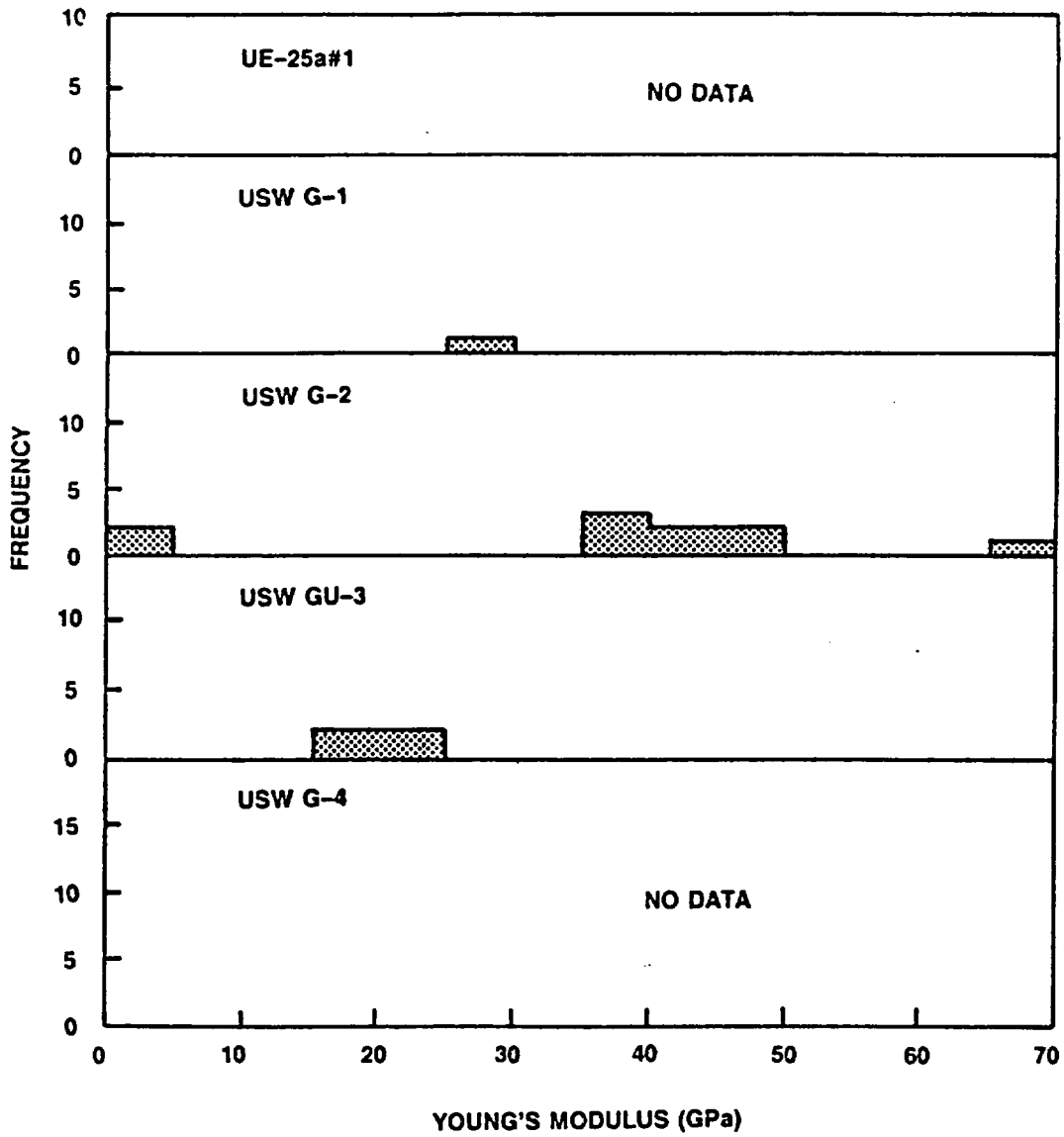


Figure 6.3-4. Comparison of Ranges of Young's Modulus for Unit TSw1. Data from Nimick and Schwartz (1987).

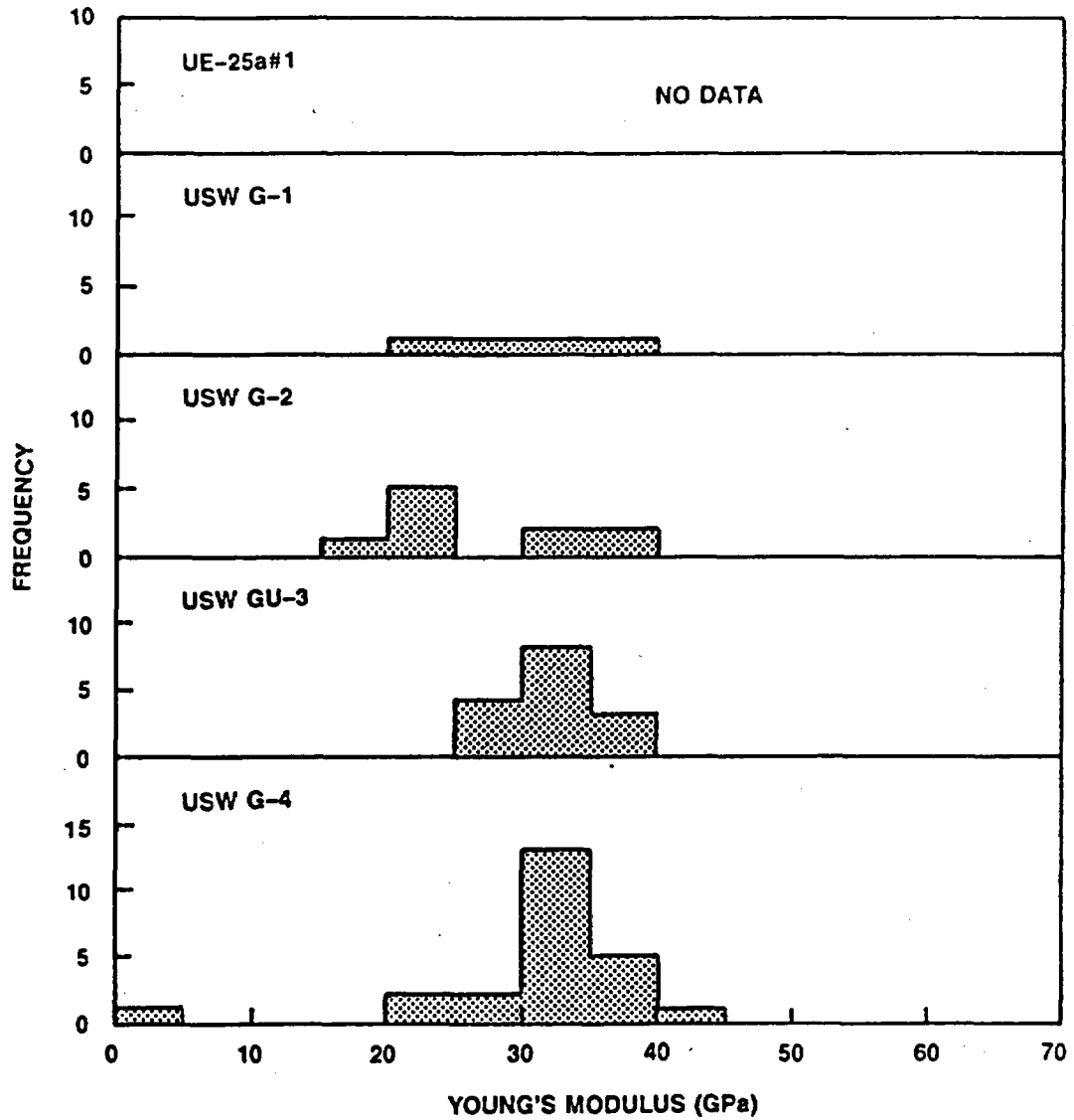


Figure 6.3-5. Comparison of Ranges of Young's Modulus for Unit TSw2. Data from Nimick and Schwartz (1987).

when combined with a description for the mechanical response of fractures, can be used in the assessment of the stability of underground openings.

Very few experimental data are available on which to base a decision concerning the representativeness of the ES-1 location in terms of the Mohr-Coulomb parameters. Nimick and Schwartz (1987) have described relationships between the two parameters and porosity. These relationships could be used to make inferences about representativeness. However, in the absence of experimental data, we cannot draw firm conclusions about the representativeness of Mohr-Coulomb parameters.

#### 6.3.5 Tensile Strength

The tensile strength of the matrix of the welded, devitrified Topopah Spring Member may be relevant in estimating the stability of waste emplacement holes and thus to the question of retrievability. In addition, tensile strength is used in the interpretation of hydraulic fracturing data that can be used to estimate in situ stress.

No data are available for the tensile strength of units TSw1 or TSw2 at the ES-1 location, or from any location other than UE-25a#1. Price (1983) suggested a linear relationship between tensile strength (as determined by the "Brazilian" technique) and matrix porosity. This relationship could be used to make inferences about representativeness. However, in the absence of experimental data we cannot draw firm conclusions about the representativeness of tensile strength.

### 6.4 Thermal Properties of the Welded, Devitrified Portion of the Topopah Spring Member

#### 6.4.1 Thermal Conductivity

The thermal conductivity of the welded, devitrified portion of the Topopah Spring Member contributes to the calculation of temperature fields induced by heat-producing material. In turn, these temperatures are used in analysis of allowable power density and in the estimation of thermally induced stresses.

Available data for the thermal conductivity of the welded, devitrified portion of the Topopah Spring Member are tabulated in Appendix B. Figure 6.4-1 compares the ranges of data for nominally saturated samples ( $s = 0.90-0.95$ ). For unit TSw1, the data ranges for all five core holes overlap extensively, so that the ES-1 location (as represented by USW G 4) may be considered to be representative of the entire area for the underground facilities.

The ranges of thermal conductivity data for unit TSw2 are entirely disparate. Thus, based on the limited number of available data, the ES-1 location may not be representative of the area for the underground facilities. Sampling opportunities provided by the lateral drifts at the main test level may ameliorate this situation.

The above paragraph is based on tests performed on samples containing no lithophysal cavities and very little vapor-phase altered material. The representativeness of the thermal conductivity of tuff in ES-1 containing lithophysal cavities, or vapor-phase altered material, or both is related to the representativeness of these components (Section 4.3). However, in the absence of experimental data, we cannot draw firm conclusions on the representativeness of thermal conductivity of this material.

#### 6.4.2 Heat Capacity

Heat capacity is used in calculations of the temperatures induced in the tuff by heat-producing waste. In turn, these temperatures are used in analysis of allowable power density and in the estimation of thermally induced stresses.

To date, no experimental data are available for the heat capacity of the tuffs at Yucca Mountain. However, heat capacities of the solid portion of samples of the welded, devitrified portion of the Topopah Spring Member have been estimated from data on bulk chemical composition (Nimick and Schwartz, 1987). Although these data are insufficient to analyze spatial variability, the extremely small variations between the

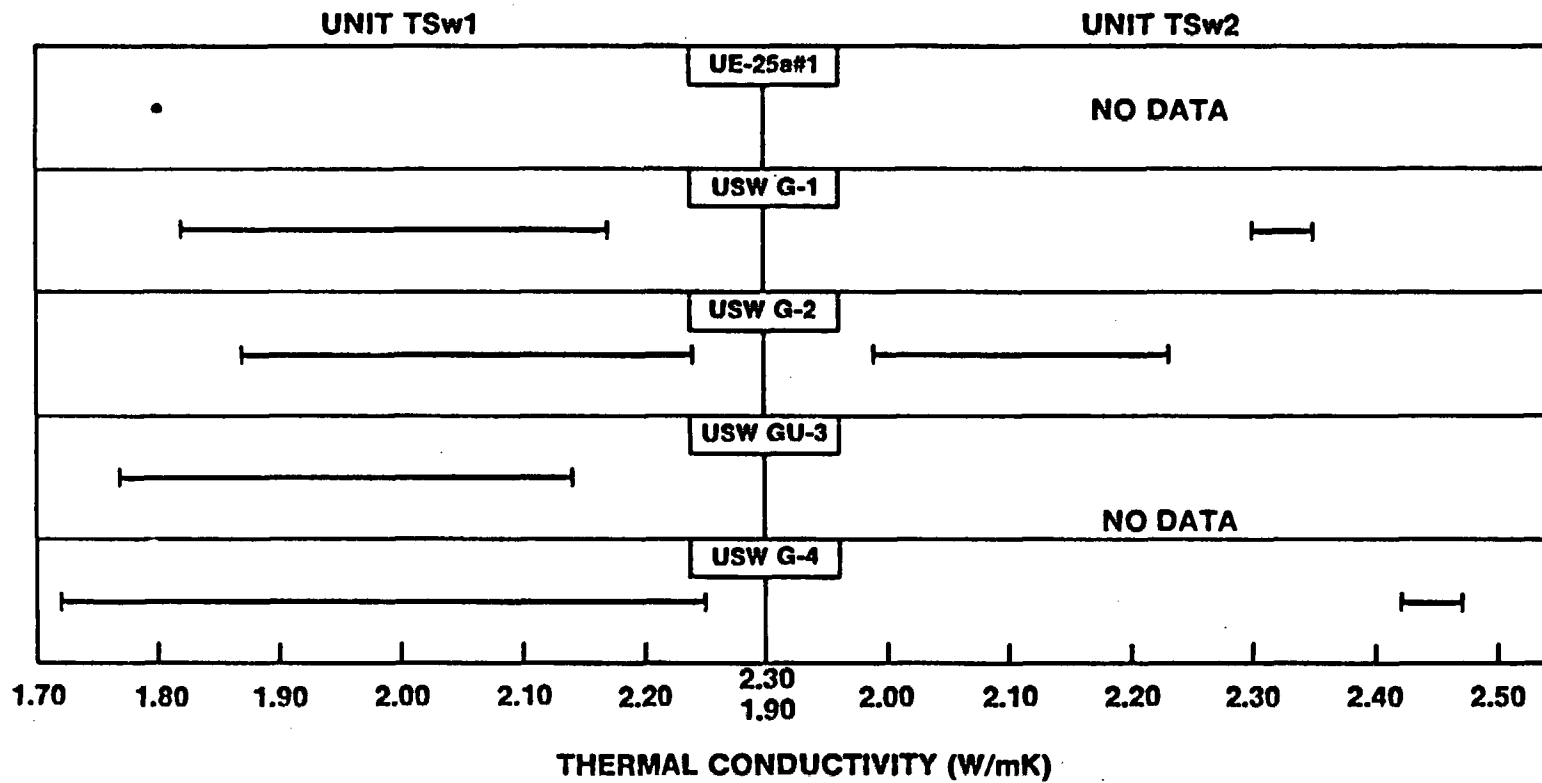


Figure 6.4-1. Comparison of Ranges of Thermal Conductivity for Units TSw1 and TSw2

calculated heat capacities of the samples ( $\leq 1.0$  percent of the mean value) imply that the heat capacities of the solid components will be approximately the same for units TSw1 and TSw2 throughout the area for the underground facilities.

Additional data for the bulk chemistry and mineralogy of these units (e.g., in Bish and Chipera, 1986) could be used to expand the data base of calculated heat capacities of solid components. However, two other parameters must be considered in evaluating the representativeness of heat capacity data - porosity, including matrix porosity and lithophysal cavity abundance, and saturation. Data are not available with which to evaluate the representativeness of saturation. In the absence of these data and experimentally determined heat capacities, no firm conclusions can be drawn about the representativeness of heat capacity.

#### 6.5 Thermal Expansion Behavior of the Welded, Devitrified Portion of the Topopah Spring Member

The coefficient of thermal expansion of the welded, devitrified portion of the Topopah Spring Member is used with the Young's modulus to calculate the stress induced by a given temperature change in the rock. Estimation of these thermally induced stresses is important to the design of geometries and support systems for underground openings.

Thermal expansion of the welded, devitrified portion of the Topopah Spring Member has been measured both with and without confining pressure. Statistical analyses of data obtained for each pressure condition separately indicates that no differences exist within the boundary of the underground facilities for unit TSw1 (Nimick and Schwartz, 1987). Thus, the ES-1 location (as represented by USW G-4) is expected to be representative of the area for the underground facilities.

Statistical analysis of thermal expansion data for samples of unit TSw2 indicate significant differences between mean values for data collected both unconfined and with confining pressure (Nimick and Schwartz, 1987). The differences are attributed to differences in

mineralogy, and specifically to differences in the content of tridymite and cristobalite.

For experiments with confining pressure, significant differences are found for two temperature ranges: 150 to 200°C (302 to 392°F) and 25 to 200°C (72 to 392°F). The single sample from USW G-4 with data in these ranges has a higher thermal expansion coefficient than do the samples from USW G-2 and USW GU-3. However, a decision about representativeness is unwarranted based on data from a single sample that originates at a depth [737.9 ft (225 m)] far removed from the depths to be encountered by excavations at the main test level.

No data are available for thermal expansion coefficients at unconfined conditions for samples from USW G-4. Given this and the paucity of data for confined experiments, no conclusions can be made about the representativeness of the thermal expansion behavior of unit TSw2.

Data contributing to the preceding discussion have been collected for samples that do not contain lithophysal cavities. The thermal expansion behavior of tuff that does contain lithophysal cavities is expected to be similar throughout the area for the underground facilities, but no data are presently available to test this assumption. Again, no conclusions about representativeness can be made.

#### 6.6 Fracture Characteristics of the Welded, Devitrified Portion of Topopah Spring Member

Fracture characteristics such as spatial orientation, absolute abundances, and mechanical properties are used in empirical, analytical, and numerical techniques that address design and performance assessment activities. Thus far, none of the fracture characteristics have been sufficiently evaluated at all of the core holes to make a definitive statement about the representativeness of the fracture characteristics to be found in the ES-1 and the anticipated fractures in the subsurface portions of a repository. In addition, existing data are constrained

because they are obtained from vertical coreholes and are a sample of a fracture population for which the dominant orientations are near-vertical.

In terms of spatial orientation, fractures in USW G-4 (Figure 17B of Spengler et al., 1984) and USW GU-3 (Figure 26 of Scott and Castellanos, 1984) compare well. Fracture densities (fractures/m<sup>3</sup>) differ somewhat, with more in USW GU-3 (42/m<sup>3</sup>) than in USW G-4 (34/m<sup>3</sup>). However, the proximity of USW GU-3 to a fault suggests that the fracture density at USW GU-3 may be high relative to the fracture density to be expected in the (unfaulted) majority of the area for the underground facilities. For core holes USW G 1 (Spengler et al., 1981), UE-25a#1 (Spengler et al., 1979), USW GU-3 (Scott and Castellanos, 1984) and USW G-4 (Spengler et al., 1981) the angular inclination frequencies (fractures/m) compare well, with the USW G 4 data falling within the range of all the drill holes. Finally, for fracture mechanical properties, sufficient data have not been collected to make a statement about representativeness.

Other fracture characteristics (e.g., spacing, continuity, aperture, and roughness) would be pertinent to an evaluation of representativeness. However, existing data are insufficient to permit the evaluation.

## 7.0 HYDROLOGICAL CHARACTERISTICS

Flow of water through unsaturated rock is thought to be the principal mechanism for the transport of most of the soluble radionuclides and other contaminants from a repository to the biosphere at an arid site such as that proposed in Yucca Mountain. The lateral drifts extending from ES-1 will intersect a number of geological features (Drill Hole Wash, Ghost Dance Fault, and imbricate faulting) with variable lithology, fracture density, porosity, and saturations. The effects of these structural features on the hydrologic conditions at Yucca Mountain are not known but will be assessed at specific locations during excavation and drifting. Note that the representativeness of the ES-1 location in terms of such structural features was incorporated into the process of selecting a site for an exploratory shaft, as discussed in Section 1.0.

A number of parameters and characteristics can contribute to hydrologic flow patterns at Yucca Mountain including moisture flux, hydraulic conductivity, maximum moisture content, saturation as a function of pressure head, and unit thickness. (Unit thickness is addressed separately in Section 4.0.) Rather than attempting to assess the representativeness of each of the parameters and characteristics separately, a single variable: sample travel time has been formed by combining the other parameters. The variable represents the length of time necessary for water to move a length of 1.5 cm (0.6 in.) based on hydrologic properties measured on specific hydrologic test samples under a constant assumed flux of 0.1 mm/yr, which is a reasonable value for Yucca Mountain until more in situ information becomes available. If the matrix hydrologic conductivity for a sample is less than this assumed flux, flow is assumed to occur, at least in part, through fractures and sample travel times are assumed to be zero. A more detailed description of the calculation of sample travel times and the resulting values are given in Rutherford et al. (in preparation).

Note that the assumed flux could be decreased until all samples had conductivities that were greater than the flux, and hence non-zero travel times. Although this would result in the removal of discussion of

"fracture flow" in the remainder of Section 7.0, the overall conclusions would remain unchanged.

#### 7.1 Unit TSw1

Figure 7.1-1 compares the matrix sample travel times for unit TSw1. Because of the absence of data for USW G-4, no conclusions can be made about the representativeness of the ES-1 location.

In addition to the five data points on Figure 7.1-1, zero travel times have been estimated for five other samples (two each from USW G-1 and USW GU-3 and one from USW G-4). However, even when considering these additional samples, data are insufficient to evaluate the representativeness of the ES-1 location.

#### 7.2 Unit TSw2

Figure 7.2-1 compares the matrix sample travel times for unit TSw2. The range of data for samples from USW G-4 includes the few data points obtained for samples from other core holes. In addition, four other samples (two from USW G-1 and one each from USW GU-3 and USW G-4) have sample travel times of zero. Thus, the ES-1 location (as represented by USW G-4) appears to be representative in terms of travel times through the matrix.

#### 7.3 Unit TSw3

Sample travel times for unit TSw3 are limited to five samples (including samples with travel times of zero). Data are insufficient to reach conclusions about the representativeness of the ES-1 location.

#### 7.4 Unit CHnv

Figure 7.3-1 compares the matrix sample travel times for unit CHnv (all but one data point are for unit CHnv). No samples had travel times of zero. Samples from USW G-4 have significantly higher travel times

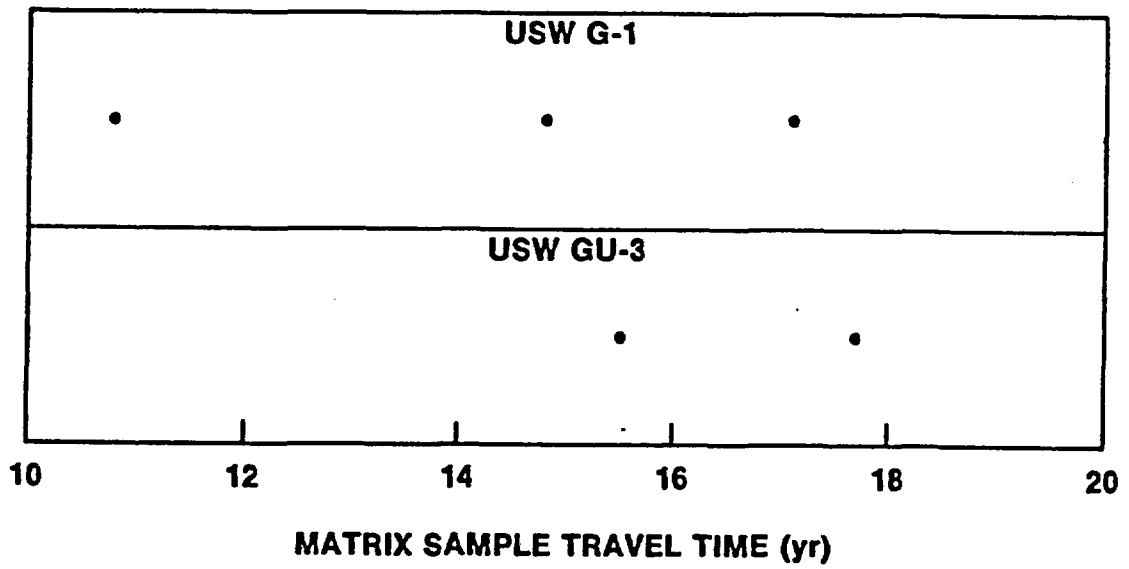


Figure 7.1-1. Comparison of Matrix Sample Travel Times for Unit TSw1. Data from Rutherford et al. (in preparation).

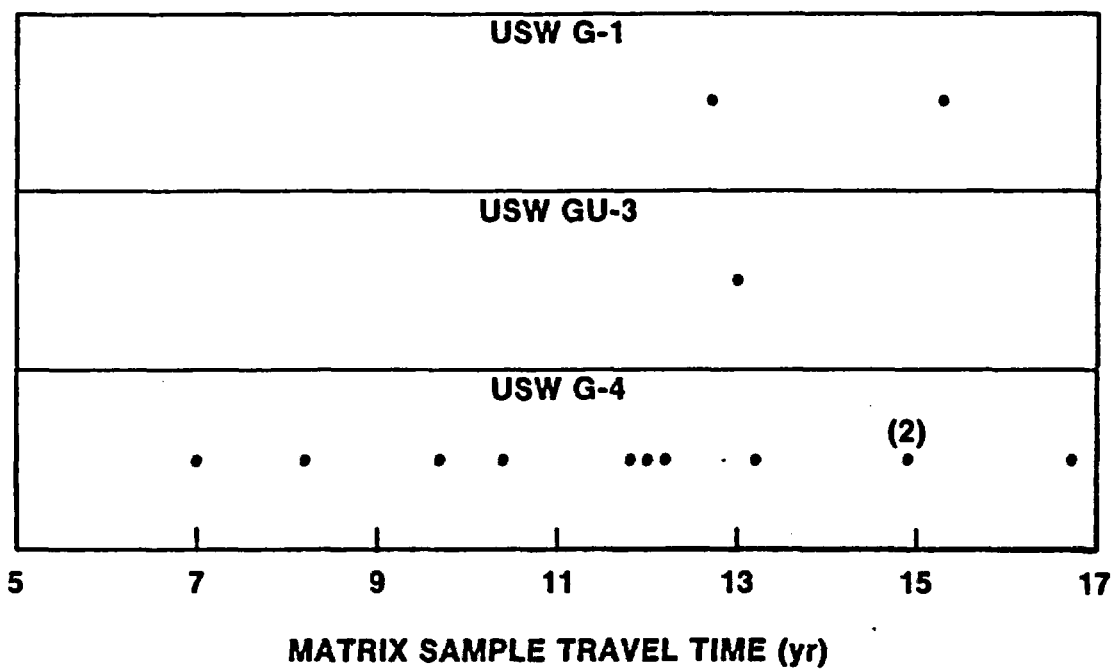


Figure 7.2-1. Comparison of Matrix Sample Travel Times for Unit TSw2. Data from Rutherford et al. (in preparation).

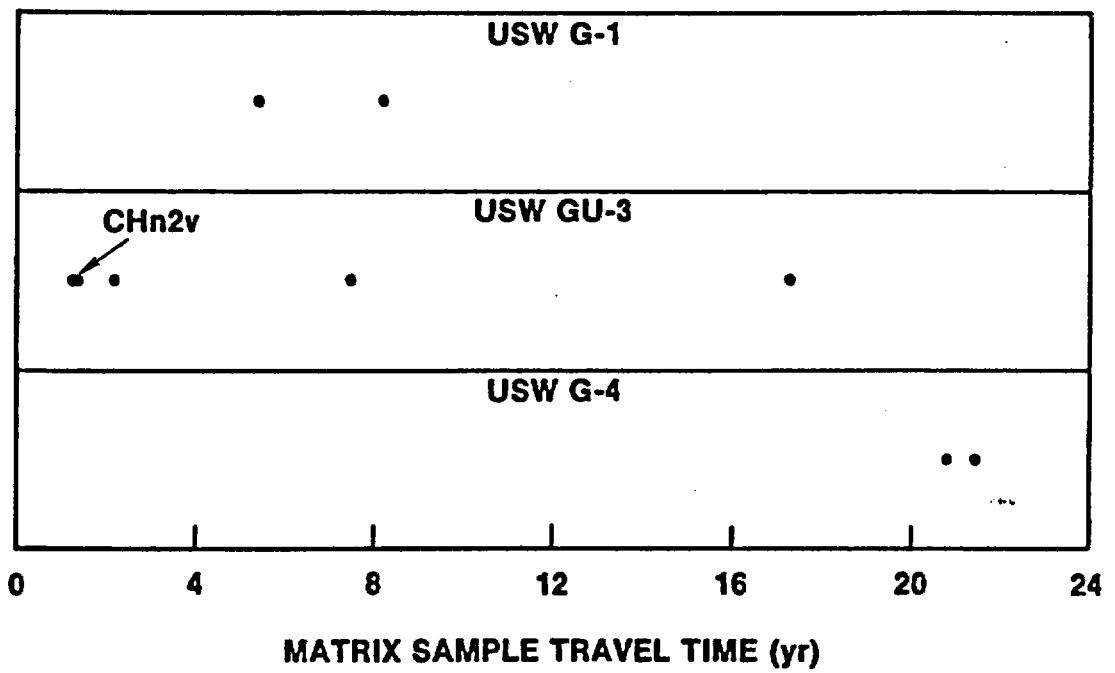


Figure 7.3-1. Comparison of Matrix Sample Travel Times for Unit CHn2v. Data from Rutherford et al. (in preparation).

than samples from the other two core holes. Thus, the ES-1 location may not be representative in terms of hydrologic conditions in unit CHn1v.

#### 7.5 Unit CHnz

Data for matrix sample travel times for unit CHnz are shown in Figure 7.5-1. When data for the unit as a whole are compared, the range for USW G-4 includes all data for samples for USW G-1, and the ES-1 location would be representative.

However, differences appear when unit CHnz is subdivided according to the units described in Ortiz et al. (1985). The data range for unit CHn1z in USW G-4 includes all data from CHn1z in USW G-1. For unit CHn2z, matrix travel times for samples from USW G-4 are higher than those for samples from CHn2z in USW G-1. Finally, matrix travel times for samples from CHn3z from USW G-4 are lower than those for samples of CHn3z from USW G-1. Assuming that this comparison is representative of east-west spatial variation in the northern portion of the area for the underground facilities, the ES-1 location (as represented by USW G-4) may be representative for CHn1z, but may not be representative for CHn2z or CHn3z.

The contrast between samples of unit CHn2z from the two core holes is increased when samples having zero travel times are considered. Two of six samples from USW G-1 would have some fracture flow, compared to only one of six samples from USW G-4. Similarly, the only sample from unit CHn3z having a travel time of zero comes from USW G-4, substantiating the generally lower travel times relative to those for unit CHn3z in USW G-1.

Unit CHnz does not exist in the southern portion of the area for the underground facilities because material above the central welded Prow Pass Member has not been zeolitized (see Sections 4.2 and 5.4). In order to complete the evaluation of hydrologic conditions, the following comparisons need to be made: CHn1z (USW G-1, USW G-4) to CHn1v (USW GU-3); CHn2z (USW G-1, USW G-4) to CHn2v (USW GU-3); and CHn3z (USW G-1, USW G-4) to CHn3v (USW GU-3). The last comparison is not possible at present because no data are available for CHn3v.

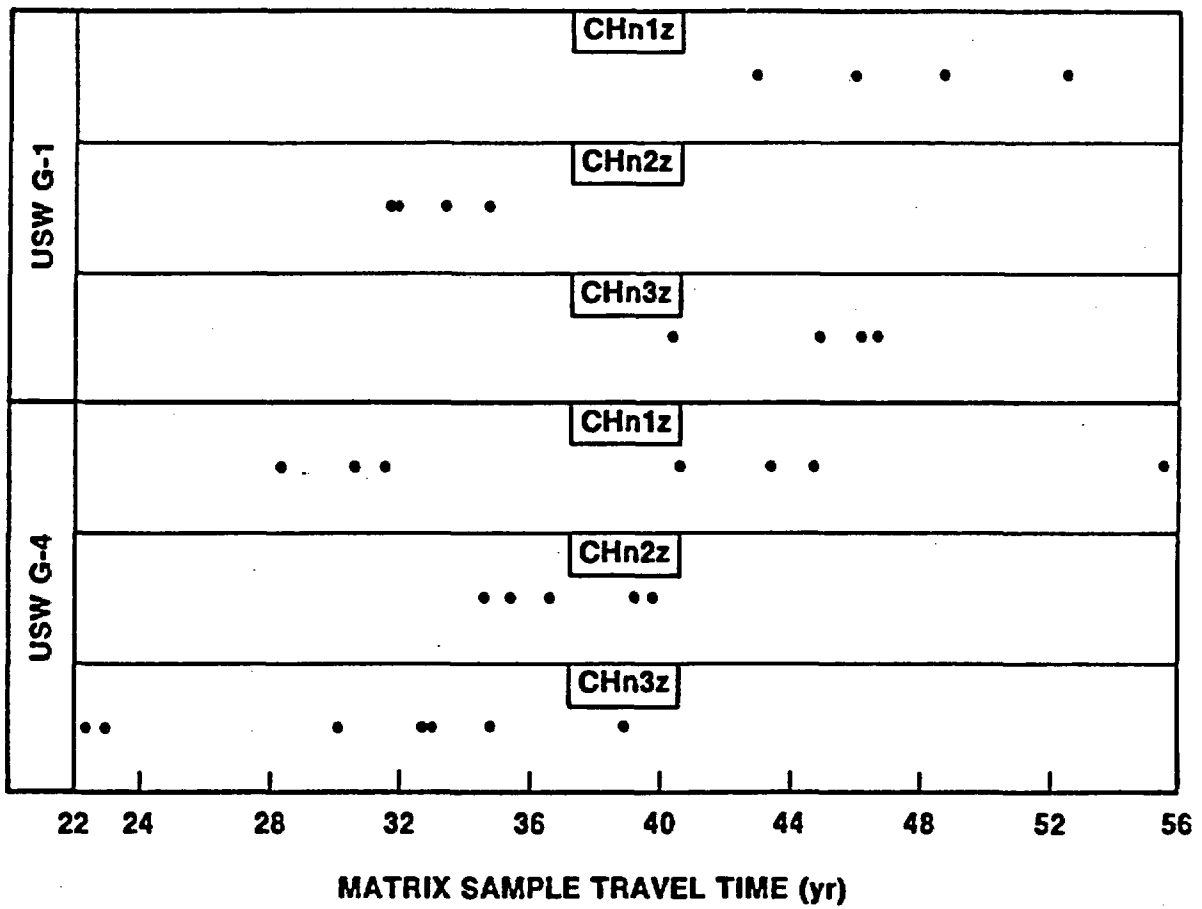


Figure 7.5-1. Comparison of Matrix Sample Travel Times for Unit CHnz. Data from Rutherford et al. (in preparation).

Examination and comparison of Figures 7.3-1 and 7.5-1 indicate that matrix sample travel times in CHn1v and CHn2v from USW GU-3 are significantly lower than matrix travel times for samples from CHn1z and CHn2z from USW G-1 and USW G-4. Thus, the ES-1 location may not be representative of hydrologic conditions in any of the CHn subunits in the southern portion of the area for the underground facilities or of units CHn2z or CHn3z in the northern portion of the area.

Finally, it should be noted that the processes associated with hydrologic flow in the unsaturated tuffs will be investigated during some of the in situ hydrologic tests planned in the ESF. The results of these investigations may be useful in understanding and defining hydrologic conditions elsewhere at Yucca Mountain even in cases for which hydrologic characteristics are different from those at the ES-1 location.

## 8.0 WASTE PACKAGE ENVIRONMENT

The performance of the waste package is largely contingent on the natural and perturbed physical and chemical environment in the proposed waste emplacement horizon. The characterization of this environment will require a detailed description of the preemplacement (ambient) environment and a determination of the changes that will occur when this environment is perturbed by waste emplacement.

### 8.1 Natural and Perturbed Physical Environment

The physical environment surrounding the waste package will be controlled largely by the rock-mass mechanical properties and the response of the rock mass to mechanical and thermomechanical loading and unloading as a result of excavation and waste emplacement. The representativeness of the ambient rock-mass mechanical properties (i.e., in situ stress, Poisson's ratio, Young's modulus, unconfined compressive strength, tensile strength, and fracture characteristics) and thermal properties (i.e., thermal conductivity, heat capacity, and coefficient of thermal expansion) has been discussed for units TSw1 and TSw2 in Chapter 6.0.

The data base which can be used to predict the changes that occur in the thermal and mechanical properties as a result of temperature perturbations caused by waste emplacement is extremely limited. Thus, the representativeness of the properties in the perturbed environment cannot be evaluated. Data pertinent to the evaluation will be obtained during in situ heater experiments in the ESF.

### 8.2 Natural and Perturbed Chemical Environment

The chemical environment in contact with the waste package will be controlled largely by the interactions between mineralogical components of the rock, the chemistry of the water contained in the rock, the duration of the contact between the waste package and water or water vapor, and possibly radiolysis. Perturbations to the natural environment

that occur as a result of waste emplacement may greatly alter the amount and composition of water in the rock and the characteristics of the environment immediately adjacent to the waste package.

The mineralogy of the rock mass in units TSw1 and TSw2 and an assessment of the representativeness thereof is discussed in Chapter 5.0. The major phases in the rock (quartz, cristobalite and feldspar) should not be affected by the increase in temperature caused by the waste package, with the possible exception of conversion of cristobalite to quartz over long periods of time. No data are available to estimate the likelihood of such a conversion. The representativeness of this aspect of the waste package test should be similar to the representativeness of the cristobalite abundance, which is discussed in Section 5.1.2.

Another potential perturbation to the chemical environment is temperature-enhanced dissolution of minerals in the pore water. However, pore waters are expected to vaporize at approximately 95 to 100°C. Changes in solubility of the major phases between ambient temperature and 100°C is not expected to have a significant effect on the chemical environment of the waste package.

Fractures in units TSw1 and TSw2 contain some hydrous minerals (e.g., clinoptilolite, montmorillonite) that can be expected to dehydrate as temperature increases. However, the volume percentage of such minerals is negligible relative to the entire rock mass. Thus, any changes in the fracture mineralogy should have little or no effect on the chemical environment.

Analyses of the chemistry of the water in the saturated zone at Yucca Mountain reported by Benson et al. (1984) and Ogard and Kerrisk (1984) indicate that the range in chemical composition is very limited and appears similar to the composition of the vadose zone water sampled from Ranier Mesa (White et al., 1980; Henne, 1982). No water samples have been analyzed from the vadose zone at Yucca Mountain. However, on the basis of available data from the saturated zone at Yucca Mountain and the vadose zone at Ranier Mesa, it is presumed that the chemical composition of the vadose zone water at Yucca Mountain will fall within the range

encountered at these other two locations. These results suggest that the chemistry of the water in the rock encountered in the ESF where the waste package experiments will be conducted should be representative of the conditions encountered elsewhere in the subsurface portions of the repository.

A limited data base exists which can be used to predict the changes in the chemical environment during the heating and cooling phases related to waste emplacement. The relative changes that occur in the chemical environment at increased temperature may be unaffected by any spatial variability in the chemical characteristics, so that the representativeness of the properties at ambient conditions will apply for the perturbed environment. Conversely, the composition of the pore fluid phase may change significantly as the environment is perturbed by the emplacement of waste. Evaporation, fluid migration, and condensation will occur at various times as the rock mass gradually heats up and then cools. Each of these processes may result in a change in the composition of the environment surrounding the waste package although the results of these processes and the controlling parameters (e.g., temperature, humidity, etc.) are not clearly defined. A better definition of these controlling parameters is required to adequately assess the representativeness of the test-alcove environment relative to the remainder of the subsurface portions of a repository.

The regional hydrologic conditions (i.e., the conditions in Yucca Mountain before any excavations occur) controlling the water flux within units TSw1 and TSw2 will probably vary significantly from the flux that occurs within a test alcove even though the intrinsic hydrologic characteristics may be quite similar. These variations possibly may be more significant as the far-field environment is perturbed, although our understanding of the processes occurring at high temperature is limited.

In addition to the changes that are expected in the chemical environment as a result of waste emplacement, other factors also may cause time-dependent changes to the chemical environment that may not occur in the ESF. Contaminants introduced during the construction and operational phase of the subsurface portions of a repository may

significantly influence the waste package environment in some locations. These conditions may not be simulated in the environment developed during the waste package experiments in the test alcove.

The physical and chemical characteristics of the ambient environment encountered in the ESF are likely to be representative of the conditions encountered throughout the area of the underground facilities. Only a limited number of data are available on the processes controlling the changes expected in the environment surrounding the waste package or on the magnitude of these changes. However, in the absence of external contaminants introduced during excavation or operation of the subsurface portions of a repository, perturbation of the chemical environment by the waste package experiment should be approximately representative of similar perturbations that will occur around actual waste packages elsewhere within the boundary of the underground facilities.

## 9.0 REPOSITORY DESIGN PARAMETERS

Many of the activities planned for the ESF will provide data for the repository design process. The stability of variously sized underground openings will be monitored, the performance of ground support systems in different rock conditions will be evaluated, the response to vibratory ground motion caused by weapons tests will be measured, the adequacy of the ventilation system design in the ESF will be estimated, and data will be obtained on dust generated by the dry drilling process so that an evaluation can be made of compliance with silica and fibrous dust standards.

### 9.1 Variations in the Depth of the ESF

Several parameters that are used as input for the design of the subsurface portions of a repository can vary significantly as a function of depth. Many of these parameters (e.g., geological characteristics, rock mechanics characteristics) have been discussed in preceding chapters. In the present layout of the subsurface facilities (MacDougall et al., 1987), depths to the base of the design subsurface facilities range from about 980 ft (300 m) to a maximum of about 1420 ft (430 m) (Figure 9.1-1). Depths encountered at the main test level of the ESF will vary from 1055 ft (322 m) at the ES-1 location to a maximum depth of 1200 ft (370 m) where one of the lateral drifts is expected to intersect the Ghost Dance Fault.

In the present layout of the underground portion of a repository, approximately 80 percent of the subsurface facilities will be at a depth that is within  $\pm 200$  ft ( $\pm 60$  m) of the depths of the ESF and 50 percent of the subsurface facilities will be located at depths within  $\pm 50$  ft ( $\pm 15$  m) of the ESF depths. The maximum depth penetrated by ES-1 is expected to be 1430 ft (436 m); the entire range of depths at which the subsurface facilities will be located is less than this maximum depth. These data indicate that the depth of the ESF is representative of the depths that will be encountered within the subsurface portions of a repository.

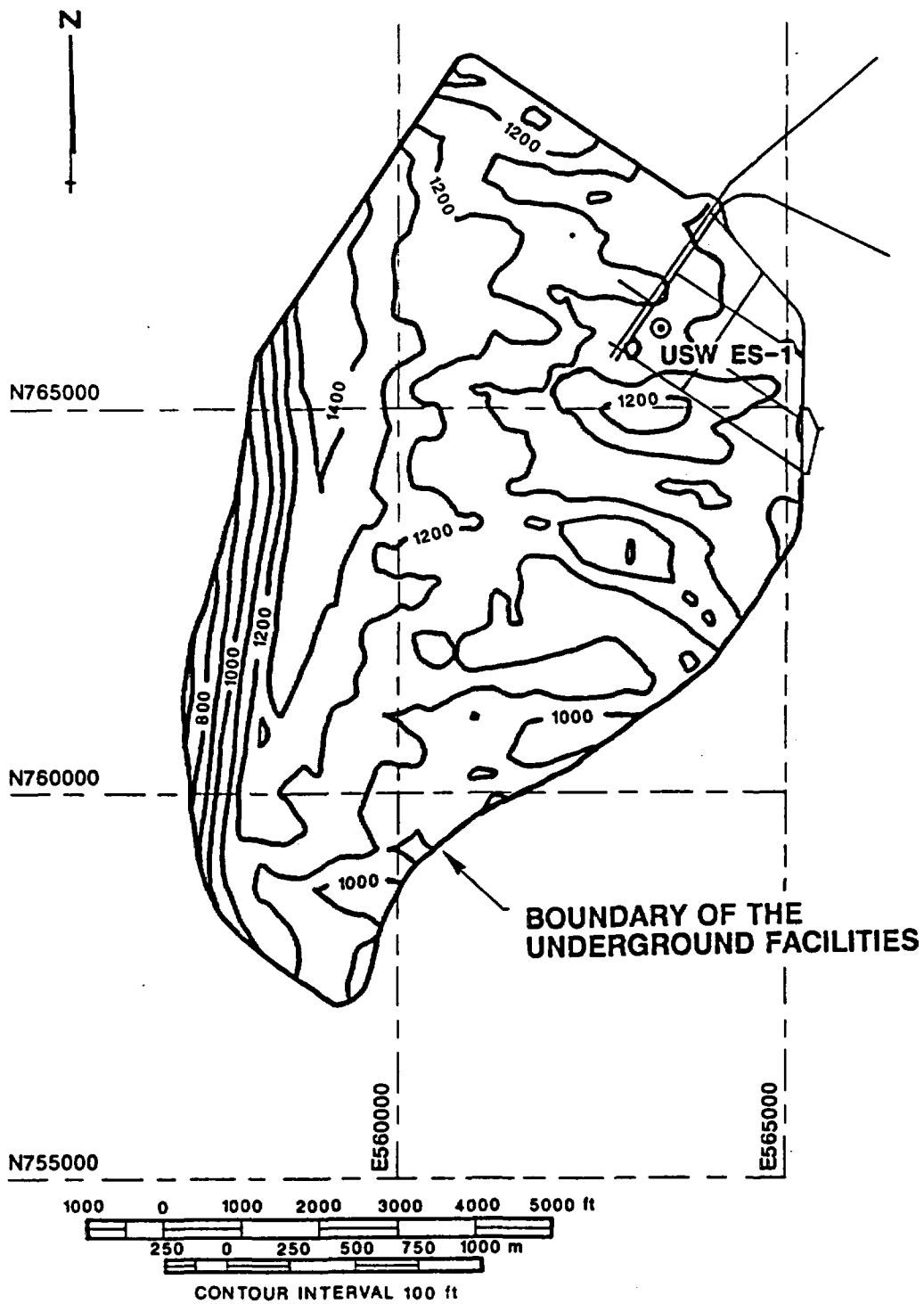


Figure 9.1-1. Thickness of Overburden Overlying the Proposed Waste Emplacement Horizon and the ESF. The approximate location of the ESF illustrates the variations in depth that should be encountered during construction of the underground facilities. Contour interval is 100 ft.

## 9.2 Excavation Techniques, Orientations, and Sizes of the Underground Openings in the ESF

All underground openings that will be included in the subsurface facilities were designed by considering a number of factors including long-term stability requirements, ventilation requirements, the dimensions of the various types of equipment that will be required for drilling, mining, waste emplacement and retrieval, and other types of utility and support functions that may be required (MacDougall et al., 1987). The design and size of the major openings in the subsurface facilities vary considerably depending on the intended use (MacDougall et al., 1987). Some of the openings (i.e., waste ramp, tuff ramp, waste main, and perimeter drift) will be excavated using mechanical boring techniques, whereas other openings will be excavated using drill and blast techniques. The sizes of the openings range up to 25 ft (8 m) diameter for the bored openings and up to a maximum of 25 ft (8 m) wide and 21.5 ft (7 m) high for drifts to be excavated using drill and blast techniques.

The size of the underground openings in the ESF will vary depending on the requirements for testing associated with the experimental program. All openings will be excavated using controlled-blasting techniques. The minimum size for the underground openings associated with the ESF (exclusive of the lateral-exploration drifts) is being determined on the basis of the mining methodology employed, the required clearances for the mining equipment, drift geometry, and ventilation and utility requirements. This drift size currently is expected to be 16 ft (5 m) wide by 14 ft (4 m) high. This dimension will provide adequate overhead clearance for the operation of the drill jumbo and the ventilation system while providing the required operating width for equipment, utility, and personnel clearances.

The lateral drifts to be driven to intersect geologic structures will be 14 ft (4 m) wide by 14 ft (4 m) high. These drifts will be selectively enlarged by controlled-blasting techniques to sizes representative of drifts in the subsurface facilities so that the performance of

such openings can be evaluated for the different qualities of rock encountered.

The design of the subsurface portions of the repository is such that all long exploratory drifts to be developed as part of the ESF will be incorporated into the design. Therefore, almost by definition the orientation of the lateral drifts at the main test level will be representative of the orientations planned for the underground portion of the repository.

### 9.3 Ground Support Systems in the ESF

The ground support requirements for the subsurface portions of a repository may vary over relatively short distances depending on the local geologic conditions encountered. These conditions are expected to fall within the limits encountered in work that has been completed in the G Tunnel Underground Facility (Zimmerman et al., 1987) and in the River Mountains Tunnel in Nevada (Sperry, 1969). There are numerous options available for ground support in the proposed waste-emplacement horizon; of these, five have been proposed for use in the subsurface facilities (MacDougall et al., 1987). These five categories of ground support (Table 9.3-1: from MacDougall et al., 1987) are considered adequate for the full range of conditions expected within the subsurface facilities based on available rock mass classification data for tuffs of the Topopah Spring Member (Langkopf and Gnirk, 1986).

The ground-support system that will be used in the ESF will depend on the geologic conditions encountered. The primary ground-support system is expected to consist of wire mesh and rock bolts. The lateral exploratory drifts to the major structural features evident in Yucca Mountain are expected to encounter rock conditions that will require several different types of ground support. Because these drifts are intended to intersect geologic features (primarily faults) with rock conditions different from those prevalent in most of the area for the underground facilities, the geologic conditions probably will span the range of conditions expected for the proposed waste-emplacement horizon.

Table 9.3-1. Recommended Ground Support Requirements for the Expected Rock Conditions Within the ESF (After MacDougall et al., 1987)

Ground Class	A	B	C	D	E
NGI* Relative Description	Very Good	Good	Fair	Poor	Very Poor
General Ground Condition Relative to Yucca Mountain	Massive, welded tuff; little or no jointing; dry or slightly damp.	Densely welded tuff with one to three joint sets; joints are tight with no alteration.	Densely welded tuff with multiple or random joint sets; little or no joint alteration.	Heavily jointed, welded tuff; typical of conditions at transition within flow units.	Fault zone; crushed tuff in a matrix of low-strength gouge; heavy alteration and possibly minor water.
Ground Support System Recommended for Conceptual Design	Untensioned friction-type bolts on variable spacing as needed; typical grid spacing of 6.5 to 10 ft.	Untensioned grouted dowels on a 5- to 6.5-ft grid spacing with wire mesh or chain-link fabric on ribs and crown.	Untensioned grouted dowels on a 5- to 6.5-ft spacing with welded wire mesh and 2 to 3 in. of shotcrete.	Initial support: friction bolts on a 5-ft spacing with 2- to 3-in fiber-reinforced shotcrete; final support: welded wire mesh, grouted dowels with 3 in. of additional shotcrete.	Light steel ribs or lattice girders placed near face; fiber-reinforced shotcrete 3 to 4 in. followed by welded wire mesh, grouted dowels, and 2 in. of shotcrete.

\*Norwegian Geotechnical Institute (Barton et al., 1974).

Tests will be conducted specifically to evaluate the performance of the ground support system for various ground conditions having different rock mass classifications. On the basis of this experience and the various rock conditions that should be encountered in the lateral drifts, it is expected that the ground support system requirements for the ESF will be representative of the requirements for the remainder of the subsurface portions of a repository.

#### 9.4 Construction-Related Conditions in the ESF

The general construction techniques used for the ESF will be similar to those employed during construction of the subsurface portions of a repository except that all excavations will be completed using drill-and-blast techniques. These controlled-blasting techniques will have a greater influence on the rock mass immediately adjacent to the openings than will mechanical boring techniques.

The procedures to be employed for monitoring and controlling the introduction of contaminants and water in the subsurface facilities also will be used in the ESF. Similar types and quantities of materials that may adversely impact the environment of the subsurface facilities will be monitored in the ESF and their long-term impact on the ambient environment will be assessed.

Based on the considerations discussed above, the construction-related conditions in the ESF and their potential impacts should be representative of those encountered in the subsurface portions of a repository for drill-and-blast excavation techniques.

#### 9.5 Effects of Potential Vibratory Ground Motion

The evaluation of seismicity at Yucca Mountain must address both natural seismicity (earthquakes) and underground nuclear explosions which are conducted periodically at the Nevada Test Site. Ground motion amplitudes for both natural and weapons-related seismicity at any given point are a function of the coupling between the source and the

geological medium at the source, the geologic structure between the source and receptor, and the geology in the vicinity of the receptor (Vortman, 1986). An evaluation of the effects of seismic activity on the repository will include a determination of the response spectra at the proposed waste-emplacement horizon and measurements of the peak ground motion parameters (i.e., particle velocity, acceleration, and displacement) at the ground surface (alluvium), at the bedrock surface below the alluvium, and at the proposed waste-emplacement horizon.

The limited data base available for natural seismicity at Yucca Mountain indicates that this region is a seismically quiet area. The limited data available from naturally occurring seismic events are insufficient to directly assess representativeness on the basis of natural seismic activity. However, the ESF and the subsurface facilities have four characteristics in common that would suggest that the ESF will be representative in terms of a response to natural seismic loading: (1) both facilities will be at approximately the same depth; (2) both will be at approximately the same location (vertically within an extensive geologic unit; (3) the facilities will have similarly sized openings with similar orientations; and (4) both will utilize the same methods of ground support.

On the basis of data collected at several measurement locations on and near Yucca Mountain (Long, 1987) from two weapons tests, peak particle accelerations appear to be highly variable but may be somewhat higher at the northern and southern ends of the area for the underground facilities. This variability is such that the present location of the ESF will be as representative as any other location within the area relative to weapons-related seismicity.

#### 9.6 Ventilation Requirements in the ESF

Two independent ventilation systems are planned for the subsurface portion of a repository: one system will provide air for the development (e.g. construction, excavation) activities and the second will provide ventilation to support the waste-emplacement activities. The estimates

of airflow demands for both ventilation systems are based primarily on minimum requirements for airflow, the need to dilute diesel exhaust fumes and minimize engine heat loads, and shop demands. Airflow volume requirements were derived primarily from dust abatement needs, fan operating costs, and comfort considerations. It is not expected that the air will need to be cooled in the ventilation system for the development area of the repository because the heat from the waste package is expected to have little impact on the overall system.

The ventilation system planned for the ESF will perform the same functions as the development ventilation system designed for the subsurface portions of a repository. It is expected that the demands placed on this system from construction-related activities (i.e., excavation, experimental work) will be comparable to those imposed in the subsurface portions of a repository, except that the size of the area requiring ventilation will be significantly less. The smaller area may reduce the level of complexity required for the full-scale system (e.g., exhaust shafts, layout, blower size) but the requirements for both areas should be similar. Monitoring for dust and radon levels will be conducted to ensure that air quality standards are achieved. Additionally, the effects of heat on radon emanation from the rock will be monitored. The ventilation requirements during development of the ESF will be representative of the requirements for the subsurface portions of a repository.

These data indicate that the ventilation system incorporated into the ESF will be representative of the system that will be employed for development of the subsurface portions of a repository.

## 10.0 PERFORMANCE-ASSESSMENT PARAMETERS

The performance assessment program will examine the potential for release of radionuclides to the accessible environment. Contributing to such an examination are three factors that will be measured during testing in the ESF: (1) the age of the groundwater; (2) hydrologic properties of the tuff units that occur between the proposed waste emplacement horizon and the accessible environment; and (3) the solubility of radionuclides in the groundwater (groundwater chemistry). The hydrologic properties are discussed in Chapter 7.0. Few data are available to determine whether the ESF location will be representative in terms of factors (1) and (3).

## 11.0 CONCLUSIONS

Results of studies conducted during and after the construction of the ESF will form an integral component of the information that is required to complete a comprehensive evaluation of Yucca Mountain as a potential high-level waste repository. For this reason, it is important that the information obtained from the ESF be representative of the conditions and characteristics encountered in the subsurface portions of a repository that may influence waste emplacement and retrieval, radionuclide containment, and the transport of radionuclides to the accessible environment.

A preliminary assessment of the representativeness of pertinent geological, mineralogical, geomechanical, and hydrological characteristics has been completed based on available data (Table 11.0-1). In addition, available information on factors influencing the waste package environment and on the parameters influencing the repository design and performance assessment has been evaluated using the definitions of representativeness discussed in Chapter 2.0.

In many instances, data are very limited or do not exist (e.g., fracture characteristics, perturbed physical and chemical environment). For such cases, an adequate evaluation of representativeness before construction of the ESF may not be possible.

Some of the entries in Table 11.0-1 indicate that a property or characteristic is not representative. It is possible that a different location for ES-1 might be more representative for these properties and characteristics. However, given the large number of aspects considered in this document, there is no reason to believe that any other single location would be any more representative, as a whole, than the present location.

Table 11.0-1. Summary of Representativeness Evaluation for Each of the Technical Areas Considered

<u>Technical Area Evaluated</u>	<u>Results of Evaluation</u>
<b>Geology</b>	
4.1 Strata - Proposed Waste-Emplacement Unit and Above	Representative
4.2 Strata - Below Proposed Waste-Emplacement Unit to Water Table	
Unit TSw3	Inconclusive
Unit CHn1	Representative
Unit CHn2	Representative
Unit CHn3	Representative
4.3.1 Lithophysal Cavities	Representative
4.3.2 Vapor-Phase Altered Material	Inconclusive
<b>Mineralogy</b>	
5.1 Distribution of SiO <sub>2</sub>	Representative
5.2 Fracture Mineralogy	Inconclusive
5.3 Clay Content	Inconclusive
5.4 Sorptive Mineralogy	
Clinoptilolite	Inconclusive
Mordenite	Inconclusive
Clay	Inconclusive
Glass	Nonrepresentative
<b>Rock Mechanics</b>	
6.1 In Situ Stress	
Vertical	Representative
Horizontal	Representative
6.2 Physical Properties	
Grain Density	Representative
Matrix Porosity	Representative
6.3 Mechanical Properties	
Poisson's Ratio	
Unit TSw1	Inconclusive
Unit TSw2	Nonrepresentative
Unconfined Compressive Strength	
Lithophysae-poor	
Unit TSw1	Inconclusive
Unit TSw2	Representative
Lithophysae-rich	Inconclusive

Table 11.0-1. Summary of Representativeness Evaluation for Each of the Technical Areas Considered (Continued)

<u>Technical Area Evaluated</u>	<u>Results of Evaluation</u>
Young's Modulus Lithophysae poor Unit TSw1 Unit TSw2 Lithophysae rich	Inconclusive Representative Inconclusive
Mohr-Coulomb Parameters Tensile Strength	Inconclusive Inconclusive
6.4 Thermal Properties Thermal Conductivity Unit TSw1 Lithophysae poor Lithophysae rich Unit TSw2 Heat Capacity	Representative Inconclusive Inconclusive Inconclusive
6.5 Thermal Expansion Behavior Unit TSw1 Unit TSw2	Representative Inconclusive
6.6 Fracture Characteristics	Inconclusive
<b>Hydrology</b>	
7.1 Unit TSw1	Inconclusive
7.2 Unit TSw2	Representative
7.3 Unit TSw3	Inconclusive
7.4 Unit CHnv	Nonrepresentative
7.5 Unit CHnz	Nonrepresentative
<b>Waste Package</b>	
8.1 Natural and Perturbed Physical Environment	Inconclusive
8.2 Natural and Perturbed Chemical Environment	Inconclusive
<b>Repository Design</b>	
9.1 Depth of ESF	Representative

**Table 11.0-1. Summary of Representativeness Evaluation for Each of the Technical Areas Considered (Concluded)**

---

9.2	Excavation Techniques/Opening Sizes and Orientations	Representative
9.3	Ground Support Systems	Representative
9.4	Construction-Related Conditions	Representative
	<u>Technical Area Evaluated</u>	<u>Results of Evaluation</u>
9.5	Seismicity	
	Natural Seismicity	Inconclusive
	Weapon-Related Seismicity	Representative
9.6	Ventilation	Representative
	<b>Performance Assessment</b>	
10.0	Performance Assessment Activities	Inconclusive

---

## 12.0 REFERENCES

- Barton, N., R. Lien, and J. Lunde, 1974. Engineering Classification of Rock Masses for the Design of Tunnel Support; Jour. Rock Mechanics, No. 6, p. 189-239.
- Benson, L. U., J. H. Robison, R. K. Blankennagel, and A. E. Ogard, 1983. Chemical Composition of Groundwater and the Locations of Permeable Zones in the Yucca Mountain Area, Nevada; USGS-OFR-83-854, U.S. Geological Survey, Denver, CO.
- Bertram, S. G., 1984. NNWSI Exploratory Shaft Site and Construction Method Recommendation Report; SAND84-1003, Sandia National Laboratories, Albuquerque, NM.
- Bish, D. L., and S. J. Chipera, 1986. Mineralogy of Drill Holes J-13, UE-25a#1, and USW G-1 at Yucca Mountain Nevada; LA-10764-MS, Los Alamos National Laboratory, Los Alamos, NM.
- Bish, D. L., and D. T. Vaniman, 1985. Mineralogic Summary of Yucca Mountain, Nevada, LA-10543-MS, Los Alamos National Laboratory, Los Alamos, NM.
- Byers, F. M., Jr., and L. M. Moore, 1987. Petrographic Variation of the Topopah Spring Matrix Within and Between Cored Drill Holes, Yucca Mountain, Nevada; LA-10901-MS, Los Alamos National Laboratory, Los Alamos, NM.
- Carlos, B. A., 1985. Minerals in Fractures of the Unsaturated Zone from Drill Core USW G-4, Yucca Mountain, Nevada; LA-10415-MS, Los Alamos National Laboratory, Los Alamos, NM.
- Carlos, B. A., 1987, Personal Communication to F. B. Nimick.
- Daniels, W. R., K. Wolfsberg, R. S. Rundberg, A. E. Ogard, J. F. Kerrisk, C. J. Duffy, T. W. Newton, J. L. Thompson, B. P. Bayhurst, D. L. Bish, J. D. Blacic, B. M. Crowe, B. R. Erdal, J. F. Griffith, S. D. Knight, F. O. Lawrence, V. L. Rundberg, M. L. Sykes, G. M. Thompson, B. J. Travis, E. N. Treher, R. J. Vidale, G. R. Walter, R. D. Aguilar, M. R. Cisneros, S. Maestas, A. J. Mitchell, P. Q. Oliver, N. A. Raybold, and P. L. Wanek, 1982. Summary Report on the Geochemistry of Yucca Mountain and Environs; LA-9328-MS, Los Alamos National Laboratory, Los Alamos, NM.
- DOE (U.S. Department of Energy), 1986. Final Environmental Assessment: Yucca Mountain Site, Nevada Research and Development Area, Nevada; DOE/RW-0073, Washington, DC.
- Henne, M. S., 1982. The Dissolution of Rainier Mesa Volcanic Tuffs and Its Application to the Analysis of the Groundwater Environment; unpublished manuscript, University of Nevada, Reno, NV.

REFERENCES (Continued)

- Langkopf, B. S., and P. R. Gnirk, 1986. Rock-Mass Classification of Candidate Repository Units at Yucca Mountain, Nye County, Nevada; SAND82-2034, Sandia National Laboratories, Albuquerque, NM.
- Lappin, A. R., 1980. Thermal Conductivity of Silicic Tuffs: Predictive Formalism and Comparison with Preliminary Experimental Results; SAND80-0679, Sandia National Laboratories, Albuquerque, NM.
- Long, J. W., 1987. Component Ground Motion at Yucca Mountain from Pahute Mesa Underground Nuclear Explosions; SAND86-0439, Sandia National Laboratories, Albuquerque, NM.
- MacDougall, H. R., L. W. Sculley, and J. R. Tillerson, 1987. Site Characterization Plan Conceptual Design Report; SAND84-2641, Sandia National Laboratories, Albuquerque, NM.
- Nimick, F. B., and B. M. Schwartz, 1987. Bulk, Thermal, and Mechanical Properties of the Topopah Spring Member of the Paintbrush Tuff, Yucca Mountain, Nevada; SAND85-0762, Sandia National Laboratories, Albuquerque, NM.
- Nimick, F. B., and R. L. Williams, 1984. A Three Dimensional Geologic Model of Yucca Mountain, Southern Nevada; SAND83-2593, Sandia National Laboratories, Albuquerque, NM.
- Ogard, A.E, and J. F. Kerrisk, 1984. Groundwater Chemistry Along Flow Paths Between a Proposed Repository Site and the Accessible Environment; LA-10188-MS, Los Alamos National Laboratory, Los Alamos, NM.
- Ortiz, T. S., R. L. Williams, F. B. Nimick, B. C. Whittet, and D. L. South, 1985. A Three-Dimensional Model of Reference Thermal/Mechanical and Hydrological Stratigraphy at Yucca Mountain, Southern Nevada; SAND84-1076, Sandia National Laboratories, Albuquerque, NM.
- Peters, R. R., E. A. Klavetter, I. J. Hall, S. C. Blair, G. W. Heller, and G. W. Gee, 1984. Fracture and Matrix Hydrologic Characteristics of Tuffaceous Materials from Yucca Mountain, Nye County, Nevada; SAND84-1471, Sandia National Laboratories, Albuquerque, NM.
- Price, R. H., and S. J. Bauer, 1985. Analysis of the Elastic and Strength Properties of Yucca Mountain Tuff, Nevada; Proc. 26th U.S. Symp. Rock Mech., pp. 89-96.
- Price, R. H., F. B. Nimick, J. R. Connolly, K. Keil, B. M. Schwartz, and S.J. Spence, 1985. Preliminary Characterization of the Petrologic, Bulk, and Mechanical Properties of a Lithophysal Zone Within the Topopah Spring Member of the Paintbrush Tuff; SAND84-0860, Sandia National Laboratories, Albuquerque, NM.
- Rautman, C., 1985. Potential Problems with Topopah Spring Stratigraphy; Internal Memorandum to S. Sinnock, December 11, 1985.

## REFERENCES (Continued)

- Rutherford, B. M., I. J. Hall, R. G. Easterling, R. R. Peters, and E. A. Klavetter, (in preparation). Statistical Analysis of Hydrologic Data for Yucca Mountain; SAND87-2380, Sandia National Laboratories, Albuquerque, NM.
- Savage, W. Z., H. S. Swolfs, and P. S. Powers, 1985. Gravitational Stress in Long Symmetric Ridges and Valleys; *Int. J. Rock Mech. Min. Sci. and Geomech. Abstr.*, Vol. 22, No. 5, pp. 291-302.
- Scott, R. B. and M. Castellanos, 1984. Stratigraphic and Structural Relations of Volcanic Rocks in Drillholes USW GU-3 and USW G 3, Yucca Mountain, Nye County, Nevada; USGS-OFR-84-491, U.S. Geologic Survey, Denver, CO.
- Spengler, R. W., D. C. Muller, and R. B. Livermore, 1979. Preliminary Report on the Geology and Geophysics of Drillhole UE25a 1, Yucca Mountain, Nevada; USGS-OFR-79-1244, U.S. Geological Survey, Denver, CO.
- Spengler, R. W., F. M. Byers, Jr., and J. B., Warner, 1981. Stratigraphy and Structure of Volcanic Rocks in Drillhole USW-G1, Yucca Mountain, Nye County, Nevada; USGS-OFR-81-1349, U.S. Geologic Survey, Denver, CO.
- Spengler, R. W., and M. P Chornack, 1984. Stratigraphic and Structural Characteristics of Volcanic Rocks in Core Hole USW G-4, Yucca Mountain, Nye County, Nevada, with a Section on Geophysical Logs by D. C. Muller and J. E. Kibler; USGS-OFR-84-781, U.S. Geological Survey, Denver, CO.
- Sperry, P. E., 1969. River Mountains Tunnel; in: H. L. Hartman (ed.), *Proc. Second Symp. on Rapid Excavation*, Sacramento, CA.
- Stock, J. M., J. H. Healy, S. H. Hickman, and M. D. Zoback, 1985. Hydraulic Fracturing Stress Measurements at Yucca Mountain, Nevada, and Relationship to the Regional Stress Field; *Jour. Geophys. Res.*, Vol. 90, No. B10, pp. 8691-8706.
- Tillerson, J. R., and F. B. Nimick (eds.), 1984. *Geoengineering Properties of Potential Repository Units at Yucca Mountain, Southern Nevada*; SAND84-0021, Sandia National Laboratories, Albuquerque, NM.
- U.S. Department of Energy, 1986. *Issues Hierarchy for a Mined Geologic Disposal System (OGR/B-10)*; DOE/RW-0101, U.S. Department of Energy, Office of Civilian Radioactive Waste Management, Washington, DC.
- Vaniman, D. T., D. Bish, D. Broxton, F. Byers, G. Heiken, B. Carlos, E. Semarge, F. Caporuscio, and R. Gooley, 1984. Variations in Authigenic Mineralogy and Sorptive Zeolite Abundance at Yucca Mountain, Nevada, Based on Studies of Drill Cores USW GU-3 and G 3; LA-9707-MS, Los Alamos National Laboratory, Los Alamos, NM.

REFERENCES (Concluded)

- Vortman, L. J., 1986. Ground Motion Produced at Yucca Mountain from Pahute Mesa Underground Nuclear Explosions; SAND85-1605, Sandia National Laboratories, Albuquerque, NM.
- White, A. F., H. C. Claassen, and L. V. Benson, 1980. The Effect of Dissolution of Volcanic Glass on the Water Chemistry in a Tuffaceous Aquifer, Rainier Mesa, Nevada; USGS-WSP-1535-Q, U.S. Geological Survey, Washington, DC.
- Zimmerman, R. M., R. A. Bellman, Jr., K. L. Mann, D. P. Zerga, M. Fowler, and R. L. Johnson, 1987. Final Report: G-Tunnel Welded Tuff Mining Evaluations; SAND87-1433, Sandia National Laboratories, Albuquerque, NM.

## APPENDIX A

### REVISION OF INPUT DATA FOR THE TSw1-TSw2 CONTACT

Originally, the contact between thermal/mechanical units TSw1 and TSw2 was assigned at the base of the ash flow described in a lithologic log as containing 20 percent (or more) lithophysae. In addition, the lithophysae themselves were assumed to be 50 percent lithophysal cavities, leading to the inference that the contact divides material with more than 10 percent cavities from material with less than 10 percent cavities. However, as discussed by Nimick and Schwartz (1987), use of lithologic logs to define this contact resulted in erroneous picks of the contact because the assumption that cavities comprise 50 percent of lithophysae was incorrect.

Spengler and Chornack (1984) report point-counting data for four core holes (USW G-1, USW G-2, USW GU-3, and USW G-4) that enable more accurate assignment of the 10 percent-cavity dividing line. Thus, new elevations for the TSw1 TSw2 contact were obtained for these four core holes. These new data were combined with the two contact locations on the ground surface [see Ortiz et al. (1985) for description] to complete a new data set for calculation of a three-dimensional representation of the contact. The new version of the contact was used to calculate new isopach maps for units TSw1 and TSw2. These maps are believed to be better representations of the true thicknesses of these two units than the isopach maps in Ortiz et al. (1985) and Nimick and Schwartz (1987).

The new input data for the TSw1-TSw2 contact are listed in Table A 1. Because no point-count data were available for core hole UE-25a#1, the core hole has been excluded from the input data set. The new three-dimensional model estimates that the contact has an elevation of 3118 ft (950 m) at UE-25a#1. This elevation is 260 ft (79 m) higher than the elevation of the contact used in estimation of the TSw1-TSw2 contact by Ortiz et al. (1985).

Table A-1. Revised Input Data for TSw1-TSw2 Contact

Core Hole	N-S Location <sup>a</sup>	E-W Location <sup>a</sup>	Elevation <sup>a,b</sup>	Elevation Assigned by Ortiz et al. (1985) <sup>a</sup>
USW G 1	770487	560999	3749	3352
USW G- 2	778809	560519	3958	3605
USW GU- 3	752676	558503	4177	4167
USW G- 4	765804	563069	3500	3430
s1 <sup>c</sup>	760704	556958	4300	4300
s2 <sup>c</sup>	755406	557481	4300	4300

<sup>a</sup>Values are in feet.

<sup>b</sup>Values include corrections for faulting given in Ortiz et al. (1985). The well deviations used previously for the TSw1-TSw2 contact have been retained; these deviations may be in error by several feet for the redefined contact elevations.

<sup>c</sup>Not changed from Ortiz et al. (1985).

## APPENDIX B

### THERMAL CONDUCTIVITY DATA

Although many measurements of thermal conductivity have been made on samples of the tuffs from Yucca Mountain, few data have been published. This appendix provides a listing of the available data for the welded, devitrified portion of the Topopah Spring Member (Table B-1).

The data in Table B-1 should be precise and accurate to  $\pm 10$  percent, based on discussion in Lappin et al. (1982). However, because of possible differences between the saturation states of laboratory samples and in situ saturations, the values in the table probably are not directly transferable for use as data for in situ thermal conductivity of the rock mass. Additional analysis of transferability is ongoing.

Table B-1. Average Measured Thermal Conductivities for Samples of the Welded, Devitrified Topopah Spring Member

Sample ID <sup>a</sup>	Thermal/Mechanical Unit	Mean Measured Conductivity (W/mK)	
		"Saturated" <sup>b</sup>	"Dry" <sup>c</sup>
A1-369.0	TSw1	1.80	1.37
G1-406.4	TSw1	1.82	1.62
G1-795	TSw1	2.13	ND
G1-810.3	TSw1	2.17	2.08
G1-1207.9	TSw2	2.30	2.08
G1-1230.8	TSw2	2.35	ND
G2-860.4	TSw1	1.87	1.48
G2-950.1	TSw1	2.22	1.90
G2-1272.4	TSw1	2.11	ND
G2-1388.0	TSw1	2.24	1.92
G2-1526.3	TSw2	1.99	1.54
G2-1559.0	TSw2	2.23	1.99
GU3-431.5	TSw1	1.77	1.69
GU3-683.8	TSw1	2.12	2.06
GU3-685.8	TSw1	2.14	1.92
G4-327.7	TSw1	1.72	1.27
G4-737.9	TSw1	2.25	1.99
G4-1155.4	TSw2	2.42	1.91
G4-1232.0	TSw2	2.47	ND

ND = No reliable data.

<sup>a</sup>A1-core hole UE-25a#1; G1-core hole USW G-1; G2-core hole USW G-2; GU3-core hole USW GU-3; G4-core hole USW G-4. Number is depth of the sample in feet.

<sup>b</sup>"Saturated" test samples are inferred to have had saturations between 0.90 and 0.95 during thermal conductivity measurements.

<sup>c</sup>The saturation state of "dry" test samples during thermal conductivity measurements is unknown. Data are for measurement temperatures above the nominal boiling temperature at the applied pore pressures.

## APPENDIX C

### INFORMATION FROM, AND CANDIDATE INFORMATION FOR, THE REFERENCE INFORMATION BASE

#### C.1 Information Taken From the Reference Information Base

No information has been used directly from Version 02.002 of the Reference Information Base (RIB). The thermal/mechanical stratigraphy used in this study is the same as that in the RIB in the sense that both are based on Ortiz et al. (1985). (For an exception to the previous statement, see Section C.2.)

Much of the data used in Chapter 6.0 has been taken from Nimick and Schwartz (1987). In turn, much of the data in Nimick and Schwartz (1987) has been recommended for inclusion in the next update of the RIB, in the Site and Engineering Property Data Base, or both. Thus, the intent in this study has been to be consistent with parameter data contained in the RIB.

#### C.2 Candidate Information For the Reference Information Base

As a part of this study, the elevation of the contact between thermal/mechanical units TSw1 and TSw2 has been revised for the four USW G holes (see Appendix A), the three dimensional representation of the contact was recalculated, and new isopach maps of the two units were generated. The revised elevation data (Table A-1) are proposed as replacements for the existing data in Section 1.3.1.1.3 of the RIB, and the new isopach maps (Figures 4.1-5 and 4.1-7) should replace the correlative maps in Section 1.3.1.1.2 (pages 7 and 8).

APPENDIX D

INFORMATION FROM, AND CANDIDATE INFORMATION FOR,  
THE SITE AND ENGINEERING PROPERTY DATA BASE

No information in this report has been taken from the Site and Engineering Property Data Base (SEPDB). The only data tabulated in this report that might be considered for entry into the SEPDB is the thermal conductivity data in Table B-1. However, these data have been synthesized from measurements at several different temperatures. The actual measured values from which the data in Table B-1 were derived will be tabulated in a forthcoming report.

DISTRIBUTION LIST

Samuel Rousso, Acting Director (RW-1)  
Office of Civilian Radioactive  
Waste Management  
U.S. Department of Energy  
Forrestal Bldg.  
Washington, D.C. 20585

Ralph Stein (RW-30)  
Office of Civilian Radioactive  
Waste Management  
U.S. Department of Energy  
Forrestal Bldg.  
Washington, D.C. 20585

M. W. Frei (RW-22)  
Office of Civilian Radioactive  
Waste Management  
U.S. Department of Energy  
Forrestal Bldg.  
Washington, D.C. 20585

B. G. Gale (RW-23)  
Office of Civilian Radioactive  
Waste Management  
U.S. Department of Energy  
Forrestal Bldg.  
Washington, D.C. 20585

Samuel Rousso (RW-10)  
Office of Civilian Radioactive  
Waste Management  
U.S. Department of Energy  
Forrestal Bldg.  
Washington, D.C. 20585

J. D. Saltzman (RW-20)  
Office of Civilian Radioactive  
Waste Management  
U.S. Department of Energy  
Forrestal Bldg.  
Washington, D.C. 20585

S. J. Brocoum (RW-221)  
Office of Civilian Radioactive  
Waste Management  
U.S. Department of Energy  
Forrestal Building  
Washington, D.C. 20585

V. J. Cassella (RW-123)  
Office of Civilian Radioactive  
Waste Management  
U.S. Department of Energy  
Forrestal Bldg.  
Washington, D.C. 20585

S. H. Kale (RW-20)  
Office of Civilian Radioactive  
Waste Management  
U.S. Department of Energy  
Forrestal Bldg.  
Washington, D.C. 20585

T. H. Isaacs (RW-40)  
Office of Civilian Radioactive  
Waste Management  
U.S. Department of Energy  
Forrestal Bldg.  
Washington, D.C. 20585

D. H. Alexander (RW-332)  
Office of Civilian Radioactive  
Waste Management  
U.S. Department of Energy  
Forrestal Bldg.  
Washington, D.C. 20585

C. Bresee (RW-10)  
Office of Civilian Radioactive  
Waste Management  
U.S. Department of Energy  
Forrestal Bldg.  
Washington, D.C. 20585

Gerald Parker (RW-333)  
Office of Civilian Radioactive  
Waste Management  
U.S. Department of Energy  
Forrestal Bldg.  
Washington, D.C. 20585

Chief, Repository Projects Branch  
Division of Waste Management  
U.S. Nuclear Regulatory Commission  
Washington, D.C. 20555

NTS Section Leader  
Repository Project Branch  
Division of Waste Management  
U.S. Nuclear Regulatory Commission  
Washington, D.C. 20555

Document Control Center  
Division of Waste Management  
U.S. Nuclear Regulatory Commission  
Washington, D.C. 20555

Carl P. Gertz, Project Manager (6)  
Waste Management Project Office  
U.S. Department of Energy  
Nevada Operations Office  
P.O. Box 98518  
Mail Stop 523  
Las Vegas, NV 89193-8518

J. L. Fogg (12)  
Technical Information Office  
U.S. Department of Energy  
Nevada Operations Office  
P.O. Box 98518  
Las Vegas, NV 89193-8518

C. L. West, Director  
Office of External Affairs  
U.S. Department of Energy  
Nevada Operations Office  
P.O. Box 98518  
Las Vegas, NV 89193-8518

W. M. Hewitt, Program Manager  
Roy F. Weston, Inc.  
955 L'Enfant Plaza, Southwest  
Suite 800  
Washington, D.C. 20024

Technical Information Center  
Roy F. Weston, Inc.  
955 L'Enfant Plaza, Southwest  
Suite 800  
Washington, D.C. 20024

L. D. Ramspott (3)  
Technical Project Officer for NNWSI  
Lawrence Livermore National  
Laboratory  
P.O. Box 808  
Mail Stop L-204  
Livermore, CA 94550

M. E. Spaeth  
Technical Project Officer for NNWSI  
Science Applications International  
Corp.  
101 Convention Center Dr.  
Suite 407  
Las Vegas, NV 89109

H. N. Kalia  
Exploratory Shaft Test Manager  
Los Alamos National Laboratory  
Mail Stop 527  
101 Convention Center Dr.  
Suite P230  
Las Vegas, NV 89109

D. T. Oakley (4)  
Technical Project Officer for NNWSI  
Los Alamos National Laboratory  
P.O. Box 1663  
N-5, Mail Stop J521  
Los Alamos, NM 87545

L. R. Hayes (6)  
Technical Project Officer for NNWSI  
U.S. Geological Survey  
P.O. Box 25046  
421 Federal Center  
Denver, CO 80225

K. W. Causseaux  
NHP Reports Chief  
U.S. Geological Survey  
P.O. Box 25046  
421 Federal Center  
Denver, CO 80225

R. V. Watkins, Chief  
Project Planning and Management  
U.S. Geological Survey  
P.O. Box 25046  
421 Federal Center  
Denver, CO 80225

Center for Nuclear Waste  
Regulatory Analyses  
6220 Culebra Road  
Drawer 28510  
San Antonio, TX 78284

R. L. Bullock  
Technical Project Officer for NNWSI  
Fenix & Scisson, Inc.  
101 Convention Center Dr.  
Suite 320  
Mail Stop 403  
Las Vegas, NV 89109-3265

James C. Calovini  
Technical Project Officer for NNWSI  
Holmes & Narver, Inc.  
101 Convention Center Dr.  
Suite 860  
Las Vegas, NV 89109

Dr. David W. Harris  
NNWSI Technical Project Officer  
Bureau of Reclamation  
P.O. Box 25007 Bldg. 67  
Denver Federal Center  
Denver, CO 80225-0007

M. D. Voegele  
Science Applications International  
Corp.  
101 Convention Center Dr.  
Suite 407  
Las Vegas, NV 89109

J. A. Cross, Manager  
Las Vegas Branch  
Fenix & Scisson, Inc.  
P.O. Box 93265  
Mail Stop 514  
Las Vegas, NV 89193-3265

P. T. Prestholt  
NRC Site Representative  
1050 East Flamingo Road  
Suite 319  
Las Vegas, NV 89109

A. E. Gurrola, General Manager  
Energy Support Division  
Holmes & Narver, Inc.  
P.O. Box 93838  
Mail Stop 580  
Las Vegas, NV 89193-3838

A. M. Sastry  
Technical Project Officer for YMP  
MAC Technical Services  
Valley Bank Center  
101 Convention Center Drive  
Suite P-113  
Las Vegas, NV 89109

B. L. Fraser, General Manager  
Reynolds Electrical & Engineering Co.  
P.O. Box 98521  
Mail Stop 555  
Las Vegas, NV 89193-8521

P. K. Fitzsimmons, Director  
Health Physics & Environmental  
Division  
U.S. Department of Energy  
Nevada Operations Office  
P.O. Box 98518  
Las Vegas, NV 89193-8518

Robert F. Pritchett  
Technical Project Officer for NNWSI  
Reynolds Electrical & Engineering Co.  
P.O. Box 98521  
Mail Stop 615  
Las Vegas, NV 89193-8521

Elaine Ezra  
NNWSI GIS Project Manager  
EG&G Energy Measurements, Inc.  
P.O. Box 1912  
Mail Stop H-02  
Las Vegas, NV 89125

SAIC-T&MSS Library (2)  
Science Applications International  
Corp.  
101 Convention Center Dr.  
Suite 407  
Las Vegas, NV 89109

Dr. Martin Mifflin  
Desert Research Center  
Water Resource Center  
2505 Chandler Avenue  
Suite 1  
Las Vegas, NV 89120

E. P. Binnall  
Field Systems Group Leader  
Building 50B/4235  
Lawrence Berkeley Laboratory  
Berkeley, CA 94720

J. F. Divine  
Assistant Director for Engineering  
Geology  
U.S. Geological Survey  
106 National Center  
12201 Sunrise Valley Dr.  
Reston, VA 22092

V. M. Glanzman  
U.S. Geological Survey  
P.O. Box 25046  
913 Federal Center  
Denver, CO 80225

C. H. Johnson  
Technical Program Manager  
Nuclear Waste Project Office  
State of Nevada  
Evergreen Center, Suite 252  
1802 North Carson Street  
Carson City, NV 89710

T. Hay, Executive Assistant  
Office of the Governor  
State of Nevada  
Capitol Complex  
Carson City, NV 89710

R. R. Loux, Jr. (3)  
Executive Director  
Nuclear Waste Project Office  
State of Nevada  
Evergreen Center, Suite 252  
1802 North Carson Street  
Carson City, NV 89710

John Fordham  
Desert Research Institute  
Water Resources Center  
P.O. Box 60220  
Reno, NV 89506

Prof. S. W. Dickson  
Department of Geological Sciences  
Mackay School of Mines  
University of Nevada  
Reno, NV 89557

J. R. Rollo  
Deputy Assistant Director for  
Engineering Geology  
U.S. Geological Survey  
106 National Center  
12201 Sunrise Valley Dr.  
Reston, VA 22092

Eric Anderson  
Mountain West Research-Southwest  
Inc.  
Phoenix Gateway Center  
432 North 44 Street  
Suite 400  
Phoenix, AZ 85008-6572

Judy Foremaster (5)  
City of Caliente  
P.O. Box 158  
Caliente, NV 89008

A. T. Tamura  
Science and Technology Division  
Office of Scientific and Technical  
Information  
U.S. Department of Energy  
P.O. Box 62  
Oak Ridge, TN 37831

L. Jardine  
Project Manager  
Bechtel National Inc.  
P.O. Box 3965  
San Francisco, CA 94119

R. Harig  
Parsons Brinckerhoff Quade &  
Douglas  
1625 Van Ness Ave.  
San Francisco, CA 94109-3679

Dr. Roger Kasperson  
CENTED  
Clark University  
950 Main Street  
Worcester, MA 01610

Robert E. Cummings  
Engineers International, Inc.  
P.O. Box 43817  
Tucson, AZ 85733-3817

Dr. Jaak Daemen  
Department of Mining and  
Geotechnical Engineering  
University of Arizona  
Tucson, AZ 85721

Department of Comprehensive Planning  
Clark County  
225 Bridger Avenue, 7th Floor  
Las Vegas, NV 89155

Economic Development Department  
City of Las Vegas  
400 East Stewart Avenue  
Las Vegas, NV 89109

Planning Department  
Nye County  
P.O. Box 153  
Tonopah, NV 89049

Director of Community Planning  
City of Boulder City  
P.O. Box 367  
Boulder City, NV 89005

Commission of the European  
Communities  
200 Rue de la Loi  
B-1049 Brussels  
Belgium

Lincoln County Commission  
Lincoln County  
P.O. Box 90  
Pioche, NV 89043

Community Planning & Development  
City of North Las Vegas  
P.O. Box 4086  
North Las Vegas, NV 89030

City Manager  
City of Henderson  
Henderson, NV 89015

ONWI Library  
Battelle Columbus Laboratory  
Office of Nuclear Waste Isolation  
505 King Avenue  
Columbus, OH 43201

Librarian  
Los Alamos Technical  
Associates, Inc.  
P.O. Box 410  
Los Alamos, NM 87544

Paul Aamodt  
Los Alamos National Laboratory  
P.O. Box 1663  
Los Alamos, NM 87545

H. Kalia  
Los Alamos National Laboratory  
P.O. Box 1663  
Los Alamos, NM 87545

T. Merson  
Los Alamos National Laboratory  
P.O. Box 1663  
Los Alamos, NM 87545

6300 R. W. Lynch  
6300-1 T. O. Hunter  
6310 J. E. Stiegler, Actg.  
6310 NNWSICF  
6310 100/124213/SAND87-1685/Q3  
6311 A. L. Stevens  
6311 C. Mora  
6312 F. W. Bingham  
6312 R. R. Peters  
6312 A. C. Peterson  
6313 T. E. Blejwas  
6313 R. E. Finley

6313 F. D. Hanson  
6313 E. A. Klavetter  
6313 F. B. Nimick (5)  
6313 R. H. Price  
6313 B. M. Schwartz (2)  
For Data Set Files  
51/L01A-06/24/80  
51/L01A-10/07/81  
51/L01A-12/02/82  
51/L01A-07/16/81  
51/L01A-09/07/82  
51/L01A-01/23/85  
6314 J. R. Tillerson  
6314 S. J. Bauer  
6314 L. S. Costin  
6314 J. A. Fernandez  
6314 T. E. Hinkebein  
6314 R. E. Stinebaugh  
6315 L. E. Shephard  
6316 R. P. Sandoval  
6317 S. Sinnock  
6332 WMT Library (20)  
6430 N. R. Ortiz  
3141 S. A. Landenberger (5)  
3151 W. I. Klein (3)  
8524 J. A. Wackerly  
3154-3 C. H. Dalin (8)  
for DOE/OSTI

